UNIVERSITY OF ZIMBABWE

MODELLING THE IMPACT OF CLIMATE VARIABILITY AND CHANGE ON HUMAN HEALTH AND DISEASES

ETHEL TSUNGAI NGARAKANA-GWASIRA

September 7, 2016

MODELLING THE IMPACT OF CLIMATE VARIABILITY AND CHANGE ON HUMAN HEALTH AND DISEASES

by

ETHEL TSUNGAI NGARAKANA-GWASIRA

Submitted in fulfilment of the academic requirements for the degree of Doctor of Philosophy in the Faculty of Science, Department of Mathematics, University of Zimbabwe

Harare

September 2016

Abstract

Malaria is a life-threatening disease caused by parasites that are transmitted to humans through the bites of infected female mosquitoes. Almost half of the world's population is at risk of malaria. Schistosomiasis is considered second only to malaria as the most devastating parasitic disease, estimated to affect 237 million people worldwide. The development, mortality and reproduction rates of the malaria and schistosomiasis parasites and their hosts are very sensitive to temperature and the availability of water bodies. The distribution and prevalence of the diseases are most likely to be affected by climate change. The aim of this thesis was to advance understanding of the potential effects of climate change on malaria and schistosomiasis transmission, using non linear differential equations. In addition, the study also sought to assess the role of mathematical models in evaluating the impact of climate variability and change on malaria and schistosomiasis transmission. The work in this thesis focused on investigating the effects of climate on malaria and schistosomiasis transmission in Africa and South America. Climate driven deterministic models were developed separately for malaria, schistosomiasis and malaria-schistosomiasis coinfection. Mathematical models of human population dynamics and the vector population dynamics were developed for both malaria and schistosomiasis. For both diseases, temperature-dependent stages of the parasites in their life cycles are considered. Temperature and rainfall were incorporated in the models to explore the effects of climate variability and change on the diseases transmission dynamics. The equilibrium states for the models were determined and analysed. The reproductive rates were computed for

each model and accordingly analysed. Mathematical packages (Mathematica, Matlab and C++) were used to perform sensitivity analyses and numerical simulations. Projections for future transmission dynamics were made from climate change projection models in order to inform policy makers on how to deal with the diseases in the future. Results from the malaria model suggest that temperature range 23^oC to 38^oC is ideal for malaria transmission. The reproduction number increases as temperature increases to attain a maximum at 31.5^oC, beyond which the reproduction number starts declining. This result suggests the optimal temperature for malaria transmission is around 31^oC. The analytic results are also supported by numerical simulations which show an increase in malaria cases as temperature increases to about 38^oC and a decrease thereafter. Furthermore, results from model analysis suggest daily rainfall in the range of $15 - 17mm$ is ideal for the spread of malaria. The models' reproductive rates were simulated using climate models for Africa to determine the current transmission patterns and to aid prediction of future trends. The results of the simulated current transmission pattern of malaria fall within the observed spatial distribution of falciparum limits on the African continent. Results from future projections of malaria transmission suggest that due to climate change, endemic malaria will die out on the southern fringe of the disease map in Africa by 2040, while malaria endemicity is going to become a problem in the African highlands. A drying trend is the likely driving force for the reduction in malaria transmission in the regions to the south of the continent, while a warming trend is the likely factor driving the projected increase in malaria endemicity in the highlands, although increases in malaria incidences in these ar-

eas can also be attributed to socioeconomic factors such as land use change and drug resistance. The model has the following limitations: it did not consider the role of human migration, other climate variables, in particular relative humidity as the tropical anopheline mosquitoes prefer humidities above 60% and the role of socioeconomic factors in malaria transmission dynamics. Despite these limitations, the model is reasonable enough to be able to give a realistic picture of malaria in the African continent. Thus, results from the study will be useful at various levels of decision making, for example, in setting up an early warning system and sustainable strategies for climate change adaptation for malaria vectors control programmes in Africa. These results can be generalized to other tropical regions outside Africa. A mathematical model to explore the impact of temperature and rainfall (in the context of its effect on water bodies) on schistosomiasis transmission is presented as a system of differential equations and analysed. The model analysis suggests that the optimal temperature for schistosomiasis transmission is around 23^OC. Geographical information systems (GIS) was used to map the reproduction number for Zimbabwe using temperature and rainfall data from 1950 to 2000. It was noted that high reproduction numbers, which suggest high incidences of schistosomiasis, are found in the Zambezi valley catchment area and the lowveld of the country. A mathematical model for schistosomiasis and malaria coinfection incorporating rainfall and temperature was developed and analysed. The coinfection reproduction number was computed and mapped on the continents of Africa and South America. Results from the mapping suggest that environmental ambient conditions in the equatorial regions of Africa and Latin America promote

malaria and schistosomiasis coinfection with a heavier burden of coinfection in South America, especially in Brazil. Within Africa, there are some countries where it is beneficial to target both diseases, for example Angola, Democratic Republic of Congo and Madagascar. However there are some areas where targeting Malaria only is warranted. In the sub-tropical regions, including Namibia, South Africa, the greater part of Zimbabwe and the areas on the northern fringe of the Sahara, schistosomiasis is more dominant than malaria. Results also show that coinfection is a greater problem in general in South America than in Africa. These findings suggest that both schistosomiasis and malaria control programmes should be intensified in these regions of Africa and South America. The results of this study can be used to identify areas which need special attention with regard to malaria and schistosomiasis control. This can be extended to incorporate other aspects like the terrain of the region under study to capture the real transmission dynamics of schistosomiasis and malaria.

Declaration

This thesis is a presentation of work done at the University of Zimbabwe in the Faculty of Science, Department of Mathematics, during the period May 2012 to April 2016. It was completed under the supervision of Professor E Mashonjowa and the late Professor C.P Bhunu. I declare that this thesis has been composed solely by myself and that it has not been submitted, in whole or in part, in any previous application for a degree. Except where stated otherwise by reference or acknowledgement, the work presented is entirely my own

Ethel T Ngarakana-Gwasira

September 2016

Articles published from the thesis

Part of the work presented in this thesis has been published in international reviewed journals.

1. Ngarakana-Gwasira ET, Bhunu CP & Mashonjowa E, (2014). Assessing the impact of temperature on malaria transmission dynamics. *Afrika Matematika*, 25:1095-1112.

2. Ngarakana-Gwasira ET, Bhunu CP, Masocha M, Mashonjowa E, (2016). Transmission dynamics of schistosomiasis in Zimbabwe: A mathematical and GIS Approach. *Communication in Nonlinear Science and Numerical Simulation*, 35:137-147.

3. Ngarakana-Gwasira ET, Bhunu CP, Masocha M, Mashonjowa E, (2016). Impact of climate change on malaria transmission in Africa. *Malaria Research and Treatment* http://dx.doi.org/10.1155/2016/7104291

Acknowledgements

All glory and honour be unto the Most High God for taking me this far. I would like to express my gratitude towards my advisors, Professors C.P Bhunu and E. Mashonjowa. I appreciate their guidance, dedication and exemplary academic standards. Their courtesy, professionalism and patience made working with them very rewarding and gratifying.

I would like to acknowledge Dr M.Masocha whose expertise in Geographic Information Systems was very valuable to my research.

I would like to thank all the staff members in the department of Mathematics at the University of Zimbabwe for their constructive criticism and useful suggestions. l would like to thank you for the wonderful times we shared during my studies. Special thanks goes to Professor Mushayabasa, Professor A.G.R Stewart, Professor S. Mukwembi and Mr Mazorodze.

I would like to thank my father Mr Yotam Jacob who inspired me to pursue mathematics. I would like to thank my Pastor, Mrs Francisca Zinyemba who instilled in me the strength and confidence to fulfil my dreams.

Finally I wish to thank my husband Esau and children for their love and unlimited support. They were and will always be the inspiration of all my goals in life.

"Every place upon which the sole of your foot shall tread, that I have given to you as I promised". Joshua 1:3

Dedication

To my husband Esau, sons Tinashe and Jayden and daughters Debrah and Deanne.

Contents

List of Figures

List of Tables

Chapter 1

Introduction

1.1. Background

The impact of climate variability and change on the transmission of infectious diseases is a complex and pressing public health issue. Schistosomiasis is endemic in 78 tropical and subtropical countries (WHO, 2014). The World Health Organisation estimates that globally, 779 million people are at risk of schistosomiasis and at least 237 million people are infected with Schistosoma species (Chitsulo *et al.*, 2000; Steinmann *et al.*, 2006; Vos *et al.*, 2012; Colley *et al.*, 2014). Africa bears the brunt of the epidemic where more than 90% of the infections occur worldwide (WHO, 2013). Malaria on the other hand remains endemic in 97 countries with an estimated 214 million cases worldwide and an estimated 438 000 deaths in 2015 (WHO, 2015). It is considered one of the most important vector-borne disease re-

sponsible for the fifth greatest number of deaths due to infectious diseases and is the second leading cause of death in Africa behind HIV/ AIDS (Gubler, 1998). Globally, malaria caused an estimated 453 000 under-five deaths in 2013 of which 437 000 were from Africa (WHO, 2014).

Climate change projections show increasing temperatures across Africa (Stocker *et al.*, 2013), where the burden of both schistosomiasis and malaria are highly concentrated. What remains unclear is how climate change might affect the transmission potential of both malaria and schistosomiasis in different locations, given that rainfall and temperature are key determinants of both snails and mosquitoes geographical distribution and all aspects of their life cycles. Although the impact of climate change on human health has received increasing attention in recent years, current comprehension of the relationships between environmental variables, including temperature, rainfall and hydrology and vector borne diseases is still limited (Remais, 2010).

The aim of this thesis was to advance understanding of the potential effects of climate change on malaria and schistosomiasis transmission, using non linear differential equations. Mathematical models of human population dynamics and the vector population dynamics were developed for both malaria and schistosomiasis. For both diseases, temperature-dependent stages of the parasites in their life cycles are considered.

1.2.   Mathematical modelling of infectious diseases

Mathematical modelling is an attempt to describe some part of the real world phenomenon using functions and equations. Mathematical models take us beyond verbal or graphical reasoning and provide a solid frame-work upon which to build experiments and generate hypotheses. Mathematical models have been used in the physical, biological, and social science. The building blocks for mathematical models have been taken from calculus, algebra, geometry and nearly every other field within mathematics. The main thrust of creating and analysing mathematical models is to develop a clear understanding of the real world phenomenon under investigation with aid of virtual models instead of experimenting with lives. A virtual model is a mathematical model with a biological meaning.

Population dynamics are complex, non-linear systems that cannot be understood without the help of detailed mathematical analysis. In population dynamics, populations in different states are denoted by variables. These variables are used to construct ordinary differential equations that describe the interactions and relationships between the different variables. After the mathematical model has been developed, it is then analysed or is used in biological investigations from which biological results are obtained analytically or numerically. Mathematical models can be used to,

- understand the mechanisms through which infectious diseases spread;

- understand, predict and control disease outbreaks;

- quantify the relative contribution of vaccination, chemotherapy and preventive measures to the reduction of the disease;

- determine the effectiveness of interventions currently in place;

- study the impact of poverty on disease epidemiology;

- explore the effects of drug interactions in situations where an individual is co-infected with different pathogens;

- determine the effects of drug-resistant strains in a population;

- determine the effectiveness of current vaccines on multifactorial interaction between different diseases;

- predict the future course of an epidemic.

Mathematical models can be classified in several ways some of which are described as

- Linear and non-linear: Mathematical models are usually composed of variables, which are abstractions of quantities of interest in the described systems, and operators that act on these variables, which can be algebraic operators, functions and differential operators. If all the operators in a mathematical model present linearity the resulting mathematical model is defined as linear. A model is considered to be non linear otherwise.

- Deterministic and stochastic: A deterministic model is one in which every set of variables is uniquely determined by parameters in the model and by sets

of previous states of these variables. Therefore, deterministic models perform the same way for a given set of initial conditions. Deterministic models are also called compartmental models as individuals in a population are classified into compartments depending on their status with regard to infection under study. Usually they are classified by a string of letters that provides information about the model structure. Conversely, in a stochastic model, randomness is present, and variable states are not described by unique values, but rather by probability distributions.

In this thesis a deterministic approach is used in the modelling of malaria and schistosomiasis dynamics. Data from published work and reasonable estimates will be used in this thesis. Differential equations are preferred because a lot is known about their behaviour and they are suitable to model population dynamics. For instance given a set of parameters and particular set of differential equations, one can predict the behaviour of the system and tell the range of parameter values the system make biological sense and bifurcate from one state to the other. Almost all modern epidemic models (Anderson and May, 1991; Daley and Gani, 1999; Hethcote, 2000) make use of a multiple-state approach, segmenting the modelled population into a set of distinct classes, each exhibiting a different characteristic with respect to the disease.

The states that are modelled would typically include those described in Table 1.1. The existence (or otherwise) of each of these five states, together with the links

between the respective states, is usually sufficient to provide a broad outline of the particular epidemic model being used, particularly in describing acute epidemics, which develop and spread over a short period of time. However, models for more chronic and long-term epidemics would also need to consider births and deaths. A further enhancement for models dealing with diseases for which vaccines have been developed is to include a further state for those lives that have been immunized against a particular disease. The states used in conventional epidemic modelling are described in Table 1.1.

Symbol	Epidemic State	Description
M	Passively Immune	Individuals who have acquired temporary immunity to a particular disease without having ever been infected. An example of this state would be newborn infants with antibodies against the disease passed from their mother. These antibodies eventually disappear from the body at which time the infant moves into the Susceptible state.
S	Susceptible	Lives who are healthy, but who could potentially develop the disease.
E	Exposed	Individuals who have been infected and with the disease, but who are still in the latent period (with or without symptoms of the disease) and who cannot transmit the disease to others.
I	Infective	Individuals who are infected with the disease (with or without symptoms of the disease) and who are capable of transmitting the infection to others.
R	Removed	Individuals who have either died or recovered from infection thereby acquiring immunity (temporary or permanent) from infection.

Table 1.1: States used in conventional epidemic modelling.

Making use of the states outlined above, it is conventional to name epidemic models after the states considered in the modelling process and the possible transitions between the various states. For example, one of the simplest epidemic models is called the Susceptible, Infective, and Removed (SIR) model after the 3 states considered in the modelling. Various other epidemic models, considering combinations of the above five states are shown in Table 1.2.

Model	Characteristics
SI	Once a susceptible member of the population (S) has been infected with the disease, he or she is immediately infective (I) and capable of transmitting the infection to others. No recovery from the disease is possible.
SIS	Same as the SI model, except that recovery from the disease is possible. However, upon recovery, a life is immediately susceptible (S) once again. That is, recovery from the disease does not confer any immunity against future infection.
SEI	Same as the SI model, except that, following initial exposure (E) to the disease leading to infection, there is a latent or incubation period during which the disease cannot be passed on to others.
$SEIS$	Same as the SIS model, except that, following initial exposure (E) to the disease leading to infection, there is a latent or incubation period during which the disease cannot be passed on to others.
SIR	Same as the SI model, except that recovery (R) from the disease is possible. Once recovered from the disease, there is lifelong immunity from reinfection.
$SIRS$	Same as the SIR model, except that postrecovery immunity is only temporary. Following a period of immunity, a life may become susceptible (S) once again.
$SEIR$	Same as the SIR model, except that following initial exposure (E) to the disease leading to infection, there is a latent or incubation period during which the disease cannot be passed on to others.
$SEIRS$	Same as the $SEIR$ model, except that postrecovery immunity is only temporary.
$MSEIR$	Same as the $SEIR$ model, with the addition of lives who are passively immune (M) from infection when they enter the population.
$MSEIRS$	Same as the $MSEIR$ model, except that postrecovery immunity is only temporary.

Table 1.2: Conventional epidemic models.

In many such models, there is a sharp threshold behaviour and the asymptotic dynamics are determined by a parameter $\mathcal{R}_0$ known as the basic reproduction number. When $\mathcal{R}_0 < 1$, the disease-free equilibrium is asymptotically stable (usually globally) and when $\mathcal{R}_0 > 1$ there exists a unique endemic equilibrium which is also asymptotically stable. $\mathcal{R}_0$ represents the average number of new infectious cases caused by an infectious case in a fully susceptible population, during the entire infectious period. It is worth noting here that not all $SEIR$-type models have an $\mathcal{R}_0$ threshold; see Heffernan *et al.* (2005) for the review of $\mathcal{R}_0$ estimation in different kinds of models.

The first mathematical model to predict epidemics was developed in 1760 by Daniel Bernoulli who used mathematical methods to evaluate the effectiveness of variolation of healthy people with small pox virus in an effort to tame the disease. However deterministic epidemiology modelling seems to have started in the 20th century. In 1906 Hamer formulated and analysed a discrete time model in an attempt to understand the recurrence of measles epidemics. His model may have been the first to assume that incidence depends on the product of the susceptibles and infectives (Hamer, 1906). This concept of mass action in analogy to its origin in chemical reaction kinetics is fundamental to the modern theory of deterministic epidemic modelling (Roberts and Heesterbeek, 2003). The popularity of mass action is explained by its mathematical convenience and the fact that at low population densities it is a reasonable approximation of a much more complex contact process (Roberts and Heesterbeek, 2003). For a complete undestanding of the con-

cept of mass action in epidemiological models see Roberts and Heesterbeek (2003).

Ross who was interested in the incidence and control of malaria developed a differential equation model for malaria as a host-vector disease (Ross, 1911). Other deterministic models were later, developed by Ross, Ross and Hudson, Martini and Lotka (Bailey, 1975; Dietz, 1967, 1988). Kermark and McKendrick developed a number of epidemic models starting in 1926 which show that an epidemic threshold result that the density of susceptibles must exceed a critical value in order for an epidemic outbreak to occur (Bailey, 1975).

1.3. Malaria

Malaria is a disease that is transmitted between female Anopheles mosquitoes and mammals. Four Plasmodium parasite species are responsible for malaria infection in humans: Plasmodium falciparum, Plasmodium vivax, Plasmodium ovale, and Plasmodium malariae. Of the four parasites, P. falciparum causes the most severe clinical symptoms and is responsible for the greatest number of malaria induced deaths. Malaria is transmitted between humans through bites by infected female Anopheles mosquitoes. The incubation period is usually $7 - 30$ days; this is the time it takes for the sporozoites from a new mosquito bite to travel to the liver and develop into merozoites in the blood stream. Malaria is both a preventable and treatable disease. The objective of treating is to ensure a rapid and complete elimination of the Plasmodium parasite from the patients blood in order to prevent progression of uncomplicated malaria to severe disease or death, and to chronic

infection that leads to malaria-related anaemia. Treatment is meant to reduce transmission of the infection to others, by reducing the infectious reservoir and to prevent the emergence and spread of resistance to antimalarial medicines. Clinical manifestations of severe infection include cerebral malaria, anaemia, respiratory distress syndrome, and acute renal failure (Kochar *et al.* 2009).

The malaria parasite has two main life stages, one which requires a human host and the other requires a mosquito host. An infectious mosquito bites a human, the parasites in form of sporozoites in the saliva of the mosquito enter the human blood and move to the liver. In the liver, the sporozoites invade the hepatic cells. After some $5-16$ days, the sporozoites develop into schizonts which contain thousands of merozoites. The merozoites exit the liver cells and re-enter the bloodstream, beginning a cycle of invasion of red blood cells, known as asexual replication. In the red blood cells they develop into mature schizonts, which rupture, releasing newly formed merozoites that then reinvade other red blood cells. The rupture is what frees the parasite and causes it to affect other blood cells. This cycle of invasion and cell rupture repeats every $1-3$ days and can result in thousands of parasite-infected red blood cells in the host bloodstream, leading to illness and complications of malaria that can last for months if not treated. Some of the merozoites differentiate into sexual forms known as gametocytes.

When a mosquito takes a blood meal from an infected human being it ingests the gametocytes. These gametocytes fuse to form the zygote that matures to form an ookinete which penetrates the stomach wall. The ookinete develops into an oocyst

which in a week or more releases sporozoites. This process is ambient temperature dependent. Some of the merozoite-infected blood cells leave the cycle of asexual replication. Instead of replicating, the merozoites in these cells develop into sexual forms of the parasite, called male and female gametocytes. In some malaria species, young gametocytes sequester in the bone marrow and some organs while late stage gametocytes, circulate in the bloodstream. It takes $7 - 12$ days for the gametocytes to form new sporozoites in the mosquito but this incubation period varies greatly depending on the environmental temperature, humidity and the species of plasmodium. The optimal environmental conditions for development of sporozoites are temperatures between 20^oC and 30^oC and relative humidity greater than 60%. The malaria parasite life cycle is shown in Figure 1.1.
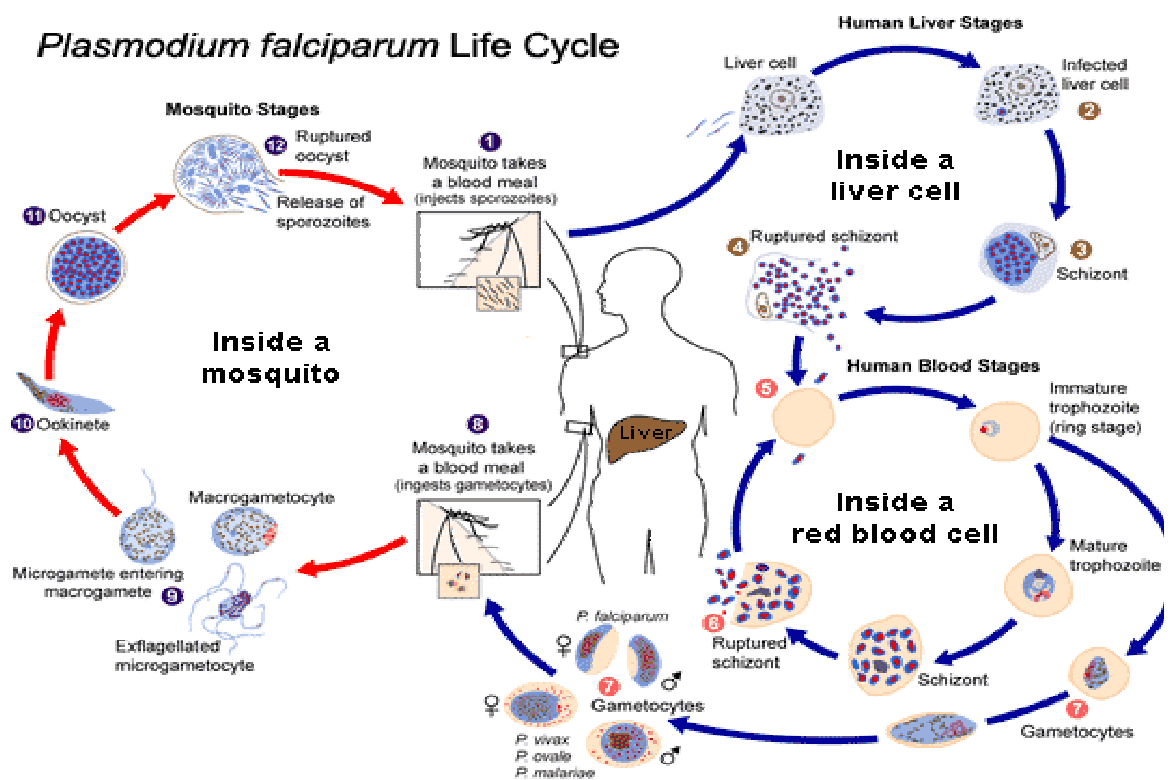
Figure 1.1: Malaria parasite life cycle (Adopted from www.cdc.gov/dpdx/malaria/)

The mosquito has four separate and distinct stages of its life cycle. The eggs require water for successful hatching. They hatch into larvae in about $2-3$ days depending on temperature. However, the hatching may even take weeks in cold weather. The larvae stage requires water, they live in water for $7-14$ days depending on water temperature as they develop into pupa. Pupa requires water and may take $1-4$ days depending on the species and temperature. The egg, larva and pupa stage belong to the immature stage and do not participate in the infection cycle. This stage is water bound and depends on the existence of water bodies. The pupa develops to an adult mosquito. The average lifespan of an adult male is about a week while the female mosquito can live up to a month.

The adult female mosquito requires a blood meal for the protein needed to produce eggs. After the blood meal it rests until the eggs develop and this process is temperature dependent and usually lasts for $2-3$ days in tropical conditions. The lifespan of the adult mosquito depends on temperature, humidity, sex of the mosquito and time of the year. Temperature and moisture, in form of precipitation and relative humidity, are critical regulators of the growth and development within each stage, in determining the end of one stage and the beginning of the next and in regulating the length of the gonotrophic cycle. Thus, the transition usually occurs in $10-14$ days in tropical conditions. The development time for the mosquito depends on the environmental conditions and on the species of the mosquito with warmer temperatures promoting quicker development.

To control the population of mosquitoes, people in Africa in the past, removed or

poisoned the breeding grounds of mosquitoes and the aquatic habitats of the larva stages by applying oil to places with standing water (Killeen *et al*, 2002). In recent years, pesticides have been widely used to eliminate mosquitoes. The use of mosquito nets, bedclothes and mosquito-repellent incense (indoor residual spraying) also helps to minimize the biting rate, greatly reducing the chances of infection and transmission of malaria as mosquitoes are kept away from humans. There are effective drugs for malaria treatment, Chloroquine, Quinuine, Primaquine and combinations of some other drugs like sulfadoxine and pyrimethamine(SP) are effective medicines for treating infections caused by the malaria parasites. Once recovered, an individual does possess temporary immunity, but it only lasts for a short time. The road to malaria vaccine clinics has been long and filled with darkness, even with the support of global funds. A completely effective vaccine has not yet been developed for malaria infection, although several vaccines are under clinical trials.

1.3.1. Review of mathematical models for Malaria

For over a century, mathematical models have been used to provide a framework for understanding malaria transmission dynamics in human population. In early 1900, Sir Ronald Ross was one of the first to publish a series of papers using mathematical functions to study transmission of Malaria (Ross 1915 , 1916a, 1916b, 1916c, 1916d). Ross developed a simple mathematical model, commonly known as the Ross model (Ross 1916a), which explained the relationship between the number of mosquitoes and incidence of malaria in humans. His results showed that

reduction of mosquito numbers below the transmission threshold was sufficient to counter malaria. Several mathematical models have been developed as researchers extended Ross's model. In the 1950s George Macdonald reasserted the usefulness of mathematical models by modifying Ross's model by integrating the latent period of infection in mosquitoes due to parasite development (Macdonald, 1957). Anderson and May also introduced latency of infection in humans in Macdonald's model (Anderson and May, 1991). All other models are developed from these three basic models by incorporating different factors to make them biologically more realistic in explaining disease prevalence and prediction.

While Ross was a pioneer in using mathematical models to understand malaria transmission, he did not look into the aspects of climate variables and the mosquito life cycle. The mosquito lifecycle is generally not considered in most mathematical models because eggs, larvae and pupae are not involved in the transmission cycle. In malaria transmission, the mosquito population dynamics are strongly influenced by the environmental conditions which directly affect the juvenile stage dynamics. Though neglecting the juvenile stage in modelling malaria transmission simplifies the modelling aspect, results of such models do not predict malaria intensity in most malaria endemic regions (Smith and McKenzie, 2004).

1.4.   Schistosomiasis

Schistosomiasis, also known as bilharzia, is a water-borne infection caused by a microscopic worm called Schistosoma, belonging to the family of flukes. There

are three types of human schistosomiasis, two of which occur in Africa and South America and the other one in the Far East. Schistosoma mansoni worms live in the veins supplying the intestine and their eggs are passed out with faeces, while S. haematobium worms live in the veins supplying the bladder and their eggs are voided with urine. The S. japonicum species of the Far East behave like S. mansoni. The male and female worms are small enough to lie within blood vessels where they feed and reproduce. The male has a groove along his body in which the female lives. The fertilised female lays thousands of eggs in her lifetime. Some are swept along in the bloodstream to the liver, while others find their way directly into the intestine or bladder from where they exit the host, either in urine or faeces.

An infected human passes eggs in stool or urine in or near fresh water. The eggs will hatch upon contact with water into tiny, hairy larvae called miracidia. The miracidia penetrates the tissues of freshwater snails, where they multiply. After several days, the snails shed many hundred swimming larvae called cercariae into the water. One egg excreted in human waste can give rise to thousands of aquatic cercariae. These larvae penetrate human skin during activities in water such as washing clothes, bathing, swimming, planting rice and fishing which expose humans to infection by schistosome larvae. However, the deeper the water, the lower the risk of infection as the snail host prefers shallow water with plenty of vegetation. In the water, the cercariae penetrate human skin, transforming into larvae called schistosomulae. The schistosomulae mature into worms in the blood supply of the liver, intestines, and bladder. These worms lay thousands of eggs that cause

damage as they work through tissues. The eggs, released into the water in urine or feaces, restart the cycle.

The eggs of S. mansoni and S. haematobium are equipped with a sharp spine to enable them to burrow out of the blood vessels and penetrate into other tissues on their migration out of the host. While most eggs find their way out of the host, many become trapped in tissue and die before completing their journey. It is these trapped eggs which eventually lead to tissue damage and cause problems to the human host. S. mansoni eggs tend to lodge in the liver while S.haematobium eggs become trapped in the bladder wall. The heavier the worm infection, the greater the number of eggs which remain stuck. The body defenses of the host produce an inflammatory reaction around each egg. Over time, the inflamed tissue hardens and blockages of blood and lymph vessels occur, leading in turn to complications for the host.

Different control measures have been used to interupt the life cycle of schistosomes. These include improved sanitation which reduces surface water contamination by urine or stool, construction of dams and supply of clean water which also reduces contact with water, killing of worms in the human host through chemotherapy and using mollucides for snail control (WHO, 1993). Schistosomiasis infection caused by any of the schistosome human species can be treated using a single dose of Praziquantel.

1.4.1. Review of mathematical models for schistosomiasis

Mathematical models have been used to provide a framework for understanding schistosomiasis transmission dynamics in the human and snail populations. The models have been developed for evaluating possible control strategies; limitations and uncertainties (Barbour, 1978), heterogeneities; snail dynamics; miracidia and cercaria dynamics and acquired immunity (Anderson and May, 1985; Woolhouse, 1991). The first mathematical model for schistosomiasis transmission was developed by George MacDonald in 1965 (Macdonald, 1965). The model has shown some potential for understanding the disease transmission and control although it was based on oversimplified biological assumptions. Latent period in snails has been incorporated into transmission models since 1976, (Bradley and May, 1978; Lee and Lewis, 1976; Nasell, 1976). The latent period is epidemiologically significant to snails since the life expectancy of snail is comparable to the length of latent period. Mathematical models that ignore latent period would predict an unrealistically high prevalence of shedding snails (Bradley and May, 1978; Barbour, 1978). Mathematical models exploring the effects of temperature on schistosomiasis transmission have been developed (McCreesh and Booth, 2014; Martens *et al.*,1995; Martens *et al.*, 1997; Mangal *et al.*, 2008; Zhou *et al.*, 2008; Mas-Coma *et al.*, 2009). While most incorporated projected increases in mean temperature, McCreesh developed a mathematical model of water temperature, snail population dynamics incorporating temperature dependent stages of the parasite and snail lifecycles (McCreesh and Booth, 2014). Some attempts have been made to develop

more realistic models incorporating both rainfall and temperature to capture the seasonal environmental factors in snail dynamics (Liang *et al.*, 2002; Woolhouse and Chandiwana, 1990). The models of Liang (Liang *et al.*, 2002) used temperature and rainfall to formulate the effective growth rate of snail population based on earlier work of Woolhouse and Chandiwana (Woolhouse and Chandiwana, 1990). These models from previous works laid a foundation for our work and shed light on direction of our research in modeling schistosomiasis transmission.

1.5. Mathematical background

In this thesis ordinary differential equations are used. This section therefore provides a synoptic discussion of these ordinary differential equations that are used in the formulation of the models in this work.

An ordinary differential equation system is a system of equations of the form

$$\frac{dx_1}{dt} = f_1(x_1, x_2, \ldots, x_n),$$

$$\frac{dx_2}{dt} = f_2(x_1, x_2, \ldots, x_n), \tag{1.1}$$

$$\ldots\ldots$$

$$\frac{dx_n}{dt} = f_n(x_1, x_2, \ldots, x_n),$$

which can be written more concisely in vector notation

$$\frac{d\mathbf{x}}{dt} = \mathbf{f}(\mathbf{x}), \tag{1.2}$$

where x and f are vectors with components x_i and f_i, respectively, and the functions f_i are assumed to be smooth enough so that through each point x_0 there passes a unique solution of equation (1.1). It is worth noting here that the x_is correspond to the states of the disease being modelled as shown in Table 1.1 and the system corresponds to various epidemic models shown in Table 1.2. In disease modelling the variables represent numbers of individuals, or fractions of the whole population, therefore they should be positive or zero for all times $t \geq 0$, and if this fails then the model should be discarded since it violates a basic aspect of the biological reality.

Let $\mathbb{R}^n$ be an n-dimensional space $(n \geq 1)$, and let Ω be a subset of $\mathbb{R}^n$. We say that Ω is positively invariant for (1.1) if, when $(x_1(0), x_2(0), \ldots, x_n(0))$ is in Ω, the solution starting with these initial values has the property that the trajectory $(x_1(t), x_2(t), \ldots, x_n(t))$ is in Ω for all $t \geq 0$,

$$\mathbb{R}^n_+ = \{(x_1, x_2, \ldots, x_n) : x_1 \geq 0, x_2 \geq 0, \ldots, x_n \geq 0\}.$$

Positive invariance of the non-negative orthant $\mathbb{R}^n_+$ for any given system (1.1) will be assured if no trajectory can leave $\mathbb{R}^n_+$ by crossing through one of its faces.

In the analysis of system (1.1), often the first step is to determine whether there are steady states or equilibria. An equilibrium is a constant vector $\bar{x}$ (that is, $x_i = \bar{x}_i, i = 1, \ldots, n$ are constant) that satisfies the equations (1.1). Since this

solution is constant, it may be found by solving the equations

$$f_1(\bar{x}_1, \ldots, \bar{x}_n) = 0,$$

$$\ldots \tag{1.3}$$

$$f_n(\bar{x}_1, \ldots, \bar{x}_n) = 0.$$

A set of values that satisfy (1.3) represents a system state such that if the system is in that state at some time t_1, it remains in that state for all $t \geq t_1$, in the absence of external disturbance. The effects that these disturbances have on an equilibrium are important, hence it is necessary to distinguish between stable and unstable equilibria. We now describe, the analysis of finding stability by restricting ourselves to the case $n = 2$, to keep the notation simple. For $n = 2$, equations (1.1) are

$$\frac{dx_1}{dt} = f_1(x_1, x_2),$$

$$\tag{1.4}$$

$$\frac{dx_2}{dt} = f_2(x_1, x_2).$$

If $(x_1(t), x_2(t))$ is a solution of this system for $t \geq 0$ such that $(x_1(0), x_2(0))$ is near an equilibrium $(\bar{x}_1, \bar{x}_2)$, we define

$$y_1(t) = x_1(t) - \bar{x}_1, \quad y_2(t) = x_2(t) - \bar{x}_2. \tag{1.5}$$

Then

$$\frac{dy_1(t)}{dt} = f_1(\bar{x}_1 + y_1(t), \bar{x}_2 + y_2),$$

$$\frac{dy_2(t)}{dt} = f_2(\bar{x}_1 + y_1(t), \bar{x}_2 + y_2). \tag{1.6}$$

Assuming that the functions f_1 and f_2 are sufficiently differentiable, the expressions (1.6) can be expanded in Taylor series. Since $y_1(t)$ and $y_2(t)$ are assumed to be small disturbances from the equilibrium, we drop terms of degree two or higher and consider linear parts of the equations. We note that since $(\bar{x}_1, \bar{x}_2)$ is an equilibrium state, $f_1(\bar{x}_1, \bar{x}_2) = f_2(\bar{x}_1, \bar{x}_2) = 0$. Therefore, the appropriate linear equations are obtained as

$$\frac{dy_1}{dt} = a_{11}y_1 + a_{12}y_2,$$

$$\frac{dy_2}{dt} = a_{21}y_1 + a_{22}y_2, \tag{1.7}$$

where $a_{11}, a_{12}, a_{21}, a_{22}$ are the partial derivatives of the f_i evaluated at $(\bar{x}_1, \bar{x}_2)$. System (1.7) can be in a more compact form as

$$\frac{d\mathbf{Y}}{dt} = J\mathbf{Y},$$

where $\mathbf{Y} = (y_1, y_2)^T$ and

$$J = \begin{pmatrix} \frac{\partial f_1}{x_1}(\bar{x}_1, \bar{x}_2) & \frac{\partial f_1}{x_2}(\bar{x}_1, \bar{x}_2) \\ \frac{\partial f_2}{x_1}(\bar{x}_1, \bar{x}_2) & \frac{\partial f_2}{x_2}(\bar{x}_1, \bar{x}_2) \end{pmatrix} = \begin{pmatrix} a_{11} & a_{12} \\ a_{21} & a_{22} \end{pmatrix} \tag{1.8}$$

is the Jacobian matrix of system (1.4) evaluated at $(\bar{x}_1, \bar{x}_2)$. System (1.7) is called the linearisation of (1.4) near $(\bar{x}_1, \bar{x}_2)$. Behaviour of solutions of (1.7) is determined by the eigenvalues of J, which are the roots λ of the equation

$$\det(J - \lambda I) = 0. \tag{1.9}$$

According to the Hartman-Grobman theorem, every solution of (1.7) has the property that $y_1(t) \to 0$ and $y_2(t) \to 0$ as $t \to +\infty$ if all the roots of (1.9) are negative or are complex with negative real parts. In this case, it can therefore be proved that any solution of (1.4) with initial value sufficiently close to $(\bar{x}_1, \bar{x}_2)$ will tend to $(\bar{x}_1, \bar{x}_2)$ as $t \to +\infty$. Then $(\bar{x}_1, \bar{x}_2)$ is said to be a locally asymptotically stable equilibrium of (1.4). If one or both eigenvalues are positive or have positive real parts, then most solutions of (1.7) become unboundedly large as $t \to +\infty$ and consequently most solutions of (1.4) do not remain near $(\bar{x}_1, \bar{x}_2)$, even if they start very close and in this case, $(\bar{x}_1, \bar{x}_2)$ is said to be unstable.

We now illustrate some of the basic mathematical concepts used in modelling by analysing a simple malaria model, which is a system of deterministic ordinary differential equations.

1.5.1.   A basic malaria transmission model

A basic model for malaria has four compartments for the human population namely the susceptibles $S_h(t)$, latently infected (exposed) $E_h(t)$, the infectious $I_h(t)$ individuals and the recovered $R_h(t)$. The mosquito population is subdivided into susceptibles $S_m(t)$, latently infected (exposed) $E_m(t)$ and the infectious $I_m(t)$. The total human population is given by $N_h(t) = S_h(t) + E_h(t) + I_h(t) + R_h(t)$ while the total

mosquito population is $N_m(t) = S_m(t) + E_m(t) + I_m(t)$. The basic model is given by

$$\frac{dS_h}{dt} = \Lambda_h - \lambda_h S_h - \mu_h S_h + \gamma_h R_h,$$

$$\frac{dE_h}{dt} = \lambda_h S_h - (\mu_h + k_h)E_h,$$

$$\frac{dI_h}{dt} = k_h E - (\mu_h + \delta_h + \eta)I_h,$$

$$\frac{dR_h}{dt} = \delta_h I_h - (\mu_h + \gamma_h)R_h \qquad (1.10)$$

$$\frac{dS_m}{dt} = \Lambda_m - \lambda_m S_m - \mu_m S_m,$$

$$\frac{dE_m}{dt} = \lambda_m S_m - (\mu_m + k_m)E_m,$$

$$\frac{dI_m}{dt} = k_m E - \mu_m I_m,$$

with $\lambda_h = \dfrac{ab_h I_m(t)}{N_m(t)}$, $\lambda_m = \dfrac{ab_m I_h(t)}{N_h(t)}$ where Λ_h and Λ_m are constant human and mosquito recruitment rates respectively; a is the mosquito biting rate and b_h or b_m is the proportion of bites by infectious mosquitoes on susceptible human or by a susceptible mosquito on an infectious human that produce infection. k_h / k_m is the rate at which the individual leaves the latently infected class by becoming infectious, δ_h is the disease induced death rate, μ_h is the natural death rate of humans while μ_m is the mortality rate of mosquitoes, η is the treatment rate of individuals who also gain partial immunity, γ_h is the rate of loss of immunity as individuals rejoin the susceptible class. We assumed that an individual becomes infected only through contacts with infectious individuals. The initial conditions of

model system (1.10) are given by

$$S_h(0) = S_{h0} \geq 0, \ E_h(0) = E_{h0} \geq 0, \ I_h(0) = I_{h0}, \ R_h(0) = R_{h0},$$
$$S_m(0) = S_{m0} \geq 0, \ E_m(0) = E_{m0} \geq 0, \ I_m(0) = I_{m0} \geq 0. \quad (1.11)$$

The equilibrium states of model system (1.10) can be calculated by setting

$$\frac{dS_h}{dt} = \frac{dE_h}{dt} = \frac{dI_h}{dt} = \frac{dR_h}{dt} = \frac{dS_m}{dt} = \frac{dE_m}{dt} = \frac{dI_m}{dt} = 0. \quad (1.12)$$

Solving (1.12) we get

$$\mathcal{E}^0 = \left(S_h^0, E_h^0, I_h^0, R_h^0, S_m^0, E_m^0, I_m^0 \right) = \left(\frac{\Lambda_h}{\mu_h}, 0, 0, 0, \frac{\Lambda_m}{\mu_m}, 0, 0 \right), \quad (1.13)$$

being the disease-free equilibrium which is defined as a situation in which there is

no infection in the population. We now determine an important threshold param-

eter in epidemic modelling known as the basic reproduction number. It is defined

as the number of new infections generated by a single infectious individual in a

completely susceptible population (Anderson and May, 1991) and mathematically

as the spectral radius of the next generation matrix (Diekman *et al.*, 1990; van den

Driessche and Watmough, 2002). For model system (1.10), the basic reproduction

number ($\mathcal{R}_0$) is defined as the number of secondary malaria cases (in mosquitoes

or humans) produced by one infectious individual (human or mosquito) in a to-

tally susceptible population. We now follow the method of van den Driessche and

Watmough (2002), in using the vector notation to rewrite the equations in which

infections appear in terms of the difference between f_j, the rate of appearance of

new infections in compartment j, and v_j, the rate of transfer into and out of compartment j by all other processes. Progression from S_T to E_T is considered to be new infection:

$$
\frac{d}{dt}
\begin{bmatrix}
E_h(t) \\
I_h(t) \\
E_m(t) \\
I_m(t)
\end{bmatrix}
= f - v =
\begin{bmatrix}
\lambda_h S_h \\
0 \\
\lambda_m S_m \\
0
\end{bmatrix}
-
\begin{bmatrix}
(\mu + k)E_h \\
(\mu_h + \delta_h + \eta)I_h - k_h E_h \\
(\mu_m + k_m)E_m \\
\mu_m I_m - k_m E_m
\end{bmatrix}.
\tag{1.14}
$$

The corresponding Jacobian matrices, $\mathcal{F}$ and $\mathcal{V}$, describes the linearisation of the system about the disease-free equilibrium,

$$
\mathcal{F} =
\begin{bmatrix}
0 & ab_h & 0 & 0 \\
0 & 0 & 0 & 0 \\
0 & 0 & 0 & ab_m \\
0 & 0 & 0 & 0
\end{bmatrix},
\quad
\mathcal{V} =
\begin{bmatrix}
\mu_h + k_h & 0 & 0 & 0 \\
-k_h & \mu_h + \delta_h + \eta_h & 0 & 0 \\
0 & 0 & \mu_m + k_m & 0 \\
0 & 0 & -k & \mu_m
\end{bmatrix},
\tag{1.15}
$$

and the basic reproduction number, $\mathcal{R}_0$ is given as the spectral radius of the dominant eigenvalue of $\mathcal{F}\mathcal{V}^{-1}$ (van den Driessche and Watmough, 2002):

$$
\mathcal{R}_0 = \rho(\mathcal{F}\mathcal{V}^{-1}) = \sqrt{\left(\frac{ab_m k_m}{\mu_m(k_m + \mu_m)}\right)\left(\frac{ab_h k_h}{(\eta + \delta_h + \mu_h)(\kappa_h + \mu_h)}\right)}.
\tag{1.16}
$$

Theorem 1.1. *The disease-free equilibrium is locally asymptotically stable whenever $\mathcal{R}_0 < 1$ and unstable otherwise.*

Theorem 1.1 can also be proven using the Jacobian matrix as follows. The Jacobian

matrix of model system (1.10) evaluated at disease free equilibrium is given by

$$
J(\mathcal{E}) = \begin{bmatrix}
-\mu_H & 0 & 0 & \gamma_h & 0 & 0 & -ab_h \\
0 & -(\kappa_h + \mu_h) & 0 & 0 & 0 & 0 & ab_h \\
0 & \kappa_h & -(\mu_h + \delta_h + \gamma_h) & 0 & 0 & 0 & 0 \\
0 & 0 & \eta & -(\gamma_h + \mu_h) & 0 & 0 & 0 \\
0 & 0 & -ab_m & 0 & -\mu_m & 0 & 0 \\
0 & 0 & ab_m & 0 & 0 & -(\kappa_m + \mu_m) & 0 \\
0 & 0 & 0 & 0 & 0 & \kappa_m & -\mu_m
\end{bmatrix}.
$$

$$(1.17)$$

Finding the eigenvalues of the Jacobian matrix at $\mathcal{E}^0$, we set $\det[J(\mathcal{E}^0 - \lambda] = 0$. The eigenvalues of $J(\mathcal{E}^0)$ are negative whenever $(-1)^3 \det[J(\mathcal{E}^0)] > 0$ and $\text{trace}[J(\mathcal{E}^0)] < 0$.

From (1.17), we have

$$
\text{trace}[J(\mathcal{E}^0)] = -(4\mu_h + 3\mu_m + \kappa_h + \delta_h + 2\gamma_h + \kappa_m) < 0,
$$

$$
\det[J(\mathcal{E}^0)] = -\mu_h \mu_m (\gamma_h + \mu_h)[-(a^2 b_h b_m \kappa_h \kappa_m) + \mu_m(\eta + \delta_h + \mu_h)(\kappa_h + \mu_h)(\kappa_m + \mu_m)].
$$

$$(1.18)$$

Thus $(-1)^3 \det[J(\mathcal{E}^0] > 0$ whenever,

$$
\mathcal{R}_0 = \frac{ab_m k_m}{\mu_m(k_m + \mu_m)} \frac{ab_h k_h}{(\eta + \delta_h + \mu_h)(\kappa_h + \mu_h)} < 1 \tag{1.19}
$$

Thus all the eigenvalues of $\det[J(\mathcal{E}^0 - \lambda] = 0$ have negative real parts whenever $\mathcal{R}_0 < 1$. This implies that the disease-free equilibrium point $\mathcal{E}^0$ is locally asymptotically stable whenever $\mathcal{R}_0 < 1$.

Numerical simulations and mapping

Numerical simulations were done with the ODE solver of Matlab, a numerical mathematical software package. Matlab is also used to compute the partial rank correlation coefficient, (PRCC) for sensitivity analysis. The PRCC is a very efficient tool for identifying the most important parameters on the output variable in this study it is the reproduction number. The PRCC have a sign ($+$ or $-$) indicating the direction of change in the reproduction number if there is an increase or decrease in the input parameter.

Geographic Information System (GIS) software (ArcGIS 10.1) was used to produce maps of the distribution of malaria and schistosomiasis in terms of the reproduction number. Data on mean annual temperature and total annual precipitation for the baseline climate (i.e, average values for the period 1950 to 2000) were downloaded from the worldclim database as raster grids with a spatial resolution of 30 arc-seconds (approximately 1 km at the equator) (World Climate Database, 2014). For the future climate, we used temperature and precipitation projections of the HadCM3 and CSIROMK3 general circulation models (GCM) based on the A2a emission scenario. Data for the future climate (average values for the 2020-2039, hereafter 2040) were downloaded from the Inter-governmental panel on climate change (IPCC) database in raster format at the same 30 arc-seconds spatial resolution (IPCC Database, 2014).

1.6.   Structure of the thesis

In Chapter 2, a malaria model incorporating the juvenile mosquito population is considered. The model is used to determine the effect of temperature on the transmission dynamics of malaria. In Chapter 3, the effects of both rainfall and temperature is investigated on the transmission of malaria. In this chapter, the future dynamics of malaria transmission are considered in Africa. In Chapter 4, a schstosomiasis transmission model is presented. The model is used to assess the effects of both rainfall and temperature on schistosomiasis transmission. We present in Chapter 5, a model for malaria and schistosomiasis coinfection. Finally we present the conclusion and possible extensions to our work in Chapter 6. Due to the complexity of the models involved, global stability analysis of the equilibrium points was not considered. Parts of Chapters 2, 3 and 4 were published as follows

1. Ngarakana-Gwasira ET, Bhunu CP & Mashonjowa E, (2014). Assessing the impact of temperature on malaria transmission dynamics. *Afrika Matematika*, 25:1095-1112.

2. Ngarakana-Gwasira ET, Bhunu CP, Masocha M, Mashonjowa E, (2016). Transmission dynamics of schistosomiasis in Zimbabwe: A mathematical and GIS Approach. *Commun Nonlinear Sci Numer Simul*, 35:137-147.

3. Ngarakana-Gwasira ET, Bhunu CP, Masocha M, Mashonjowa E, (2016). Impact of climate change on malaria transmission in Africa. *Malaria Research and Treatment* http://dx.doi.org/10.1155/2016/7104291

Chapter 2

Assessing the impact of temperature on malaria transmission dynamics

2.1. Introduction

Malaria is a major cause of morbidity and mortality, with an estimated 216 million cases worldwide and at least 655 000 deaths in 2011 (WHO, 2011). Understanding the role of temperature in malaria transmission is of particular importance in light of climate change. The global mean temperature has increased by 0.7^0C during the past 100 years and is predicted to increase by an additional $1.1 - 6.4^0C$ during the twenty-first century (IPCC, 2007). This additional warming is likely to affect malaria transmission because temperature changes can alter vector development

rates, shift their geographical distribution and alter transmission dynamics.

Temperature is known to play a major role in the life cycle of the malaria vector. The development of the three aquatic stages and their emergence to adulthood are strongly dependent on temperature. It takes one, three and ten days for eggs of some mosquitoes to hatch at temperatures of $30^0C, \; 20^0C$ and 10^0C, respectively and water temperature regulates the speed of mosquito breeding (Jia Li, 2011). The development of the parasite within the mosquito (sporogonic cycle) depends on temperature. It takes about nine to ten days at temperatures of 28^0C, but stops at temperatures below 16^0C (Alemu $et \; al.$, 2011). The minimum temperature for parasite development of P. falciparum approximates 18^0C and the daily survival of the vector is dependent on temperature. At temperatures between 16^0C and 36^0C, the daily survival is about 90% (Alemu $et \; al.$, 2011).

Incorporating climate effects into models of disease dynamics is now very crucial as the evidence for climate impacts on disease transmission and potential vector distribution increases. Climate change is known to affect several parameters in the epidemiology of malaria and hence predicting climate change effects on disease transmission requires a framework that specifically incorporates the role of each climate sensitive parameter. Some models examining the contribution of climate change have been explored (Alonso $et \; al.$, 2010; Craig $et \; al.$, 1999; Hoshen and Morse, 2005; Martens $et \; al.$, 1997; Parham and Michael, 2010). However, this study incorporates the juvenile stage of the mosquito into malaria transmission

dynamics which is highly dependent on the environmental ambient conditions.

We begin by formulating the model, illustrating some of its basic properties, determining the equilibria and stability analysis performed in Section 2. The effect of temperature on the dynamics of malaria is presented and the numerical simulations in section 3. A discussion of the results is presented in Section 4.

2.2. Malaria transmission model

2.2.1. Model description

In developing a framework for understanding the impact of temperature on malaria dynamics, a deterministic transmission model is developed. The human population is subdivided into four classes: susceptible (S_H), exposed or incubating E_H, infectious (I_H) and recovered individuals who become partially immune (R_H). The rate of infection of a susceptible individual is dependent on the mosquito's biting rate $a(T)$ and the proportion of bites by infectious mosquitoes on susceptible humans that produce infection b_H. Blood meal taken by an infectious female anopheles mosquito on a susceptible human will cause sporozoites to be injected into the human bloodstream and will be carried to the liver.

Upon infection, individuals will then move to the exposed class E_H, where parasites in their bodies are still in the asexual stages. We assume that exposed individuals are not capable of transmitting the disease to susceptible mosquitoes as they do not have gametocytes. Exposed humans progress at a rate κ_H to the infectious class,

in which they now have gametocytes in their bloodstream making them capable of infecting the susceptible anopheles mosquitoes. Treated individuals recover at a rate α. A proportion p recovers with temporary immunity and the compliment $(1-p)$ recovers with no temporary immunity. Temporarily immune individuals lose immunity at a rate γ. Infected individuals who do not seek treatment die from infection at a rate η. The birth rate for humans is θ and individuals die naturally at a rate μ_H. Both human and mosquito infections take time to develop into an infectious state. Within host parasite dynamics are weather independent, but within vector, parasite dynamics, as well as the mosquito life cycle, are weather dependent.

The mosquito population is divided into the juvenile $(J_M(t))$ and adult population of which the adult population is subdivided into three classes: susceptible $(S_M(t))$, exposed $E_M(t)$ and infectious $(I_M(t))$. The juvenile stages describe the development of the aquatic stages which mature to become susceptible adult mosquitoes at a rate β_M. The rate of infecting a susceptible mosquito depends on the mosquitoes' biting rate a and the proportion of bites by susceptible mosquitoes on infected humans that produce infection b_M. Susceptible mosquitoes that feed on infectious humans will take gametocytes in blood meals, but as they do not have sporozoites in their salivary glands, they enter into the exposed class. After fertilisation, sporozoites are produced and migrate to the salivary glands ready to infect any susceptible host, the vector is then considered as infectious. Mosquitoes die at a rate μ_M which is independent of infection status. Infected mosquitoes are not harmed by the in-

fection, never clear their infection and the infective period of the mosquito ends with its death.

A coupled mosquito-human compartmental model of malaria dynamics is presented in Figure 2.1.
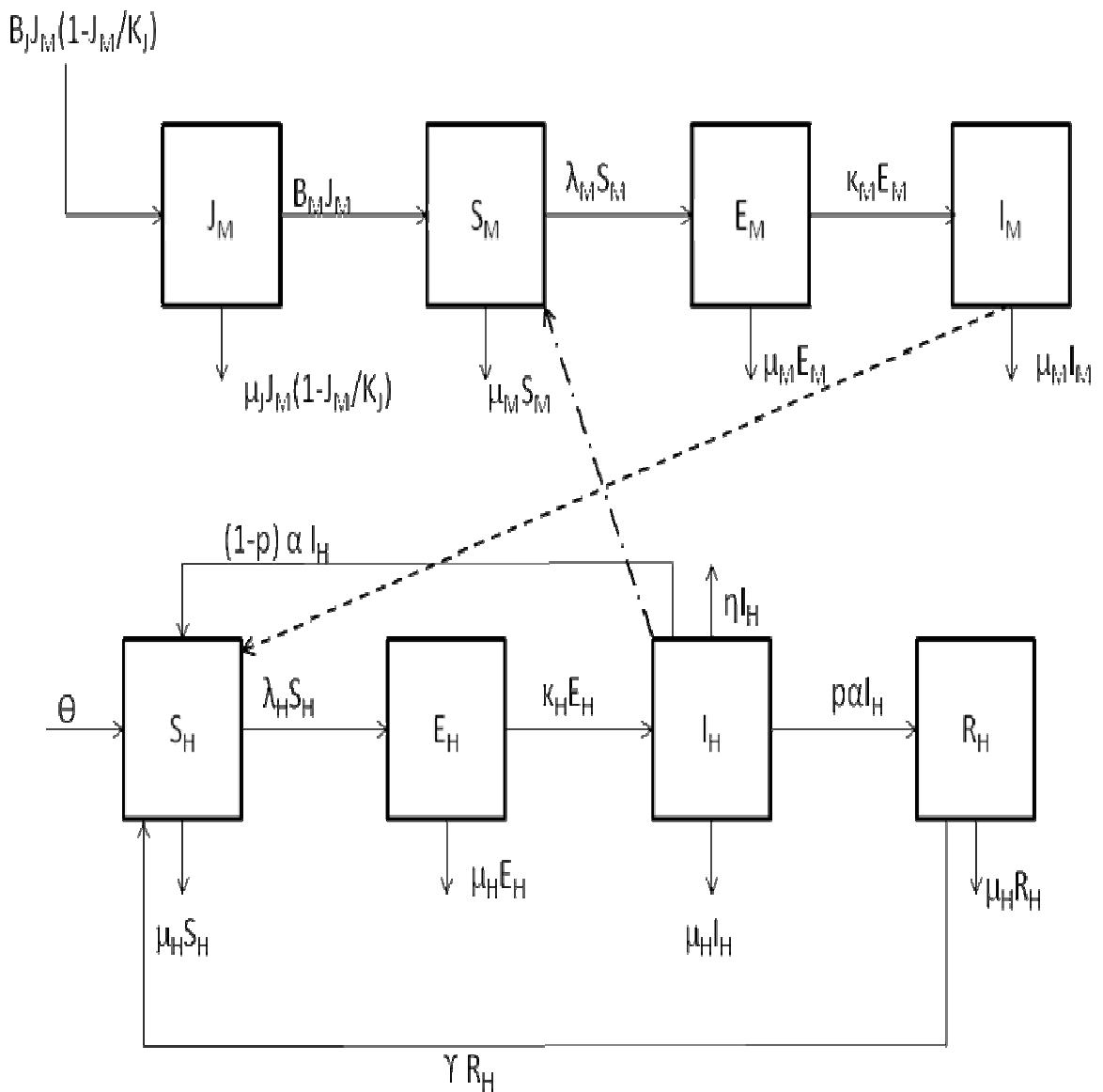
Figure 2.1: Mosquito-human model of malaria dynamics.

The following system of differential equations describe the model.

$$S'_H(t) = \theta - \lambda_H(T)S_H - \mu_H S_H + p\alpha I_H + \gamma R_H,$$

$$E'_H(t) = \lambda_H(T)S_H - (\kappa_H + \mu_h)E_H,$$

$$I'_H(t) = \kappa E_H - (\mu_H + \alpha + \eta)I_H,$$

$$R'_H(t) = (1 - p)\alpha I_H - (\gamma + \mu_H)R_H,$$

$$J'_M(t) = [\beta_J(T)N_M - \mu_J(T)\ \ J_M](1 - \tfrac{J_M}{K}) - \beta_M(T)J_M,$$ (2.1)

$$S'_M(t) = \beta_M(T)J_M - \lambda_M(T)S_M - \mu_M(T)S_M,$$

$$E'_M(t) = \lambda_M(T)S_M - (\kappa_M(T) + \mu_M(T))E_M,$$

$$I'_M(t) = \kappa_M(T)E_M - \mu_M(T)I_M,$$

where $\lambda_H = \dfrac{a(T)b_H I_M}{N_M}$ and $\lambda_M = \dfrac{a(T)b_M I_H}{N_H}$.

All parameters and state variables for model system (2.1) are assumed to be non-negative to be consistent with human and mosquito juvenile and adult populations.

2.2.2. Mathematical preliminaries

In this section, we study some basic results of the solutions of the system (2.1) which will be very useful to use into the proof of stability and persistence results.

Let $\mathbb{R}^n_+ = (0, \infty)$ denote the set of positive vectors $x = (x_1, x_2, ..., x_n)$ with $x_j > 0$ for

$j = 1, 2, ..., n$. We will use the following results in Appendix A of Thieme (2003):

Lemma 2.1. *Let $F : \mathbb{R}_+^n \to \mathbb{R}^n$*

$$F(x) = (F_1(x), F_2(x), ..., F_n(x)), \qquad x = (x_1, x_2, ..., x_n)$$

be continuous and have partial derivatives $\dfrac{\partial F_j}{\partial x_k}$ which exist and are continuous in $\mathbb{R}^n$ for all $j, k = 1, 2, ..., n$. Then F is locally Lipschitz continuous in $\mathbb{R}_+^n$.

Theorem 2.1. *Let $F : \mathbb{R}_+^n \to \mathbb{R}^n$ be locally Lipschitz continuous and for each $j = 1, 2, ..., n$ satisfy*

$$F_j(x) \geq 0 \quad whenever \quad x \in \mathbb{R}_+^n, x_j = 0.$$

Then for every $x_0 \in \mathbb{R}_+^n$, there exists a unique solution of $x' = F(x), x(0) = x_0$ with values in $\mathbb{R}_+^n$ which is defined in some interval $(0, b]$ with $b \in (0, \infty]$. If $b < \infty$, then

$$\sup_{0 \leq t \leq b} \sum_{j=1}^{n} x_j(t) = \infty.$$

Assumption 2.1. *$C(H), C(M) : \mathbb{R}_+^4 \to \mathbb{R}$ are continuously differentiable functions of (S_H, E_H, I_H, R_H) and (J_M, S_M, E_M, I_M) respectively.*

Theorem 2.2. *Assume Assumption 2.1 holds.*

For all $S_H^0, E_H^0, I_H^0, R_H^0, J_M^0, S_M^0, E_M^0, I_M^0 > 0$, there exists

$S_H, E_H, I_H, R_H, J_M, S_M, E_M, I_M : (0, \infty) \to (0, \infty)$ which solve (2.1) with initial conditions $S_H = S_H^0, E_H = E_H^0, I_H = I_H^0, R_H = R_H^0, J_M = J_M^0, S_M = S_M^0, E_M = E_M^0, I_M = I_M^0$.

Proof. We will apply Theorem 2.1. Define

$$
\begin{aligned}
F_1(x) &= \theta - \lambda_H S_H - \mu_H S_H + p\alpha I_H + \gamma R_h, \\
F_2(x) &= \lambda_H S_H - (\kappa_H + \mu_h)E_H, \\
F_3(x) &= \kappa E_H - (\mu_H + \alpha + \eta)I_H, \\
F_4(x) &= (1-p)\alpha I_H - (\gamma + \mu_H)R_H, \\
F_5(x) &= [\beta_J N_M - \mu_J J_M](1 - \tfrac{J_M}{K}) - \beta_M J_M, \\
F_6(x) &= \beta_M J_M - \lambda_M S_M - \mu_M S_M, \\
F_7(x) &= \lambda_M S_M - (\kappa_M + \mu_M)E_M, \\
F_8(x) &= \kappa_M E_M - \mu_M I_M.
\end{aligned}
\tag{2.2}
$$

By Assumption 2.1 and the properties of continuity over operations, we have the continuity of F_i for all $i = 1, 2, ..., 8$. Further

$$
\begin{aligned}
\frac{\partial F_1}{\partial x_1} &= -\frac{ab_H I_M}{N_M} - \mu_H, & \frac{\partial F_1}{\partial x_2} &= 0, & \frac{\partial F_1}{\partial x_3} &= p\alpha, & \frac{\partial F_1}{\partial x_4} &= \gamma, \\
\frac{\partial F_1}{\partial x_5} &= \frac{\partial F_1}{\partial x_6} = \frac{\partial F_1}{\partial x_7} = 0, & \frac{\partial F_1}{\partial x_8} &= \frac{-ab_H S_H}{N_M}.
\end{aligned}
\tag{2.3}
$$

These partial derivatives exist and are continuous, in the same way the other partial derivatives exist and are continuous. In consequence by Lemma 2.1, F is locally Lipschitz continuous.

Let $x_1 = S_H = 0$ and $x_2 = E_H > 0, \quad x_3 = I_H > 0, \quad x_4 = R_H > 0 \quad x_5 = J_M > 0,$

$x_6 = S_M > 0, \quad x_7 = E_M > 0, \quad x_8 = I_M > 0.$

Then $F_1(x) = \theta + p\alpha I_H + \gamma R_H > 0.$

Now let $x_2 = E_H = 0$ and $x_1 = S_H > 0, \quad x_3 = I_H > 0, \quad x_4 = R_H > 0, \quad x_5 = J_M > 0,$

$x_6 = S_M > 0, \quad x_7 = E_M > 0, \quad x_8 = I_M > 0.$ Then $F_2(x) = \dfrac{ab_H I_H}{N_H} > 0.$

Now let $x_3 = I_H = 0$ and $x_1 = S_H > 0$, $x_2 = E_H > 0$, $x_4 = R_H > 0$, $x_5 = J_M > 0$, ,

$x_6 = S_M > 0$, $x_7 = E_M > 0$, $x_8 = I_M > 0$. Then $F_3(x) = \kappa_H E_H > 0$.

Now let $x_4 = R_H = 0$ and $x_1 = S_H > 0$, $x_2 = E_H > 0$, $x_3 = I_H > 0$, $x_5 = J_M > 0$,

$x_6 = S_M > 0$, $x_7 = E_M > 0$, $x_8 = I_M > 0$. Then $F_4(x) = (1-p)\alpha I_H > 0$.

Now let $x_5 = J_M = 0$ and $x_1 = S_H > 0$, $x_2 = E_H > 0$, $x_3 = I_H > 0$, $x_4 = R_H > 0$,

$x_6 = S_M > 0$, , $x_7 = E_M > 0$, $x_8 = I_M > 0$. Then $F_5(x) = \beta_J N_M > 0$.

Now let $x_6 = S_M = 0$ and $x_1 = S_H > 0$, $x_2 = E_H > 0$, $x_3 = I_H > 0$, $x_4 = R_H > 0$, ,

$x_5 = J_M > 0$, $x_7 = E_M > 0$, $x_8 = I_M > 0$. Then $F_6(x) = \beta_M J_M > 0$.

Now let $x_7 = E_M = 0$ and $x_1 = S_H > 0$, $x_2 = E_H > 0$, $x_3 = I_H > 0$, $x_4 = R_H > 0$,

$x_5 = J_M > 0$, $x_6 = S_M > 0$, $x_8 = I_M > 0$. Then $F_7(x) = \dfrac{ab_M I_H S_M}{N_H} > 0$.

Furthermore let $x_8 = I_M = 0$ and $x_1 = S_H > 0$, $x_2 = E_H > 0$, $x_3 = I_H > 0$, $x_4 = R_H > 0$,

$x_5 = J_M > 0$, $x_6 = S_M > 0$, $x_7 = E_M > 0$. Then $F_8(x) = \kappa_M E_M > 0$.

By Theorem 2.1, for every $x_0 = (S_H^0, E_H^0, I_H^0, R_H^0, J_M^0, S_M^0, E_M^0, I_M^0) \in \mathbb{R}_+^4 \times \mathbb{R}_+^1 \times \mathbb{R}_+^3$,

there exists a unique solution of $x' = F(x)$, $x(0) = x_0$ with values in $\mathbb{R}_+^4 \times \mathbb{R}_+^1 \times \mathbb{R}_+^3$

which is defined in some interval $(0; b]$ with $b \in (0, \infty]$. If $b < \infty$, then

$$\sup_{0 \le t \le b} (S_H(t), E_H(t), I_H(t), R_H(t), J_M(t), S_M(t), E_M(t), I_M(t)) = \infty.$$

Suppose that $b < \infty$ and set $N_H(t) = S_H(t) + E_H(t) + I_H(t) + R_H(t)$, $N_M(t) = S_M(t) +$

$E_M(t) + I_M(t)$. Then

$$N'_H = \theta - \mu_H N_H - \eta I_H \leq \theta - \mu_H N_H.$$

Using the Gronwell inequality,

$$0 \leq N_H \leq \frac{\theta}{\mu_H} + N(0)e^{-\mu_H t},$$

where $N(0)$ represents the initial total human population. As $t \to \infty$,

$$0 \leq N_H \leq \frac{\theta}{\mu_H},$$

so $N(t)$ is bounded, a contradiction to Theorem 2.1. As a result, $b = \infty$, implying that solutions of model system (2.1) are positive and are defined on $(0, \infty)$. □

Lemma 2.2. *The model system (2.1) has solutions which are contained in the feasible region* $\Omega = \Omega_H \times \Omega_M \times \Omega_J$.

Proof. Let $(S_H, E_H, I_H, R_H) \in \mathbb{R}^4_+$, $\quad J_M \in \mathbb{R}^1_+$, $\quad (S_M, E_M, I_M) \in \mathbb{R}^3_+$ be any solution of the system with non-negative initial conditions.

Since

$$\frac{dN_H}{dt} \leq \theta - \mu_H N_H, \tag{2.4}$$

and using Birkhoff and Rota (1989) theorem on differential inequality, we have

$$0 \leq N_H \leq \frac{\theta}{\mu_H}.$$

Therefore in system (2.1), all feasible solutions of the human population only are

in the region

$$\Omega_H = \{(S_H, E_H, I_H, R_H) \in \mathbb{R}^4_+ : N_H \leq \frac{\theta}{\mu_H}\}. \tag{2.5}$$

$$\frac{dN_M}{dt} = \beta_M J_M - \mu_M N_M \geq 0. \tag{2.6}$$

$$N_M \leq \frac{\beta_M J_M}{\mu_M}.$$

$$\frac{dJ_M}{dt} = [\beta_J N_M - \mu_J J_M](1 - \frac{J_M}{K}) - \beta_M J_M$$

$$\leq \frac{J_M}{\mu_M}[(\beta_J \beta_M - \mu_J \mu_M)(1 - \frac{J_M}{K}) - \beta_M \mu_M]$$

$$0 \leq (\beta_J \beta_M - \mu_J \mu_M - \beta_M \mu_M) + \frac{J_M}{K}(\mu_J \mu_M - \beta_J \beta_M)$$

$$\frac{J_M}{K}(-\mu_J \mu_M + \beta_J \beta_M) \leq \beta_J \beta_M - \mu_J \mu_M - \beta_M \mu_M \tag{2.7}$$

$$J_M \leq \frac{K(\beta_J \beta_M - \mu_J \mu_M - \beta_M \mu_M)}{\beta_J \beta_M - \mu_J \mu_M}$$

$$N_M \leq \frac{\beta_M K(\beta_J \beta_M - \mu_J \mu_M - \beta_M \mu_M)}{\mu_M(\beta_J \beta_M - \mu_J \mu_M)}.$$

Similarly, the feasible solutions of the juvenile and adult mosquito population only

are in the region

$$\Omega_J = \{J_M \in \mathbb{R}^1_+ : J_M \leq \frac{K(\beta_J \beta_M - \mu_J \mu_M - \beta_M \mu_M)}{\beta_J \beta_M - \mu_J \mu_M}\}$$

$$\Omega_M = \{(S_M, E_M, I_M) \in \mathbb{R}^3_+ : N_M \leq \frac{\beta_M K(\beta_J \beta_M - \mu_J \mu_M - \beta_M \mu_M)}{\mu_M(\beta_J \beta_M - \mu_J \mu_M)}\}. \tag{2.8}$$

Thus all feasible solutions of model system (2.1) are positive and eventually enter

the invariant attracting region

$$\Omega = \Big\{ (S_H, E_H, I_H, R_H) \in \mathbb{R}^4_+, \quad J_M \in \mathbb{R}^1_+, \quad (S_M, E_M, I_M) \in \mathbb{R}^3_+ :$$

$$S_H, E_H, I_H, R_H, J_M, S_M, E_M, I_M \geq 0;$$

$$N_H \leq \frac{\theta}{\mu_H}; \quad J_M \leq \frac{K(\beta_J \beta_M - \mu_J \mu_M - \beta_M \mu_M)}{\beta_J \beta_M - \mu_J \mu_M}, \quad N_M \leq \frac{\beta_M K(\beta_J \beta_M - \mu_J \mu_M - \beta_M \mu_M)}{\mu_M(\beta_J \beta_M - \mu_J \mu_M))} \Big\}$$

which is a positively invariant set under the flow induced by model (2.1). Hence system (2.1) is epidemiologically meaningful and mathematically well-posed in the domain Ω. Therefore in this domain, it is sufficient to consider the dynamics of the flow generated by model (2.1). In addition, the usual existence, uniqueness and continuation of results hold for the system. $\qquad\square$

Predicting the effect of temperature on malaria dynamics requires a framework that specifically incorporates the role of each temperature sensitive parameter. The functional forms of temperature dependent parameters are presented in Table 2.1.

Table 2.1: Parameters of the basic malaria model in equation (2.1)

Description	Symbol	Value	Source
Mosquito biting rate	$a(T)$	$0.000203T(T-11.7)\sqrt{42.3-T}$	a^*
Birth rate of juveniles	$\beta_J(T)$	$2.325a(T)$	b^*
Adult mosquito birth rate	$\beta_M(T)$	$\frac{\beta_J}{10}$	b^*
Juvenille mosquito death rate	$\mu_J(T)$	$0.0025T^2 - 0.094T + 1.0257$	b^*
adult mosquito death rate	$\mu_M(T)$	$-\ln\rho(T)$	c^*
	$\rho(T)$	$e^{\frac{-1}{-0.03T^2+1.31T-4.4}}$	c^*
Progression rate of mosquitoes	κ_M	$\frac{T-T_{min}}{DD}$	d^*
Recruitment rate of humans	θ	0.028	e^*
Proportion of bites by infectious mosquitoes on susceptible humans that produce infection	b_H	0.09	f^*
proportion of bites by susceptible mosquitoes on infected humans that produce infection	b_M	0.04	f^*
per capita natural death rate for humans	μ_H	0.00004	e^*
Progression rate of humans from the exposed state to infectious	κ_H	$1/14$	e^*
Recovery rate of humans	α	0.005	e^*
Per capita disease induced death rate	η	0.0004	e^*
Per capita rate of loss of immunity	γ	$\frac{1}{20*365}$	g^*
carrying capacity of larvae	K	1000000	Est
Proportion of humans recoverig with temporary immunity	p	0.25	Est

a^* denotes parameters adapted from Paaijmans *et al.* (2013), b^* from Rubel *et al.*

(2008), c^* from Martens *et al* (1995), d^* from McDonald (1957), e^* from Chiyaka *et al.* (2007), f^* from Parham and Michael (2010) and g^* from Blayneh *et al* (2009).

2.2.3. Disease-free equilibrium and stability analysis

The disease-free equilibrium of model (2.1) is given by,

$$
\mathcal{E}_0 = (S_H^0, E_H^0, I_H^0, R_H^0, J_M^0, S_M^0, E_M^0, I_M^0)
$$

$$
= \left(\frac{\theta}{\mu_H}, 0, 0, 0, \frac{K(\beta_J\beta_M - \mu_J\mu_M - \beta_M\mu_M)}{\beta_J\beta_M - \mu_J\mu_M}, \frac{K\beta_M(\beta_J\beta_M - \mu_J\mu_M - \beta_M\mu_M)}{\mu_M(\beta_J\beta_M - \mu_J\mu_M)}, 0, 0 \right).
$$

$$(2.9)$$

The next generation operator approach as described by Diekmann (1990) is used to define the basic reproductive number, $\mathcal{R}_m$, as the number of new infections (in mosquitoes or humans) from one infectious individual (human or mosquito) over the duration of the infectious period, given that all other members of the population are susceptible (Diekmann *et al.*, 1990).

$$
\mathcal{R}_m = \sqrt{\left(\frac{a(T)b_H\kappa_H}{\mu_M(T)(\kappa_M(T) + \mu_M(T))} \right)\left(\frac{a(T)b_M\kappa_M(T)}{(\kappa_H + \mu_H)(\mu_H + \alpha + \eta)} \right)}
\qquad (2.10)
$$

Local stability of the disease-free equilibrium $\mathcal{E}_0$

The local stability of the disease free equilibrium can be discussed by examining the linearised form of the system (2.1) at the steady state $\mathcal{E}_0$.

Theorem 2.3. *The disease-free equilibrium $\mathcal{E}_0$ is locally asymptotically stable whenever $\mathcal{R}_m < 1$, and unstable otherwise.*

Proof. The Jacobian matrix of the model (2.1) evaluated at the disease free equilibrium point is given by

$$
\begin{bmatrix}
-\mu_H & 0 & \nu & \gamma & 0 & 0 & 0 & -ab_H Q_3 \\
0 & -(\kappa_H + \mu_H) & 0 & 0 & 0 & 0 & 0 & ab_H Q_3 \\
0 & \kappa_H & -Q_1 & 0 & 0 & 0 & 0 & 0 \\
0 & 0 & \alpha & -(\gamma + \mu_H) & 0 & 0 & 0 & 0 \\
0 & 0 & 0 & 0 & Q_2 & 0 & 0 & 0 \\
0 & 0 & -ab_M Q_4 & 0 & \beta_M & -\mu_M & 0 & 0 \\
0 & 0 & ab_M Q_4 & 0 & 0 & 0 & -(\kappa_M + \mu_M) & 0 \\
0 & 0 & 0 & 0 & 0 & 0 & \kappa_M & -\mu_M
\end{bmatrix},
$$

where

$$
Q_1 = (\nu + \mu_H + \alpha + \eta)
$$

$$
Q_2 = -(\mu_J + \beta_M) + 2\mu_J \frac{(\beta_J \beta_M - \mu_J \mu_M - \beta_M \mu_M)}{\beta_J \beta_M - \mu_J \mu_M}
$$

$$
Q_3 = \frac{\theta}{\mu_H} \frac{\mu_M (\beta_J \beta_M - \mu_J \mu_M)}{K \beta_M (\beta_J \beta_M - \mu_J \mu_M - \beta_M \mu_M)} \tag{2.11}
$$

$$
Q_4 = \frac{K \beta_M (\beta_J \beta_M - \mu_J \mu_M - \beta_M \mu_M)}{\mu_M (\beta_J \beta_M - \mu_J \mu_M)} \frac{\mu_H}{\theta} = \frac{1}{Q_3}.
$$

The first and the sixth columns have diagonal entries resulting in the diagonal entries being two of the eigenvalues of the Jacobian. Now excluding these columns

and the corresponding rows we calculate the remaining eigenvalues.

$$
\begin{bmatrix}
-(\kappa_H + \mu_H) & 0 & 0 & 0 & 0 & ab_H Q_3 \\
\kappa_H & -Q_1 & 0 & 0 & 0 & 0 \\
0 & \alpha & -(\gamma + \mu_H) & 0 & 0 & 0 \\
0 & 0 & 0 & Q_2 & 0 & 0 \\
0 & ab_M Q_4 & 0 & 0 & -(\kappa_M + \mu_M) & 0 \\
0 & 0 & 0 & 0 & \kappa_M & -\mu_M
\end{bmatrix}.
$$

Again the third and fourth columns have diagonal entries that result in other eigenvalues. Excluding these columns and the corresponding rows we calculate the remaining eigenvalues from

$$
\begin{bmatrix}
-(\kappa_H + \mu_H) & 0 & 0 & ab_H Q_3 \\
\kappa_H & -Q_1 & 0 & 0 \\
0 & ab_M Q_4 & -(\kappa_M + \mu_M) & 0 \\
0 & 0 & \kappa_M & -\mu_M
\end{bmatrix}.
$$

Let $a_1 = \kappa_H + \mu_H$, $a_2 = 0$, $a_3 = 0$, $a_4 = ab_H$.

In the same manner,

$b_1 = \kappa_H$, $b_2 = \mu_H + \alpha + \eta$, $c_2 = ab_M$, $c_3 = \kappa_M + \mu_M$, $d_3 = \kappa_M$, $d_4 = \mu_M$.

The eigenvalues are solutions of the characteristic equation of the reduced matrix of dimension four which is given by

$$
(\kappa_H + \mu_H + \lambda)[(\mu_H + \alpha + \eta + \lambda)(\kappa_M + \mu_M + \lambda)(\mu_M + \lambda)] - ab_H(\kappa_H ab_M \kappa_M) = 0
$$

which is simplified to

$$\lambda^4 + A_3\lambda^3 + A_2\lambda^2 + A_1\lambda + A_0 = 0, \tag{2.12}$$

where

$$
\begin{aligned}
A_3 &= a_1 + b_2 + c_3 + d_4, \\
A_2 &= (a_1 + d4)(b_2 + c_3) + a_1 d_4 + b_2 c_3, \\
A_1 &= c_3 d_4 (b_2 + a_1) + a_1 b_2 (c_3 + d_4), \\
A_0 &= a_1 b_2 c_3 d_4 - a^2 b_H \kappa_H \kappa_M b_M.
\end{aligned}
\tag{2.13}
$$

The Routh-Huwirtz conditions are sufficient and necessary conditions on the coefficients of the polynomial (2.12). These conditions ensure that all roots of the polynomial given by (2.12) have negative real parts. For this polynomial, the Routh-Hurwitz conditions are $A_3 > 0, \quad A_2 > 0, \quad A_1 > 0, \quad A_0 > 0$ and

$$H_1 = A_3 > 0,$$

$$H_2 = \begin{vmatrix} A_3 & 1 \\ A_1 & A_2 \end{vmatrix} > 0,$$

$$H_3 = \begin{vmatrix} A_3 & 1 & 0 \\ A_1 & A_2 & A_3 \\ 0 & A_0 & A_1 \end{vmatrix} > 0,$$

$$H_4 = \begin{vmatrix} A_3 & 1 & 0 & 0 \\ A_1 & A_2 & A_3 & 1 \\ 0 & A_0 & A_1 & A_2 \\ 0 & 0 & 0 & A_0 \end{vmatrix} > 0,$$

since all $A_i > 0, \quad i = 1, 2, 3.$

Note that from $A_0 = a_1 b_2 c_3 d_4 - a^2 b_H \kappa_H \kappa_M b_M$ the reproduction number reduces to

$$\mathcal{R}_m^2 = \frac{a^2 b_H \kappa_H \kappa_M b_M}{a_1 b_2 c_3 d_4}.$$

Hence if $\mathcal{R}_m < 0, \quad A_0 > 0$.

Clearly, $H_1 = A_3 > 0$.

$$
\begin{aligned}
H_2 &= A_3 A_2 - A_1 \\
&= (b_2 + c_3)(b_2 + d_4)(c_3 + d_4) + a_1^2(b_2 + c_3 + d_4) + a_1(b_2 + c_3 + d_4)^2
\end{aligned}
\tag{2.14}
$$

which is positive.

$$
\begin{aligned}
H_3 &= A_1(A_3 A_2 - A_1) - A_0 A_3^2 \\
&= a_1^3(b_2 + c_3)(b_2 + d_4)(c_3 + d_4) + b_2 c_3(b_2 + c_3)d_4(b_2 + d_4)(c_3 + d_4) + a_4 b_1 c_2 d_3(b_2 + c_3 + d_4)^2 \\
&\quad + a_1^2(a_4 b_1 c_2 d_3 + b_2^3(c_3 + d_4) + 2b_2^2(c_3 + d_4)^2 + c_3 d_4(c_3 + d_4)^2 + b_2(c_3^3 + 4c_3^2 d_4 + 4c_3 d_4^2 + d_4^3)) \\
&\quad + a_1(b_2^3(c_3 + d_4)^2 + (c_3 + d_4)(2a_4 b_1 c_2 d_3 + c_3^2 d_4^2) + b_2^2(c_3^3 + 4c_3^2 d_4 + 4c_3 d_4^2 + d_4^3) \\
&\quad + 2b_2(a_4 b_1 c_2 d_3 + c_3 d_4(c_3 + d_4)^2)),
\end{aligned}
\tag{2.15}
$$

which is also positive.

It can be easily seen that $H_4 = A_0 H_3$.

Therefore, all eigenvalues of the Jacobian matrix have negative real parts when $\mathcal{R}_m < 1$. However, $\mathcal{R}_m > 0$ implies that $A_0 < 0$, and since all coefficients of the polynomial (2.12) are positive, not all roots of this polynomial can have negative real parts. This means that when $\mathcal{R}_m > 1$, the disease free equilibrium point is unstable. $\qquad\qquad\qquad\qquad\qquad\qquad\qquad\qquad\qquad\qquad\qquad\qquad\qquad\quad\square$

2.2.4. Endemic equilibria and stability analysis

The endemic equilibrium point E_1 is a steady-state solution where the disease persists in the population. The endemic equilibrium of model system (2.1) is given by

$$\mathcal{E}_1 = (S_H^*, E_H^*, I_H^*, R_H^*, S_M^*, E_M^*, I_M^*),$$

in terms of the forces of infection λ_H and λ_M, where

$$S_H^* = \frac{\theta(\gamma+\mu_H)(\kappa_H+\mu_H)(\mu_H+\alpha+\eta)}{\mu_H(\gamma+\mu_H)(\kappa_H+\mu_H)(\mu_H+\alpha+\eta)+\lambda_H[\mu_H(\gamma+\mu_H)(+\mu_H+\alpha+\eta)+\kappa_H(\gamma\eta+\mu_H(\mu_H+\alpha+\eta))]},$$

$$E_H^* = \frac{\theta\lambda_H(\gamma+\mu_H)(\mu_H+\alpha+\eta)}{\lambda_H[\mu_H(\gamma+\mu_H)(\mu_H+\alpha+\eta)+\kappa_H(\gamma\eta+\mu_H(\mu_H+\alpha+\eta))]+\mu_H(\gamma+\mu_H)(\kappa_H+\mu_H)(\mu_H+\alpha+\eta)},$$

$$I_H^* = \frac{\theta\kappa_H\lambda_H(\gamma+\mu_H)}{\lambda_H[\mu_H(\gamma+\mu_H)(\mu_H+)\alpha+\eta)+\kappa_H(\gamma\eta+\mu_H(\mu_H+)\alpha+\eta))]+\mu_H(\gamma+\mu_H)(\kappa_H+\mu_H)(\mu_H+\alpha+\eta)},$$

$$R_H^* = \frac{(1-p)\alpha\theta\kappa_H\lambda_H}{\lambda_H[\mu_H(\gamma+\mu_H)(\mu_H+\alpha+\eta)+\kappa_H(\gamma\eta+\mu_H(\mu_H+\alpha+\eta))]+\mu_H(\gamma+\mu_H)(\kappa_H+\mu_H)(\mu_H+\alpha+\eta)},$$

$$J_M^* = \frac{K\beta_M+N_M^*\beta_J+K\mu_J\pm\sqrt{(K\beta_M+N_M^*\beta_J+K\mu_J)^2-4KN_M^*\beta_J\mu_J}}{2\mu_J},$$

$$S_M^* = \frac{\beta_M[K\beta_M+N_M^*\beta_j+K\mu_J\pm\sqrt{(K\beta_M+N_M^*\beta_J+K\mu_J)^2-4KN_M^*\beta_J\mu_J}]}{2\mu_J(\lambda_M+\mu_M)},$$

$$E_M^* = \frac{\beta_M\lambda_M[K\beta_M+N_M^*\beta_j+K\mu_J\pm\sqrt{(K\beta_M+N_M^*\beta_J+K\mu_J)^2-4KN_M^*\beta_J\mu_J}]}{2\mu_J(\kappa_M+\mu_M)(\lambda_M+\mu_M)},$$

$$I_M^* = \frac{\beta_M\kappa_M\lambda_M[K\beta_M+N_M^*\beta_j+K\mu_J\pm\sqrt{(K\beta_M+N_M^*\beta_J+K\mu_J)^2-4KN_M^*\beta_J\mu_J}]}{2\mu_J\mu_M(\kappa_M+\mu_M)(\lambda_M+\mu_M)},$$

$$N_M^* = \frac{K\beta_M(\beta_J\beta_M-\beta_M\mu_M-\mu_J\mu_M)}{\mu_M(\beta_J\beta_M-\beta_M\mu_M)},$$

$$N_H^* = \frac{\theta[(\gamma+\mu_H)(\mu_H+\alpha+\eta)(\lambda_H+\mu_H)+\kappa_H\{\lambda_H((1-p)\alpha+\gamma+\mu_H)+(\gamma+\mu_H)(\mu_H+\alpha+\eta)\}]}{\mu_H(\gamma+\mu_H)(\mu_H+)\alpha+\eta)(\lambda_H+\mu_H)+\kappa_H[\mu_H(\gamma+\mu_H)(\mu_H+\alpha+\eta+\lambda_H(\gamma\eta+\mu_H(\mu_H+\alpha+\eta))]},$$

$$\lambda_M =$$

$$\frac{a\theta b_M \kappa_H \lambda_H \mu_M (\gamma+\mu_H)(\beta_J\beta_M-\mu_J\mu_M)}{K\beta_M[\mu_H(\gamma+\mu_H)(\mu_H+\alpha+\eta)(\lambda_H+\mu_H)+\kappa_H\{\mu_H(\gamma+\mu_H)(\mu_H+\alpha+\eta)+\lambda_H[\gamma\eta+\mu_H(\mu_H+\alpha+\eta)]\}](\beta_J\beta_M-(\beta_M+\mu_J)\mu_M)}$$

$$\lambda_H = \frac{ab_H\beta_M\kappa_M\lambda_M[\mu_H(\gamma+\mu_H)(\mu_H+\alpha+\eta)(\lambda_H+\mu_H)+\kappa_H[\mu_H(\gamma+\mu_H)(\mu_H+\alpha+\eta+\lambda_H(\gamma\eta+\mu_H(\mu_H+\alpha+\eta)))]A]}{2\theta[(\gamma+\mu_H)(\mu_H+\alpha+\eta)(\lambda_H+\mu_H)+\kappa_H\{\lambda_H((1-p)\alpha+\gamma+\mu_H)+(\gamma+\mu_H)(\mu_H+\alpha+\eta)\}]\mu_J\mu_M(\kappa_M+\mu_M)(\lambda_M+\mu_M)}$$

where

$$A = \frac{2K\mu_J(\beta_J\beta_M-(\beta_M+\mu_J)\mu_M)}{\beta_J\beta_M-\mu_J\mu_M}. \tag{2.16}$$

From expanding and simplifying the equation of λ_H, we obtain third order equation in λ_H as follows

$$\lambda_H(B_1\lambda_H^2 + B_2\lambda_H + B_3) = 0, \tag{2.17}$$

where

$B_1 = 2K\mu_J\mu_M[\kappa_H((1-p)\alpha+\gamma+\mu_H)+(\gamma+\mu_H)((1-p)\alpha+\eta+p\alpha+\mu_H)](\kappa_M+\mu_M)\{\beta_J\beta_M-$

$(\beta_M+\mu_J)\mu_M\}[a\theta b_M\kappa_H(\gamma+\mu_H)(\beta_J\beta_M-\mu_J\mu_M)+\kappa\beta_M(\beta_J\beta_M-(\beta_M+\mu_J)\mu_M)(\mu_H(\gamma+$

$\mu_H)(\eta+\alpha+\mu_H)+\kappa_H(\gamma\eta+\mu_H((1-p)\alpha+\eta+\gamma+\mu_H)))],$

$B_2 = 2K\mu_J(\beta_J\beta_M-(\beta_M+\mu_J)\mu_M)\Big[a\theta b_M\kappa_H(\gamma+\mu_H)(\eta+\alpha+\mu_H)(\kappa_H+\mu_H)\mu_M(\kappa_M+$

$\mu_M)(\beta_J\beta_M-\mu_J\mu_M)+a^2Kb_Hb_M\beta_M\kappa_H\kappa_M(-\mu_H(\gamma+\mu_H)(\eta+\alpha+\mu_H)-\kappa_H(\gamma\eta+\mu_H((1-$

$p)\alpha+\gamma+\eta+\mu_H)))(\beta_J\beta_M-(\beta_M+\mu_J)\mu_M)+K\beta_M(\eta+\alpha+\mu_H)\mu_M(\kappa_M+\mu_M)(\beta_J\beta_M-$

$(\beta_M+\mu_J)\mu_M)\{\kappa_H^2\mu_H((1-p)\alpha+\gamma+\mu_H)+\kappa_H\mu_H^2(\alpha+\gamma+\mu_H)+2\kappa_H\mu_H(\gamma+\mu_H)(\eta+\alpha+$

$\mu_H) + 2\mu_H^2(\gamma + \mu_H)(\eta + \alpha + \mu_H) + 2K\kappa_H^3(\gamma\eta + ((1-p)\alpha + \gamma + \eta + \mu_H)\mu_H)^2\mu_J\mu_M(\kappa_M +$

$\mu_M)(\beta_J\beta_M - (\beta_M + \mu_J)\mu_M)\}\Big]$

$B_3 = 2K^2\beta_M\mu_H\mu_J(\gamma+\mu_H)^2(\eta+\alpha+\mu_H)(\kappa_H+\mu_H)(\beta_J\beta_M-(\beta_M+\mu_J)\mu_M)^2[-a^2b_Hb_M\kappa_H\kappa_M+$

$\mu_M(\kappa_M + \mu_M)(\kappa_H + \mu_H)(\eta + \alpha + \mu_H)]$

which reduces to

$$B_3 = C(1 - \mathcal{R}_m^2)$$

where $C = 2K^2\beta_M\mu_H\mu_J(\gamma + \mu_H)^2(\eta + \alpha + \mu_H)(\kappa_H + \mu_H)(\beta_J\beta_M - (\beta_M + \mu_J)\mu_M)^2$

In equation (2.17), $\lambda_H = 0$ corresponds to the disease free equilibrium and

$$f(\lambda_H^*) = \lambda_H(B_1\lambda_H^2 + B_2\lambda_H + B_3) = 0,$$

is associated with the endemic equilibria states. It is worth mentioning that B_1 and C are always positive, B_2 is either positive or negative and B_3 is either positive or negative depending on whether $1 >$ or $< R_m$. Solving for λ_H^* in $f(\lambda_H^*) = 0$. The roots of $f(\lambda_H^*) = 0$ are explored using Descartes rule of signs. The three possibilities are tabulated in Table 2.2.

Case	B_1	B_2	B_3	R_m	No of sign changes	Possible equilibria
Case 1	$+$	$-$	$+$	$R_m < 1$	2	2
Case 2	$+$	$-$	$-$	$R_m > 1$	1	1
Case 3	$+$	$+$	$-$	$R_m > 1$	1	1

Table 2.2: Number of possible roots of $f(\lambda_H^*) = 0$ for $R_m > 1$ and $R_m < 1$.

The analysis of the results in Table 2.2 gives the following lemma.

Lemma 2.3. *The endemic equilibrium E^* exists and is unique whenever $R_m > 1$,*

and there exists a backward bifurcation when $R_m < 1$.

2.3. Results

2.3.1. Effect of temperature dependant parameters on the reproduction number

The effect of climate change is investigated by examining the effect of climate components on the disease reproduction number. Evidence suggests that the mosquito biting rate (a), mosquito mortality rate (μ_M) and the parasite development rate κ_M are all sensitive to changes in temperature. The change in $\mathcal{R}_m$, with a change in mean temperature can be determined by the sum of the effects of temperature on each temperature sensitive component of $\mathcal{R}_m$ coupled with the corresponding change to $\mathcal{R}_m$.

$$\frac{d\mathcal{R}_m}{dT} = \frac{da}{dT}\frac{d\mathcal{R}_m}{da} + \frac{d\kappa_M}{dT}\frac{d\mathcal{R}_m}{d\kappa_M} + \frac{d\mu_M}{dT}\frac{d\mathcal{R}_m}{d\mu_M} \tag{2.18}$$

The mathematical relationships between $\mathcal{R}_m$ and the temperature-sensitive biological parameters are as follows:

$$\frac{d\mathcal{R}_m}{da} = \frac{\mathcal{R}_m}{a}$$

$$\frac{d\mathcal{R}_m}{d\kappa_M} = \frac{\mathcal{R}_m}{2}\left(1 - \frac{1}{\kappa_M + \mu_M}\right) \tag{2.19}$$

$$\frac{d\mathcal{R}_m}{d\mu_M} = -\frac{\mathcal{R}_m}{2}\left[\frac{2\mu_M + \kappa_M}{\mu_M(\kappa_M + \mu_M)}\right]$$

The system of equations in (2.19) shows that an increase in a, and κ_M will have a positive effect on $\mathcal{R}_m$, while increasing μ_M will have a negative effect. The quanti-

tative effect of temperature change on $\mathcal{R}_m$ will depend on both the individual relationships of these parameters with temperature and their combined impact within the $\mathcal{R}_m$ equation.

1. Mosquito biting rate $a(T)$

   The biting rate represents the frequency of feeding activity by mosquitoes per day.

   $$a(T) = 0.000203T(T - 11.7)\sqrt{42.3 - T}.$$

   Hence

   $$\begin{aligned}
   \frac{da}{dT} &= \frac{0.000406(T - 10.7)(42.3 - T) - 0.000203T(T - 11.7)}{2\sqrt{42.3 - T}} \\
   \frac{da}{dT} &= \frac{-0.000609T^2 + 0.023891T - 0.18376}{2\sqrt{42.3 - T}}
   \end{aligned} \tag{2.20}$$

2. Mosquito mortality rate $\mu_M(T)$

   $\mu_M(T) = -\ln p(T)$, where $p(T) = e^{\frac{-1}{AT^2 + BT + C}}$ is the daily survival rate. Therefore

   $$\frac{d\mu_M}{dT} = \frac{-(2AT + B)}{(AT^2 + BT + C)^2} \tag{2.21}$$

3. Progression rate of mosquitoes to infectious class $\kappa_M = \frac{T - T_{min}}{DD}$ where DD is the total degree days for the parasite development, T is the mean temperature in degrees centigrade and $T_{\min}$ is the temperature at which parasite development ceases.

$DD = 111$ while T_{min} is 16 for plasmodium falciparum.

$$\frac{d\kappa_M}{dT} = \frac{1}{DD} \qquad\qquad (2.22)$$

Substituting equations (2.19, 2.20, 2.21, 2.22) into equation (2.18) we have

$$\frac{d\mathcal{R}_m}{dT} = \mathcal{R}_m\left[\frac{-0.000609T^2+0.023891T-0.18376}{2a\sqrt{42.3-T}} + \frac{2AT+B}{2(AT^2+BT+C)}\left(\frac{1}{\mu_M}+\frac{1}{(\kappa_M+\mu_M)}\right) + \frac{1}{2DD}\left(1-\frac{1}{(\kappa_M+\mu_M)}\right)\right]$$

Let $\dfrac{0.023891T}{2a\sqrt{42.3-T}} = G_1,$ $\qquad \dfrac{2AT+B}{2(AT^2+BT+C)}\left(\dfrac{1}{\mu_M}+\dfrac{1}{(\kappa_M+\mu_M)}\right) = G_2,$

$$\frac{1}{2DD} = G_3 \qquad \text{and} \quad \frac{0.000609T^2+0.18376}{2a\sqrt{42.3-T}} + \frac{1}{2DD(\kappa_M+\mu_M)} = G_4$$

Then

$$\frac{d\mathcal{R}_m}{dT} = \mathcal{R}_m(G_1 + G_2 + G_3 - G_4).$$

If $G_1 + G_2 + G_3 - G_4 < 0$ then $\frac{d\mathcal{R}_m}{dT} < 0$ and increase in temperature results in a decrease in $\mathcal{R}_m$, typically in regions which experience extremely high temperatures. If $G_1 + G_2 + G_3 - G_4 > 0$ then $\frac{d\mathcal{R}_m}{dT} > 0$ and $\mathcal{R}_m$ increases as temperature increases the epidemic also increases.

2.3.2.   Numerical Simulations

In Figure 2.2, the relationship between temperature and mosquito biting rate, parasite development rate, mosquito mortality rate, and malaria reproduction number respectively, are illustrated. The mosquito biting rate is low at lower temperatures but increases to a maximum as temperature increases. Mosquito mortality is high at low temperatures, decreases to a minimum between $20 - 25^0 C$ before increasing at temperatures beyond $25^0 C$. The temperature range where $\mathcal{R}_m > 1$ for malaria is $22.34 - 38.6^0 C$. A maximum $\mathcal{R}_m$ of **3.65** occurs at $31.5^0 C$.
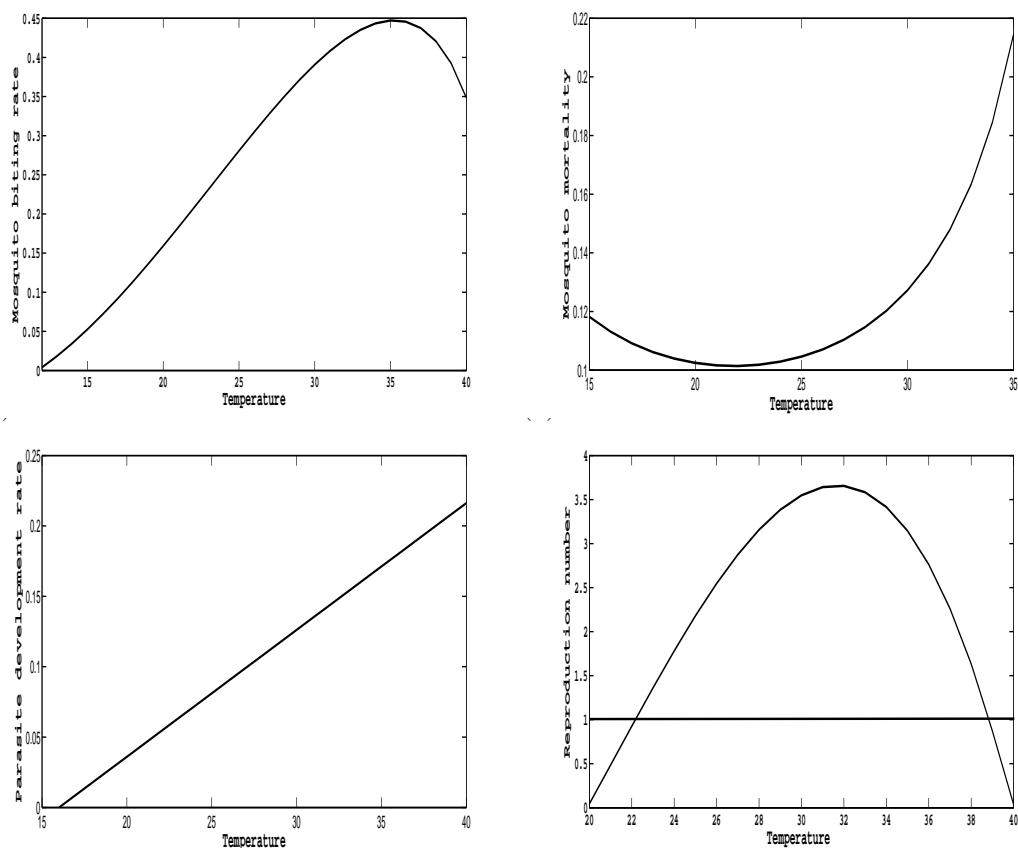

Figure 2.2: Simulation of (a) Mosquito biting rate, (b) Mosquito mortality rate, (c) Progression rate of mosquitoes, (d) $\mathcal{R}_m$ versus temperature

In Figure 2.3, we carry out numerical simulations using a fourth order Runge-Kutta scheme in Matlab with the aim of verifying some of the analytical results on the stability of the system (2.1). The parameter values that we use for numerical simulations are in Table 2.1. The following initial values are used for the numerical simulations.

$$S_H = 1000, \quad E_H = 300, \quad I_H = 200, \quad R_H = 0, \quad J_M = 30000, \quad S_M = 10000,$$

$$E_M = 1000, \quad I_M = 1000.$$

The effects of varying temperature on the infected human and mosquito populations is observed. The simulations reveal both the endemic equilibrium and the disease free equilibrium points as temperature is varied from $20 - 40^0 C$. In Figure 2.3, if temperatures are to average $20^0 C$, the infected human and mosquito population declines to asymptotically low levels as mosquito survives at above $22^0 C$ (McMichael *etal*, 1996). Furthermore, infected mosquito and human populations tend to decline to asymptotically low levels faster when temperatures average $40^0 C$ as compared to temperatures averaging $20^0 C$. This may be due to increased death rate of juvenile mosquitoes as ponds dry up quickly because of high evaporation rates at high temperatures and mosquitoes can not survive above $40^0 C$ (Shetty, 2009). Infected humans tend to be more at average temperatures of $35^0 C$ as compared to when $T = 30^0 C$ (the range of optimal temperature for malaria transmission). This is possibly due to increased mosquito biting rate and parasite development rate at higher temperatures.
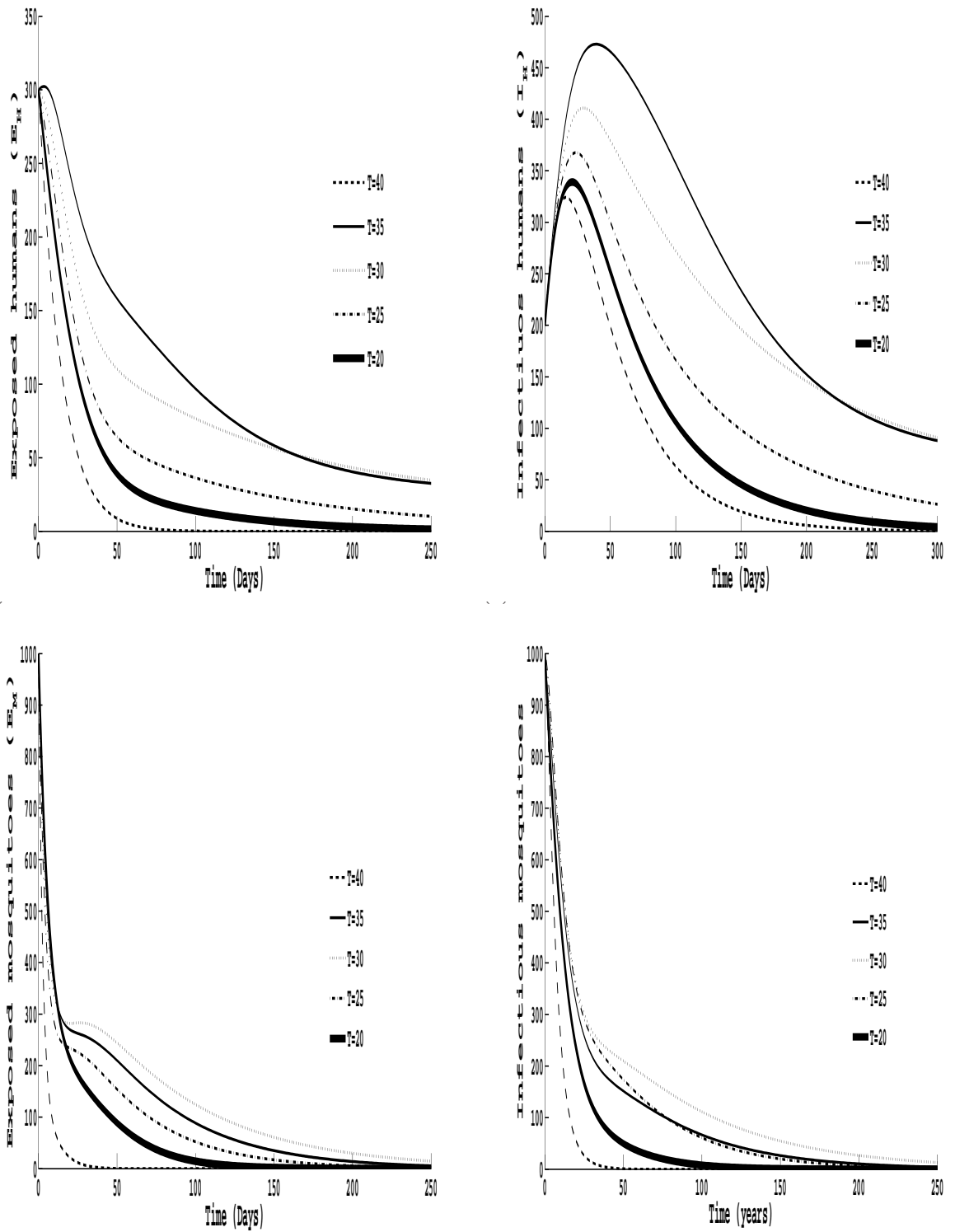
Figure 2.3: Simulation of (a) Exposed humans, (b) Infectious humans, (c) Exposed mosquitoes, and (d) Infectious mosquitoes as temperature varies

Figure 2.4, sensitivity analysis is presented using the partial rank correlation coefficients, (PRCC) which show the effect of parameter variations on $\mathcal{R}_m$. Parameters with positive PRCC will increase $\mathcal{R}_m$ when they are increased, whereas parameters with negative PRCCs will decrease $\mathcal{R}_m$ when they are increased. Results from the PRCC show that mosquito biting rate plays a more significant role in the increase of $\mathcal{R}_m$ than any other factor. This suggests that mosquito biting rate promotes malaria transmission than any other factor. Thus intervention strategies should be tailor made to prevent mosquito bites.
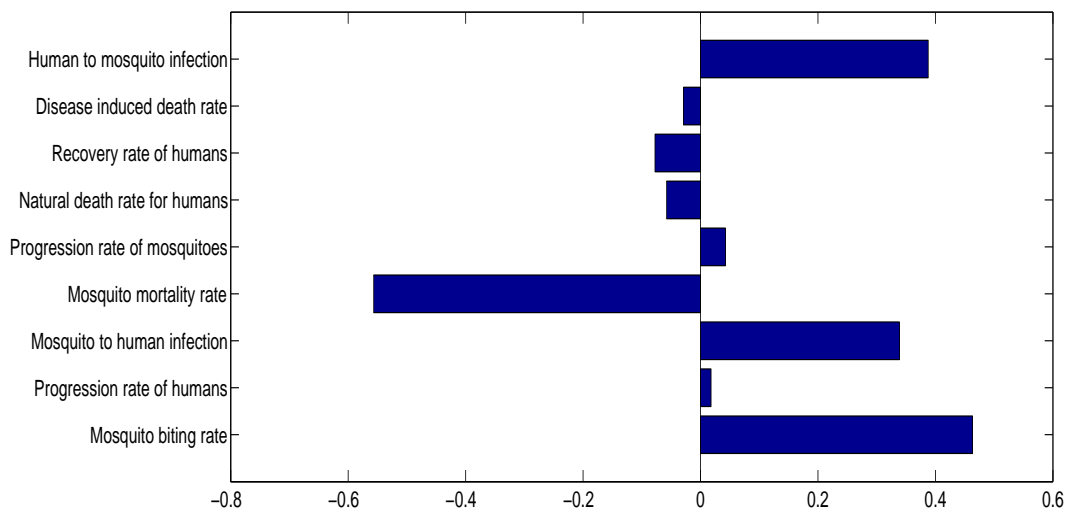
Figure 2.4: Partial rank correlation coefficients.

In Figure 2.5, Latin Hypercube Sampling and Monte Carlo simulations were used to run 1000 simulations to illustrates the effect of varying four sample parameters on the reproductive number $\mathcal{R}_m$. The results demonstrate that an increase in mosquito mortality results in a decrease in the reproduction number, while increases in both mosquito biting rate and the probability of human to mosquito infection result in an increase on the reproductive ratio.
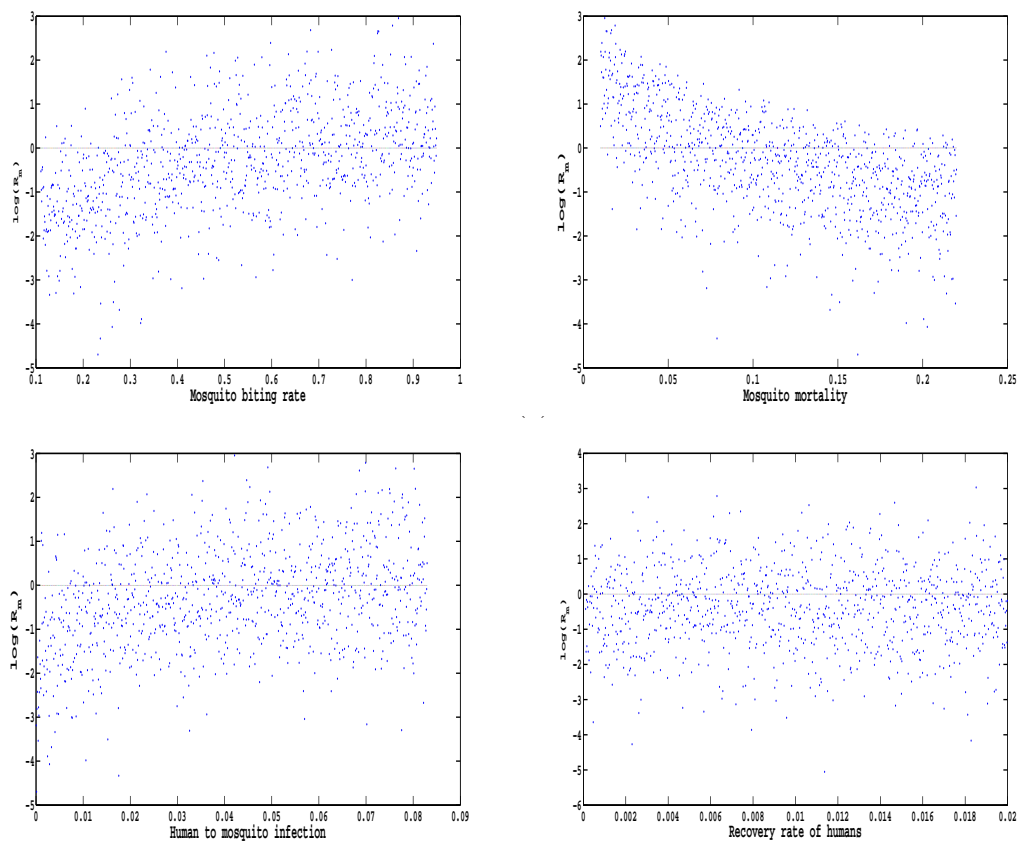
Figure 2.5: Monte Carlo simulations of (a) Mosquito biting rate, (b) Mosquito mortality, (c) Human to mosquito infection, and (d) Recovery rate of humans

2.4. Discussion

In this chapter, a mathematical model to explore the impact of temperature on malaria transmission is presented as a system of differential equations and analysed. Analysis of the model suggests that temperature range 23^0C to 38^0C is ideal for malaria transmission. The reproduction number increases as temperature increases to attain a maximum at 31.5^0C, beyond which the reproduction number starts declining.

This result suggests the optimal temperature for malaria transmission is around 31^0C. The analytic results are also supported by numerical simulations which show an increase in malaria cases as temperature increases to about 38^0C and a decrease thereafter. From the PRCCs, it is illustrated that the death rate of mosquitoes has a negative impact on the reproduction number. Thus, results suggest that any factor which contributes to increased mosquito death like spraying, use of treated mosquito nets, has potential to reduce malaria transmission. Thus, mosquito spraying, coupled with the use of treated mosquito nets has a great potential to control this deadly tropical scourge. Given high incidences of tuberculosis in Sub-saharan Africa, where malaria is also endemic, this model can be extended to incorporate the malaria and TB coinfection.

Chapter 3

Assessing the role of climate change in malaria transmission in Africa

3.1. Introduction

Climate change is projected to alter the distribution of vector borne diseases and malaria is no exception. Children under five and pregnant women continue to be at risk. One of the key Millennium development goals was to halve, halt and reverse the scourge of malaria by 2015. The disease has not yet been halved although a significant reduction in malaria incidences has been recorded (WHO, 2014). These little gains achieved to date are under threat from climate change.

Malaria is sensitive to climate change in the sense that the vector that spreads

malaria as well as the parasite that causes the disease are sensitive to climate variables especially rainfall and temperature. Research on the impact of climate change on the dynamics of malaria is still ongoing (Craig *et al.*, 1999; Martens *et al.*, 1997; Parham and Michael, 2010; Paaijmans *et al.*, 2013). However most studies tend to consider the effect of temperature alone on the dynamics of malaria, neglecting the impact of incorporating rainfall in the mathematical models of malaria transmission. Understanding the role of temperature and rainfall on malaria transmission is of particular importance in light of climate change as changes can alter vector development rates, shift vector geographical distribution and alter transmission dynamics. Climate change is widely expected to significantly affect the global spread, intensity and distribution of malaria. The question is, how is climate change going to affect the gains made thus far in trying to reduce the burden of malaria?

This study seeks to build a model that will enable prediction and mapping of the current and potential future distribution of malaria in Africa as a result of climate change. The study will highlight how combining regional climate models with mathematical models of malaria transmission provides valuable tools for better understanding future disease scenarios as climatic conditions change. We modify our previous work in Chapter 2, to incorporate rainfall into the model. We focus on the construction of a realistic, climate-based malaria transmission model that captures the combined effects of both rainfall and temperature on malaria infection dynamics. This approach permits us to gain insights into the effect of climate

change on malaria transmission.

3.2. Model description

A deterministic transmission model is developed as a framework for understanding the impact of temperature and rainfall on malaria dynamics. The human population is subdivided into four classes: susceptible ($S_H(t)$), exposed or incubating $E_H(t)$, infectious ($I_H(t)$) and recovered individuals who become partially immune ($R_H(t)$). Individuals are recruited into the susceptible class at a rate θ and individuals die naturally at a rate μ_H. The rate of infection of a susceptible individual is dependent on the mosquito's biting rate $a(T, R)$ and the proportion of bites by infectious mosquitoes on susceptible humans that produce infection b_H. Once individuals are infected, they do not automatically become infectious as they do not have gametocytes, but enter the exposed class E_H, where parasites in their bodies are still in the asexual stages. Exposed humans then progress at a rate κ_H to the infectious class, in which they now have gametocytes in their bloodstream making them capable of infecting the susceptible anopheles mosquitoes. Individuals recover through treatment at a rate α, where a proportion $(1 - p)$ recovers with temporary immunity and the compliment p recovers with no immunity. Temporarily immune individuals lose immunity at a rate γ. Infected individuals who do not seek treatment die from infection at a rate η. Both human and mosquito infections take time to develop into an infectious state. Within host parasite dynamics are weather independent, but within vector parasite dynamics, as well as the mosquito

life cycle are weather dependent.

The mosquito population is divided into the juvenile $(J_M(t))$ and adult population of which the adult population is subdivided into three classes: susceptible $(S_M(t))$, exposed $E_M(t)$ and infectious $(I_M(t))$. The juvenile stages describe the development of the aquatic stages which mature to become susceptible adult mosquitoes at a rate β_M. The rate of infecting a susceptible mosquito depends on the mosquitoes' biting rate $a(T, R)$ and the proportion of bites by susceptible mosquitoes on infected humans that produce infection b_M. Susceptible mosquitoes that feed on infectious humans will take gametocytes in blood meals, but as they do not have sporozoites in their salivary glands, they enter into the exposed class E_M. After fertilisation, sporozoites are produced and migrate to the salivary glands ready to infect any susceptible host, the vector is then considered as infectious and enters the class I_M. Mosquitoes die at a rate μ_M which is independent of infection status. Infected mosquitoes are not harmed by the infection, never clear their infection and the infective period of the mosquito ends with its death. The following system of dif-

ferential equations describe the model.

$$S'_H(t) = \theta - \lambda_H(T, R)S_H - \mu_H S_H + p\alpha I_H + \gamma R_H,$$

$$E'_H(t) = \lambda_H(T, R)S_H - (\kappa_H + \mu_h)E_H,$$

$$I'_H(t) = \kappa_H E_H - (\mu_H + \alpha + \eta)I_H,$$

$$R'_H(t) = (1 - p)\alpha I_H - (\gamma + \mu_H)R_H,$$

$$J'_M(t) = \beta_J(T, R)N_M(1 - \tfrac{J_M}{K}) - \mu_J(T) \ J_M - \beta_M(T, R)J_M,$$

$$S'_M(t) = \beta_M(T, R)J_M - \lambda_M(T, R)S_M - \mu_M(T)S_M,$$

$$E'_M(t) = \lambda_M(T, R)S_M - (\kappa_M(T) + \mu_M(T))E_M,$$

$$I'_M(t) = \kappa_M(T)E_M - \mu_M(T)I_M.$$

(3.1)

Here, $\lambda_H = \dfrac{a(T, R)b_H I_M}{N_M}$ and $\lambda_M = \dfrac{a(T, R)b_M I_H}{N_H}$, $N_H = S_H + E_H + I_H + R_H$ and $N_M = S_M + E_M + I_M$. $X(T, R)$ specifies a function of temperature and rainfall while $X(T)$ represents a function of temperature alone.

Predicting the effect of climate change on malaria dynamics requires a framework that specifically incorporates the role of each climate sensitive parameter. The functional forms of temperature and rainfall dependent parameters are presented in Table 3.1.

Table 3.1: Parameters of the basic malaria model presented. (R) shows dependance on rainfall and (T) represents dependance on temperature

Description	Symbol	Value	Source
Adult mosquito birth rate	$\beta_M(T,R)$	$\frac{B_E P_E(R) P_L(R,T) P_P(R)}{(\tau_E + \tau_L(T) + \tau_P)}$	f^*
Birth rate of juveniles	$\beta_J(T,R)$	$10 * \beta_M(T,R)$	b^*
Mosquito biting rate	$a(T,R)$	$\frac{\beta_J(T,R)}{2.325}$	b^*
Number of eggs laid per adult oviposition	B_E	200	f^*
Daily survival probability of eggs	$P_E(R)$	$\frac{4*0.9}{R_L^2} R(R_L - R)$	f^*
Daily survival probability of lavae	$P_L(T,R)$	$\frac{R(R_L - R) * e^{-0.00554T - 0.06737}}{R_L^2}$	f^*
Daily survival probability of pupae	$P_P(R)$	$\frac{4*0.75}{R_L^2} R(R_L - R)$	f^*
Duration of egg development	τ_E	1	f^*
Duration of larvae development	$\tau_L(T)$	$\frac{1}{(0.00554T - 0.06737)}$	f^*
Rainfall beyond which no immature stages survive	R_L	50	f^*
Duration of pupae development	τ_P	1	f^*
Juvenille mosquito death rate	$\mu_J(T)$	$0.0025T^2 - 0.094T + 1.0257$	b^*
adult mosquito death rate	$\mu_M(T)$	$-\ln \rho(T)$	c^*
	$\rho(T)$	$e^{\frac{-1}{-0.03T^2 + 1.31T - 4.4}}$	c^*
Progression rate of mosquitoes	κ_M	$\frac{T - T_{min}}{DD}$	d^*
Recruitment rate of humans	θ	0.028	e^*
Proportion of bites by infectious mosquitoes	b_H	0.09	f^*
Proportion of bites by susceptible mosquitoes	b_M	0.04	f^*
per capita natural death rate for humans	μ_H	0.00004	e^*
Progression rate of humans from exposed	κ_H	1/14	e^*
Recovery rate of humans	α	0.005	e^*
Per capita disease induced death rate	η	0.0004	e^*
Per capita rate of loss of immunity	γ	$\frac{1}{20*365}$	g^*
carrying capacity of larvae	K	1000000	h^*
Proportion humans recovering without temp immunity	p	0.25	h^*

b^* denotes parameters adapted from Rubel *et al.* (2008), c^* from Martens *et al* (1995), d^* from McDonald (1957), e^* from Chiyaka *et al.* (2007), f^* from Parham

and Michael (2010), g^* from Blayneh *et al* (2009) and h^* are parameters mantained from Chapter 2.

3.2.1. Model analysis

Following Van den Driessche and Watmough [**?**], the treatment induced reproduction number [$\mathcal{R}_m$] of the model in equation (3.1) is given by

$$\mathcal{R}_m = \sqrt{\left(\frac{a(T,R)b_H\kappa_H}{\mu_M(T)(\kappa_M(T)+\mu_M(T))}\right)\left(\frac{a(T,R)b_M\kappa_M(T)}{(\kappa_H+\mu_H)(\mu_H+\alpha+\eta)}\right)}. \qquad (3.2)$$

In the absence of treatment $\alpha = 0$, then $\lim\limits_{\alpha\to 0} \mathcal{R}_m = \mathcal{R}_0$ - the basic reproduction number. The treatment induced reproduction number defines the average number of new infections a single infected mosquito/ individual would produce during its/ his (her) entire infectious period where treatment is the only intervention strategy.

3.3. Mapping transmission dynamics across Africa

We applied equation (3.2) to gridded temperature and precipitation datasets for the baseline climate and future climate to compute R_0 for each pixel in Geographical information systems (GIS). The datasets used covered the entire continent of Africa. R_0 was calculated separately for the baseline climate and for each GCM model.

To determine whether falciparum malaria will persist or the disease dies out in future, we evaluated the following boolean expressions on a pixel basis, respectively: $R_0 < 1$ for the baseline map and $R_0 > 1$ for the future map; $R_0 > 1$ for the baseline

map and $R_0 < 1$ for the future map.

This allowed us to classify an area as becoming malaria endemic or malaria free. All the maps generated in this study are based on the Albers equal area conic projection. We clipped the R_0 maps by the raster maps of the digital map of dominant vectors to exclude malaria free areas such as the sahara desert.

3.4. Results

In Figure 3.1, we plot R_0 for falciparum malaria as a function of rainfall and temperature. We observe that the optimum temperature window for falciparum malaria transmission is $30 - 32^oC$.
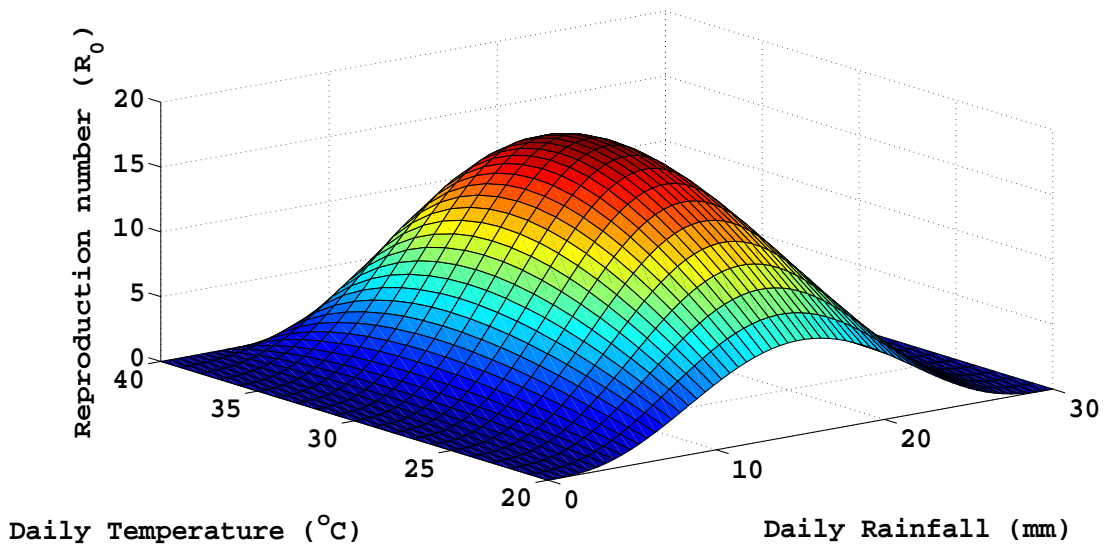
Figure 3.1: Reproduction number as a function of daily rainfall R in mm and temperature T in ^oC

Figure 3.2 illustrates the simulated R_0 for falciparum malaria on the African continent based on baseline climate. We observe distinct geographic patterns in the

intensity of falciparum malaria. The transmission intensity is highest in the tropics as well as the coastal areas of East Africa. The subtropics exhibit low levels of transmission intensity. The white areas represent areas where climatic conditions are not suitable for malaria transmission. Our simulations fall within the observed spatial distribution of falciparum malaria on the continent described by Gething *et al.* (2011).

Figure 3.2: Basic reproduction number for falciparum malaria based on the baseline climate

Figure 3.3 shows the projected R_0 for falciparum malaria in Africa based on HadCM3 and CSIRO MK3 A2a climate scenarios for 2040. Compared to the simulations for the baseline climate, we observe increases in R_0 in the tropics, the highland regions, east Africa as well as along the northern limit of falciparum malaria. By contrast, a decrease in R_0 is projected to occur on the southern fringe of the disease by 2040. These changes are similar for both HadCM3 and CSIRO MK3 A2a climate projections.
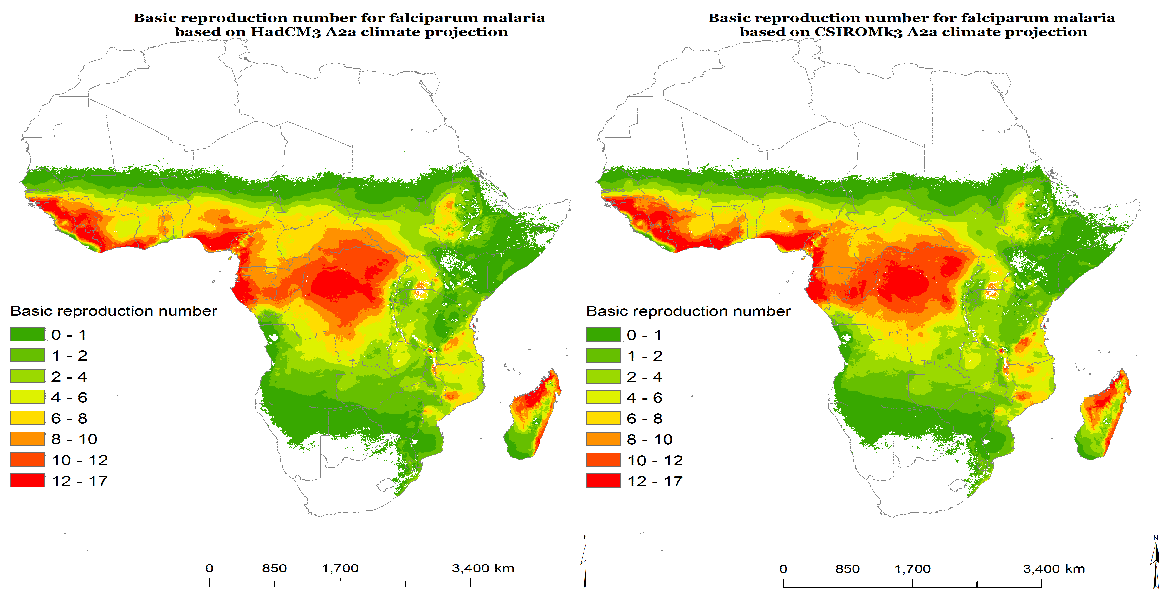
Figure 3.3: 2040 Projected basic reproduction number for falciparum malaria.

In Figure 3.4 we notice that the increases in R_0 are sufficient to turn most areas in the African highlands into malaria endemic areas by 2040. The northern limit of falciparum malaria is also projected to become an endemic region.

Areas to become malaria endemic based on HadCM3 A2a climate projection   Areas to become malaria endemic based on CSIROMk3 A2a climate projection
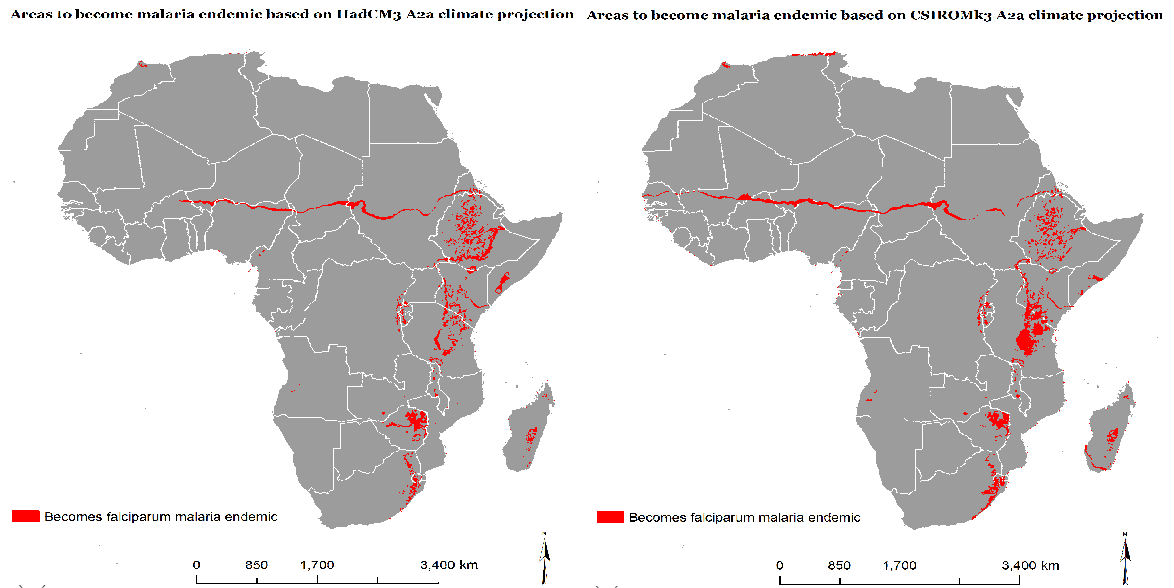
Figure 3.4: 2040 Projected malaria endemic areas previously malaria free

In contrast, the decreases in R_0 are sufficient to turn areas that fringe the southern limit of the disease into malaria-free zones. A similar trend is expected for isolated areas in the African highlands as noted in Figure 3.5.

Areas to become malaria free based on HadCM3 A2a climate projection   Areas to become malaria free based on CSIROMk3 A2a climate projection
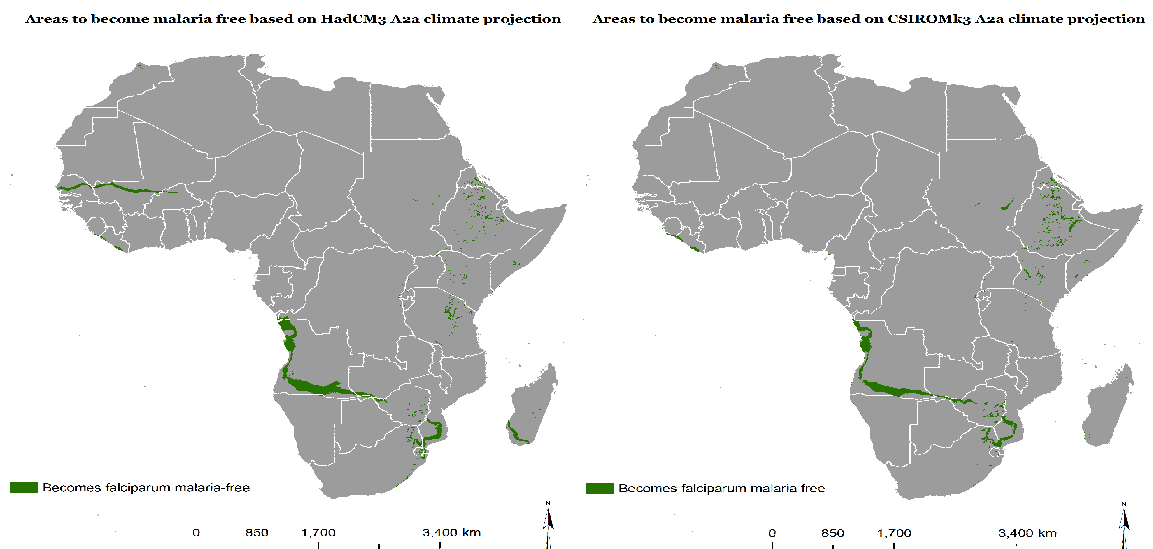
Figure 3.5: 2040 Projected malaria free areas previously malaria endemic

3.5. Discussion

A model incorporating rainfall and temperature is analysed regarding malaria transmisssion. Results from the model suggests that the optimum temperature window for peak falciparum malaria transmission is $30 - 32^oC$. This is in agreement with other studies (Parham and Michael, 2010). Furthermore, results from model analysis suggest daily rainfall in the range of $15 - 17mm$ is ideal for the spread of malaria. Perhaps the most interesting but unexpected result is that by 2040 malaria is projected to die out on the southern fringe of the disease in Africa. The fact that the same result was detected using projections from two different GCM models makes this a key result. A drying trend is the likely driving force for this change (Volker *et al.*, 2012). This finding has implications for malaria elimination in some regions of Africa. In other words, the result offers hope that the international goal of shrinking the malaria map may be achieved in southern Africa.

Results of this study suggest that due to climate change endemic malaria will become an increasing problem in the African highlands, this seems to be in agreement with other studies (Hay *et al.*, 2002; lindsay and Martens, 1998; Parham and Michael, 2010; Siraj *et al.*, 2014; Thomas *et al.*, 2004). A warming trend is the likely factor driving the projected increase in malaria endemicity in the highlands though socio-economic factors such as land use change and drug resistance can also be attributed to increases in malaria incidences in highlands too.

The model has the following limitations: (i) it did not consider the role of human migration neither did it consider other climate variables in particular relative humidity as the tropical anopheline mosquitoes prefer humidities above 60% (Martens and Thomas, 2005); (ii) the role of socio-economic factors in malaria transmission dynamics but it would be interesting to incorporate these factors to ascertain whether climate change in combination with these factors will amplify malaria transmission in the highlands. Despite these limitations, the authors believe that the model is robust enough to be able to give a realistic picture of malaria on the African continent. Thus, results from the study will be useful at various levels of decision making, for example, in setting up an early warning and sustainable strategies for climate change and adaptation for malaria vectors control programmes in Africa.

Chapter 4

Transmission dynamics of schistosomiasis in Zimbabwe

4.1. Introduction

Schistosomiasis also referred to as bilharzias (or snail fever) is an infectious disease caused by parasitic flatworms of the genus schistosoma. It is a major source of morbidity affecting over 250 million people worldwide, with 85% occuring in the developing tropical countries in Africa, Asia, South America and the Middle East (WHO, 2015; Ukoroije *et al.*, 2012). In terms of morbidity and mortality, schistosomiasis is considered the second most important human parasitic disease after malaria (Chitsulo *et al.*, 2000). Schistosomiasis continues to drain the socio-economic development of already impoverished rural communities of sub-Saharan Africa.

Schistosomiasis may localize in different parts of the body and its localization determines its particular clinical profile (Sturrock, 1993). Schistosomiasis is caused by five species of flatworms, each of which causes a different clinical presentation of the disease. Intestinal schistosomiasis is caused by Schistosoma mansoni, urinary schistosomiasis is caused by Schistosoma haematobium and Schistosoma japonicum and Schistosoma mekongi cause Asian intestinal schistosomiasis (De Jesus *et al.*, 2000). Three species of schistosomiasis, S. haematobium (prevalent in Africa), S. japonicum (prevalent in Japan, Southeast Asia, and Western Pacific) and S. mansoni (prevalent in Africa, Southwest Asia, Brazil and the Caribbean) are responsible for the majority of schistosomiasis infection while the other two species, S. intercalatum and S. mekongi parasitize humans to a much lesser extent (WHO, 2002). Flatworms infect humans by penetrating the skin when exposed to contaminated freshwater (e.g., when wading, swimming, or bathing). The flatworms spread in freshwater areas, such as rivers and lakes, where freshwater snails act as intermediate hosts for the parasites larvae. As such, the habitats of the host snails are of great importance for the spread of the disease.

The most important determinants of the population dynamics of snails are temperature and rainfall (Sturrock, 1993). The best survival temperature of snails was found to be between 20° and 25^oC while at 40^oC none of the snails survived (Dagal *et al.*, 1986). However, snails are less sensitive to low temperatures than schistosome parasites in snails. Uninfected snails can therefore be found in high altitude areas of endemic countries where low temperatures inhibit larval development in snails

(Brooker, 2007). Dagal *et al.* (1986) considered the effects of water temperatures on hatchability of eggs and survival of snails and found that at low temperatures $15^{o}C$, none of the eggs hatched. The mean survival rate of snails between $5^{o}C$ and $10^{o}C$ was found to be zero. As temperature increased, hatching rate increased but at $35^{o}C$ none of the eggs hatched.

Incorporating climate effects into models of disease dynamics is now extremely important as there is a strong need to understand the effects of climate change. The schistosome and snail life cycles are highly dependant on ambient conditions and climate change is known to affect several parameters in the epidemiology of schistosomiasis. Developing an epidemiological model to predict how these factors overally bring out the impact of climate on the dynamics of schistosomiasis transmission is crucial. The model reproduction number is applied to gridded temperature and rainfall datasets for Zimbabwe to determine the possible variation of schistosomiasis intensity in Zimbabwe.

4.2. Model formulation

The life cycle of schistosome parasites is complicated and involves two different hosts: human beings and snails. A model to trace the life cycle of schistosome parasite is formulated. The model is based on monitoring the dynamics of the populations at any time t of susceptible humans $S_H(t)$, exposed humans $E_H(t)$, infectious humans I_H, miracidia $M(t)$ (larvae of the parasite soon after hatching from the eggs), uninfected snails $U(t)$, latently infected snails $L(t)$, patent infected snails

(infected snails not yet releasing cercariae) $I_s(t)$ and cercariae $C(t)$ (larvae released into the water from infected snail ready to enter the human skin). Individuals are recruited into the human population at a rate Λ_H. Susceptible individuals acquire infection at a rate $\lambda_H = \dfrac{\beta_H C(t)}{C_0 + \epsilon C(t)}$, where β_H is the cercarial infection rate, C_0 is a saturation constant for the cercariae and ϵ is the limitation of the growth velocity of cercariae with the increase of cases. Upon infection, an individual does not automatically become infectious but enters an exposed class as the incubation period of schistosomiasis ranges from 4-8 weeks for schistosomiasis mansoni and schistosomiasis japonicum, respectively (Cohen, 1977; Spira, 2003). Individuals then progress to the infectious compartment at a rate κ_H. Susceptible and infected individuals suffer from natural death rate μ_H, but infectious individuals have an additional host mortality δ_H. Adult schistosomes within infected human hosts produce eggs which hatch and develop to free-swimming miracidia at a net rate θ_M. Miracidia either die at a rate δ_M or infect uninfected snails at rate $\lambda_S = \dfrac{\beta_S M}{M_0 + \epsilon M}$. Adult snails are recruited into the susceptible snail population at a rate Λ_S. Upon infection, snails enter the latently infected class from which they progress to the patent infected class at a rate κ_S. Adult snails die naturally at rate δ_S and infected adult snails also die due to parasite-induced mortality at an additional rate α. The patent infected snails will then release a second form of free swimming larvae called cercariae at a rate θ_C which is capable of infecting humans. Cercariae die naturally at the rate δ_C.

A compartmental model of schistosomiasis dynamics is presented in Figure 4.1.
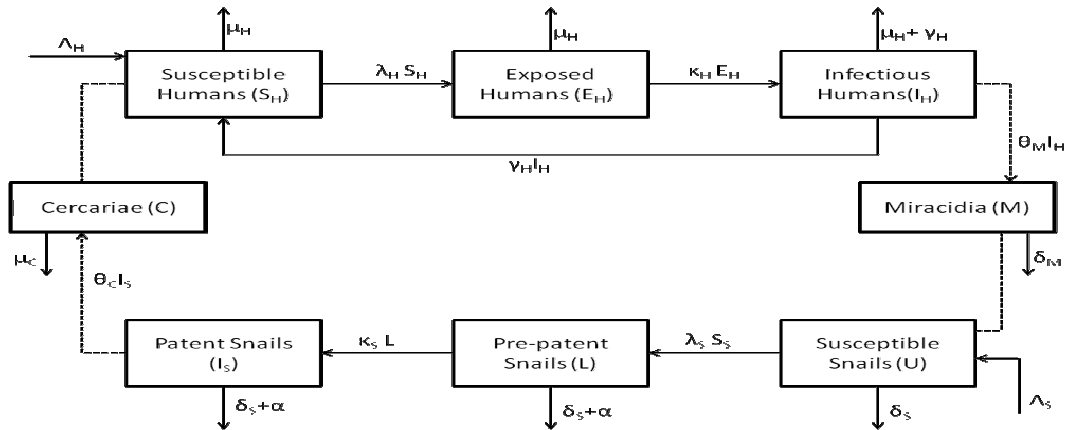
Figure 4.1: Model diagram of the mathematical model for schistosomiasis transmission. Dotted lines on the diagram denote indirect interaction.

The following system of differential equations describe the model.

$$S'_H(t) = \Lambda_H - \frac{\beta_H C S_H}{C_0 + \epsilon C} - \mu_H S_H + \gamma_H I_H,$$

$$E'_H(t) = \frac{\beta_H C S_H}{C_0 + \epsilon C} - (\kappa_H + \mu_H)E_H,$$

$$I'_H(t) = \kappa_H E_H - (\mu_H + \delta_H + \gamma_H)I_H,$$

$$M'(t) = \theta_M I_H - \frac{\beta_S M U}{M_0 + \epsilon M} - \delta_M M,$$

$$U'(t) = \Lambda_S - \frac{\beta_S M U}{M_0 + \epsilon M} - \delta_S U,$$

(4.1)

$$L'(t) = \frac{\beta_S M U}{M_0 + \epsilon M} - (\delta_S + \alpha + \kappa)L,$$

$$I'_S(t) = \kappa L - (\delta_S + \alpha)I_S,$$

$$C'(t) = \theta_C I_S - \frac{\beta_H C S_H}{C_0 + \epsilon C} - \delta_C C.$$

Table 4.1: Parameters of the basic schistosomiasis transmission model in equation (4.1) where T represents temperature and P represents rainfall. a^{**} denotes temperature dependant parameters designed using Datafit based on results from a^*.

Description	Symbol	Value	Source
Recruitment rate of humans	Λ_H	800	j^*
Cercarial infection rate	β_H	$-2.296 + 0.446 \ln T + \frac{2.96}{\ln T}$	k^{**}
Saturation constant of cercarae	C_0	9000000	j^*
progression rate of humans	κ_H	0.017857	est
Natural death rate of humans	μ_H	0.014	m^*
Disease induced death rate	δ_H	0.039	j^*
Adult snail recruitment rate	$\Lambda_S(T)$	$100 e^{A_1 + \frac{A_2}{T} + A_3 \ln T}$	k^{**}
Adult snail recruitment rate	$\Lambda_S(T, P)$	$0.321 e^{-0.5[\frac{ln(\frac{T}{21.3})}{0.087}]^2} + 0.603 e^{-0.5[\frac{P-1.927}{1.786}]^2}$	n^{**}
Miracidia infection rate	β_S	$B_1 + \frac{B_2}{T} - \frac{B_3}{T^2} + \frac{B_4}{T^3} - \frac{B_5}{T^4} + \frac{B_6}{T^5}$	p^{**}
Saturation constant for the miracidia	M_0	100000000	j^*
Adult snail mortality rate	δ_S	$C_1 - \frac{C_2}{\ln T} + \frac{C_3}{(\ln T)^2} + \frac{C_4}{(\ln T)^3} + \frac{C_5}{(\ln T)^4}$	k^{**}
Additional snail mortality due to infection	α	$D_1 + D_2 T^{2.5} + D_3 e^{-T}$	m^{**}
Net miracidial production rate	θ_M	500	m^{**}
Miracidial death rate	δ_M	$F_1 T^5 + F_2 T^4 + F_3 T^3 + F_4 T^2 + F_5 T + F_6$	k^{**}
Cercarial production rate	θ_C	$G_1 T^2 + G_2 T + G_3$	k^{**}
Cercarial mortality rate	δ_c	0.004	n^*
Within snail schistosome maturation rate	κ_S	$H_1 T^5 + H_2 T^4 + H_3 T^3 + H_4 T^2 + H_5 T + H_6$	k^{**}

j^* denotes parameters from Chiyaka and Garira (2009), k^* from Mangal et $al.$ (2008), m^* from Feng et $al.$ (2002), n^* from Remais et $al.$ (2007), p^* from Dagal et $al.$ (1986),

where $A_1 = 351.04480681884$, $A_2 = -1925.49534415329$, $A_3 = -85.1815135926783$,

$B_1 = -8.59$, $B_2 = 855$, $B_3 = 31487.35$, $B_4 = 574921.12, B_5 = 5188906$,

$B_6 = 18196700$, $C_1 = 11.4267$, $C_2 = 126.89$, $C_3 = 525.29, C_4 = -960.38$,

$D_2 = 8.738295237E - 06, \quad D_3 = 1334.208298 \quad F_1 = 3.99E - 07, \quad F_2 = -3.73E - 05,$

$F_3 = 4.97E - 04, \quad F_4 = 3.99E - 02, \quad F_5 = -1.149, \quad F_6 = 9.59, \quad G_2 = 40.19,$

$G_3 = -907.85, \quad H_1 = 2.97E - 06, \quad H_2 = -3.699E - 04, \quad H_3 = 1.83E - 02,$

$H_4 = -0.45, \quad H_5 = 5.38, \quad H_6 = -25.688 \quad a = 0.23, \quad b = -1.05,$

$B_m = 0.849, \quad T_m = 25$

We make a simplification common in models with free living particles and assume that the rate of the particle depletion by hosts or snails has negligible impact on particle dynamics (Chiyaka and Garira, 2009). This is done to reduce the complexity of the mathematics involved. In this case the interaction between the miracidia and the susceptible snail $\dfrac{\beta_S M U}{M_0 + \epsilon M}$ and the interaction between the cercariae and the humans $\dfrac{\beta_H C S_H}{C_0 + \epsilon C}$ are assumed to be negligible on pathogen dynamics. System

(4.1) can now be written as

$$S'_H(t) = \Lambda_H - \frac{\beta_H C S_H}{C_0 + \epsilon C} - \mu_H S_H + \gamma_H I_H,$$

$$E'_H(t) = \frac{\beta_H C S_H}{C_0 + \epsilon C} - (\kappa_H + \mu_H)E_H,$$

$$I'_H(t) = \kappa_H E_H - (\mu_H + \delta_H + \gamma_H)I_H,$$

$$M'(t) = \theta_M I_H - \delta_M M,$$

$$U'(t) = \Lambda_S - \frac{\beta_S M U}{M_0 + \epsilon M} - \delta_S U,$$

$$L'(t) = \frac{\beta_S M U}{M_0 + \epsilon M} - (\delta_S + \alpha + \kappa)L,$$

$$I'_S(t) = \kappa L - (\delta_S + \alpha)I_S,$$

$$C'(t) = \theta_C I_S - \delta_C C.$$

(4.2)

All feasible solutions of model system (4.2) enter the region

$$\Omega = \begin{cases} (S_H, E_H, I_H) \in \mathbb{R}^3_+ : N_H \leq \dfrac{\Lambda_H}{\mu_H}, \\[2mm] M \in \mathbb{R}_+ : M \leq \dfrac{\theta_M \Lambda_H}{\delta_M \mu_H}, \\[2mm] (U, L, I_S) \in \mathbb{R}^3_+ : N_S \leq \dfrac{\Lambda_S}{\delta_S}, \\[2mm] C \in \mathbb{R}_+ : C \leq \dfrac{\theta_C \Lambda_S}{\delta_C \delta_S}, \end{cases}$$

(4.3)

which is positively invariant and attracting and it is sufficient to consider solutions

in Ω. Existence, uniqueness and continuation results for system (4.2) hold in this region and all solutions starting in Ω remain in there for all $t \geq 0$. Hence, (4.2) is mathematically and epidemiologically well-posed and it is sufficient to consider the dynamics of the flow generated by the model system (4.2) in Ω. Also, all parameters and state variables for model system (4.2) are assumed to be non-negative since it monitors human, snail, miracidia and cercariae populations.

4.3. Model analysis

The parasite larval stages (represented by M and C) have relatively short lifespans compared with those of worms, humans and snails. So the dynamic equations for M and C are replaced with their quasi-equilibrated values $C^* = \dfrac{\theta_C I_S}{\delta_S}$ and $M^* = \dfrac{\theta_M I_H}{\delta_M}$. The original system (4.2) is reduced to a six dimensional form for

variables S_H, E_H, I_H, U, L and I_S.

$$S'_H(t) = \Lambda_H - \frac{\beta_H S_H \frac{\theta_C I_S}{\delta_S}}{C_0 + \epsilon \frac{\theta_C I_S}{\delta_S}} - \mu_H S_H + \gamma_H I_H,$$

$$E'_H(t) = \frac{\beta_H S_H \frac{\theta_C I_S}{\delta_S}}{C_0 + \epsilon \frac{\theta_C I_S}{\delta_S}} - (\mu_H + \kappa_H) E_H,$$

$$I'_H(t) = \kappa_H E_H - (\mu_H + \delta_H + \gamma_H) I_H,$$

$$U'(t) = \Lambda_S - \frac{\beta_S U \frac{\theta_M I_H}{\delta_M}}{M_0 + \epsilon \frac{\theta_M I_H}{\delta_M}} - \delta_S U,$$

(4.4)

$$L'(t) = \frac{\beta_S U \frac{\theta_M I_H}{\delta_M}}{M_0 + \epsilon \frac{\theta_M I_H}{\delta_M}} - (\delta_S + \alpha + \kappa) L,$$

$$I'_S(t) = \kappa L - (\delta_S + \alpha) I_S.$$

The equilibrium states of the basic model are obtained by setting the right hand side of system (4.2) to zero. Model system (4.2) has two steady states. At the disease free equilibrium, there are no infected humans and infected snail, thus the model system (4.4) has a disease free equilibrium

$$\mathcal{E}_0 = (S_H, E_H, I_H, U, L, I_S) = \left(\frac{\Lambda_H}{\mu_H}, 0, 0, \frac{\Lambda_S}{\delta_S}, 0, 0 \right).$$

The endemic equilibrium point for system (4.2) in terms of the forces of infection λ_H^* and λ_S^* is given by

$$
\begin{aligned}
S_H^* &= \frac{\Lambda_H(\kappa_H + \mu_H)(\mu_H + \delta_H + \gamma_H)}{(\lambda_H^* + \mu_H)(\kappa_H + \mu_H)(\mu_H + \delta_H + \gamma_H) - \gamma_H \kappa_H \lambda_H^*}, \\
E_H^* &= \frac{\lambda_H^* \Lambda_H(\mu_H + \delta_H + \gamma_H)}{\delta_H(\kappa_H + \mu_H)(\lambda_H^* + \mu_H) + \mu_H[(\kappa_H + \mu_H)(\lambda_H^* + \mu_H) + \gamma_H(\kappa_H + \lambda_H^* + \mu_H)]}, \\
I_H^* &= \frac{\kappa_H \lambda_H^* \Lambda_H}{\delta_H(\kappa_H + \mu_H)(\lambda_H^* + \mu_H) + \mu_H[(\kappa_H + \mu_H)(\lambda_H^* + \mu_H) + \gamma_H(\kappa_H + \lambda_H^* + \mu_H)]}, \\
U^* &= \frac{\Lambda_S}{\delta_S + \lambda_S^*}, \quad L^* = \frac{\lambda_S^* \Lambda_S}{(\alpha + \delta_S + \kappa_S)(\delta_S + \lambda_S^*)}, \quad I_S^* = \frac{\kappa_S \lambda_S^* \Lambda_S}{(\alpha + \delta_S)(\alpha + \delta_S + \kappa_S)(\delta_S + \lambda_S^*)}.
\end{aligned}
$$

$$(4.5)$$

4.3.1. Basic reproduction number

The next generation operator approach as described by Diekmann et al (1990) is used to define the basic reproductive number, $\mathcal{R}_s$, as the number of new infections (in snails or humans) produced by one infectious individual or snail over the duration of the infectious period in a naive population.

$$
\mathcal{R}_s = \sqrt{\frac{\kappa_H \kappa_S \beta_H \theta_C \Lambda_H \beta_S \theta_M \Lambda_S}{\delta_c C_0 \delta_H \delta_M M_0 \delta_S (\kappa_H + \mu_H)(\delta_S + \alpha + \kappa_S)(\delta_S + \alpha)(\mu_H + \delta_H + \gamma_H)}}.
\qquad (4.6)
$$

4.3.2. Local stability of the disease-free equilibrium $\mathcal{E}_0$

The local stability of the disease free equilibrium can be discussed by examining the linearised form of the system (4.4) at the steady state $\mathcal{E}_0$.

Theorem 4.1. *The disease-free equilibrium $\mathcal{E}_0$ is locally asymptotically stable whenever $\mathcal{R}_s < 1$, and unstable otherwise.*

Proof. The Jacobian matrix of the model (4.4) evaluated at the disease free equi-

librium point is given by

$$
\begin{bmatrix}
-\mu_H & 0 & \gamma_H & 0 & 0 & -\frac{\beta_H \theta_C \Lambda_H}{\delta_c C_0 \delta_H} \\
0 & -(\kappa_H + \mu_H) & 0 & 0 & 0 & \frac{\beta_H \theta_C \Lambda_H}{\delta_c C_0 \delta_H} \\
0 & \kappa_H & -(\mu_H + \delta_H + \gamma_H) & 0 & 0 & 0 \\
0 & 0 & -\frac{\beta_S \theta_M \Lambda_S}{\delta_M M_0 \delta_C} & -\delta_S & 0 & 0 \\
0 & 0 & \frac{\beta_S \theta_M \Lambda_S}{\delta_M M_0 \delta_C} & 0 & -(\delta_S + \alpha + \kappa_S) & 0 \\
0 & 0 & 0 & 0 & \kappa_S & -(\delta_S + \alpha)
\end{bmatrix}.
$$

The first and the fourth columns have diagonal entries resulting in these diagonal entries being two of the eigenvalues of the Jacobian matrix $-\mu_M$ and $-\delta_S$. Now excluding these columns and the corresponding rows we calculate the remaining eigenvalues.

$$
\begin{bmatrix}
-(\kappa_H + \mu_H) & 0 & 0 & \frac{\beta_H \theta_C \Lambda_H}{\delta_c C_0 \delta_H} \\
\kappa_H & -(\mu_H + \delta_H + \gamma_H) & 0 & 0 \\
0 & \frac{\beta_S \theta_M \Lambda_S}{\delta_M M_0 \delta_C} & -(\delta_S + \alpha + \kappa_S) & 0 \\
0 & 0 & \kappa_S & -(\delta_S + \alpha)
\end{bmatrix}.
$$

Let $a_1 = \kappa_H + \mu_H, \quad a_4 = \frac{\beta_H \theta_C \Lambda_H}{\delta_c C_0 \delta_H}$.

In the same manner,

$b_1 = \kappa_H, \quad b_2 = \mu_H + \delta_H + \gamma_H, \quad c_2 = \frac{\beta_S \theta_M \Lambda_S}{\delta_M M_0 \delta_C}, \quad c_3 = \delta_S + \alpha + \kappa_S, \quad d_3 = \kappa_S, \quad d_4 = \delta_S + \alpha.$

The eigenvalues are solutions of the characteristic equation of the reduced matrix of dimension four which is given by

$$
(\kappa_H + \mu_H + \lambda)[(\mu_H + \delta_H + \gamma_H + \lambda)(\delta_S + \alpha + \kappa_S + \lambda)(\delta_S + \alpha + \lambda)] - \frac{\kappa_H \kappa_S \beta_H \theta_C \Lambda_H \beta_S \theta_M \Lambda_S}{\delta_c C_0 \delta_H \delta_M M_0 \delta_S} = 0
$$

which is simplified to

$$\lambda^4 + A_3\lambda^3 + A_2\lambda^2 + A_1\lambda + A_0 = 0,$$
$$A_3 = a_1 + b_2 + c_3 + d_4,$$
$$A_2 = (a_1 + d4)(b_2 + c_3) + a_1d_4 + b_2c_3,$$
$$A_1 = c_3d_4(b_2 + a_1) + a_1b_2(c_3 + d_4),$$
$$A_0 = (\kappa_H + \mu_H)(\delta_S + \alpha\kappa_S)(\delta_S + \alpha)(\mu_H + \delta_H + \gamma_H) - \frac{\kappa_H\kappa S\beta_H\theta_C\Lambda_H\beta_S\theta_M\Lambda_S}{\delta_c C_0\delta_H\delta_M M_0\delta_S}.$$

(4.7)

The Routh-Huwirtz conditions are sufficient and necessary conditions on the coefficients of the polynomial (4.7). These conditions ensure that all roots of the polynomial given by (4.7) have negative real parts. For this polynomial, the Routh-Hurwitz conditions are $A_3 > 0$, $A_2 > 0$, $A_1 > 0$, $A_0 > 0$ and

$$H_1 = A_3 > 0,$$

$$H_2 = \begin{vmatrix} A_3 & 1 \\ A_1 & A_2 \end{vmatrix} > 0,$$

$$H_3 = \begin{vmatrix} A_3 & 1 & 0 \\ A_1 & A_2 & A_3 \\ 0 & A_0 & A_1 \end{vmatrix} > 0,$$

$$H_4 = \begin{vmatrix} A_3 & 1 & 0 & 0 \\ A_1 & A_2 & A_3 & 1 \\ 0 & A_0 & A_1 & A_2 \\ 0 & 0 & 0 & A_0 \end{vmatrix} > 0,$$

since all $A_i > 0$, $i = 1, 2, 3$.

Note that from

$$A_0 = (\kappa_H + \mu_H)(\delta_S + \alpha\kappa_S)(\delta_S + \alpha)(\mu_H + \delta_H + \gamma_H) - \frac{\kappa_H \kappa_S \beta_H \theta_C \Lambda_H \beta_S \theta_M \Lambda_S}{\delta_c C_0 \delta_H \delta_M M_0 \delta_S}$$

$$= (\kappa_H + \mu_H)(\delta_S + \alpha\kappa_S)(\delta_S + \alpha)(\mu_H + \delta_H + \gamma_H)(1 - R_S^2).$$

At disease free equilibrium, $R_S < 1$, which implies that $A_0 > 0$.

Clearly, $H_1 = A_3 > 0$.

$$\begin{aligned}
H_2 &= A_3 A_2 - A_1, \\
&= (b_2 + c_3)(b_2 + d_4)(c_3 + d_4) + a_1^2(b_2 + c_3 + d_4) + a_1(b_2 + c_3 + d_4)^2
\end{aligned} \tag{4.8}$$

which is positive.

$$\begin{aligned}
H_3 &= A_1(A_3 A_2 - A_1) - A_0 A_3^2, \\
&= a_1^3(b_2 + c_3)(b_2 + d_4)(c_3 + d_4) + b_2 c_3(b_2 + c_3)d_4(b_2 + d_4)(c_3 + d_4) + a_4 b_1 c_2 d_3(b_2 + c_3 + d_4)^2 \\
&+ a_1^2(a_4 b_1 c_2 d_3 + b_2^3(c_3 + d_4) + 2b_2^2(c_3 + d_4)^2 + c_3 d_4(c_3 + d_4)^2 + b_2(c_3^3 + 4c_3^2 d_4 + 4c_3 d_4^2 + d_4^3)) \\
&+ a_1(b_2^3(c_3 + d_4)^2 + (c_3 + d_4)(2a_4 b_1 c_2 d_3 + c_3^2 d_4^2) + b_2^2(c_3^3 + 4c_3^2 d_4 + 4c_3 d_4^2 + d_4^3) \\
&+ 2b_2(a_4 b_1 c_2 d_3 + c_3 d_4(c_3 + d_4)^2))
\end{aligned}$$

$$\tag{4.9}$$

which is also positive.

It can be easily seen that $H_4 = A_0 H_3$.

Therefore, all eigenvalues of the Jacobian matrix have negative real parts when $\mathcal{R}_s < 1$. However, $\mathcal{R}_s > 1$ implies that $A_0 < 0$, and since all coefficients of the polynomial (4.7) are positive, not all roots of this polynomial can have negative real parts. This means that when $\mathcal{R}_s > 1$, the disease free equilibrium point is

unstable.   □

4.4. Numerical simulations

We explore the effects of temperature and rainfall using graphical representations. In Figure 4.2, the effects of temperature on snail recruitment rate, snail mortality rate, basic reproduction number, miracidia death rate, miracidia infection rate and within snail schistosome maturation rate are illustrated. The snail recruitment rate is 0 at 15^oC and increases to a maximum at around 23^oC before declining to zero again at around 34^0C. This is in agreement with Dagal *et al* (1986) because no snail eggs hatch at temperatures lower than 15^oC and at temperatures greater or equal to 35^oC. The snail recruitment rate is maximum at 24^oC as the optimal temperatures for reproduction lie between 22^0C and 26^0C, in agreement with WHO (2015). Snail mortality is high at low temperatures but decreases to a minimum between 20^oC and 25^oC before increasing again at higher temperatures. The reproduction number is zero at 10^oC and increases to become greater than unity around 18^oC. It increases to a maximum at about 22.5^oC before declining to zero at about 35^oC. The reproduction number is greater than unity between 18^oC and 28^oC making this temperature range the ideal temperature range for endemic schistosomiasis. Matlab codes are used to obtain the numerical simulations.
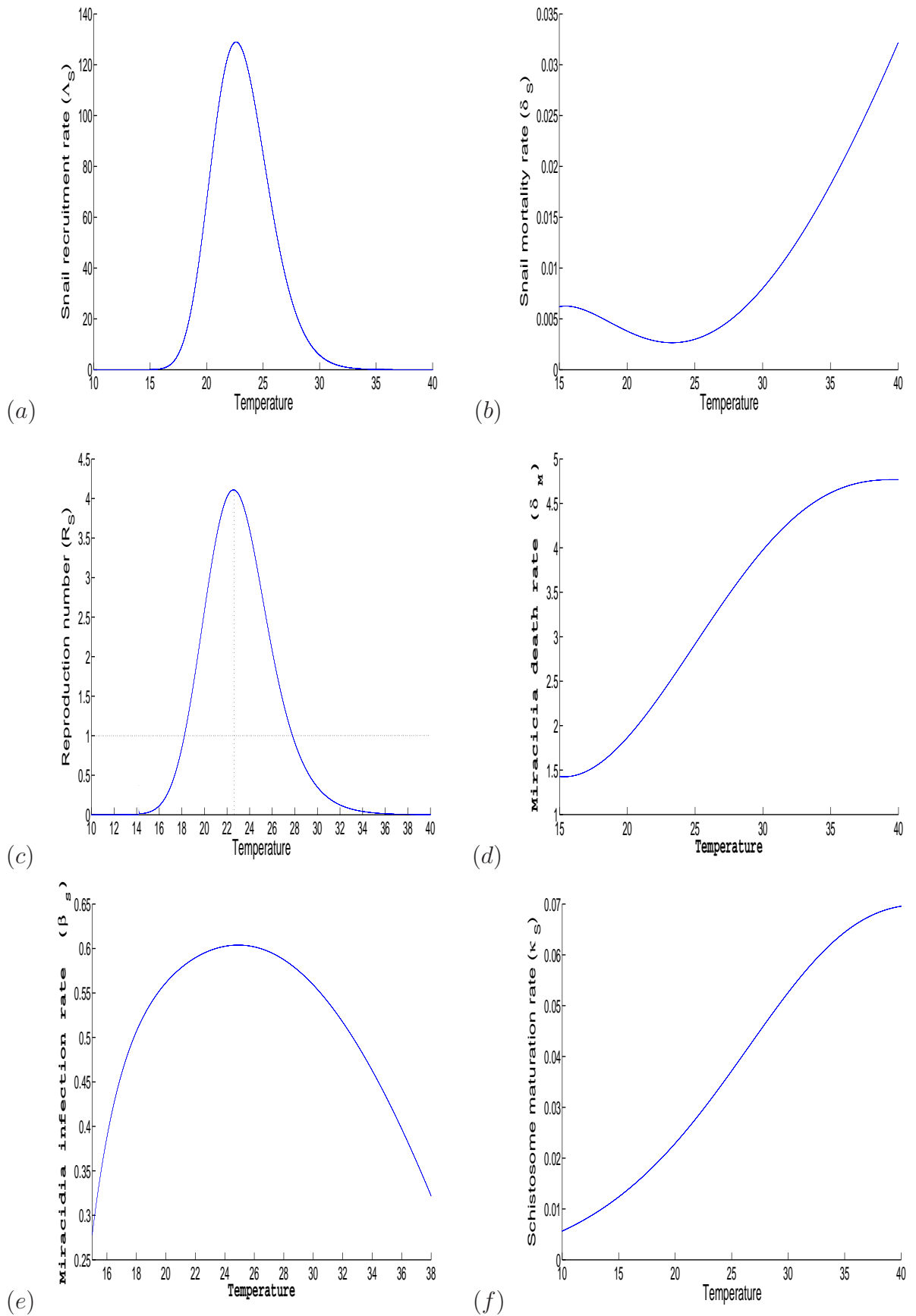
Figure 4.2: Simulation of (a) Snail egg laying rate, (b) Snail mortality rate, (c) R_s, (d) Miracidia death rate, (e) Miracidia infection rate and (f) within snail schistosome maturation rate using parameter functions in Table 1.

In Figure 4.3, simulations show convergence to the endemic equilibrium point of pre-patent snails, patent snails, exposed humans and infectious humans is illustrated. Results show that in the long term, the effects of temperature within the range $20 - 25^{o}C$ on human infectivity is more or less constant.

Figure 4.3: Simulation of infected snails and human populations with varying temperature, using model system (2).

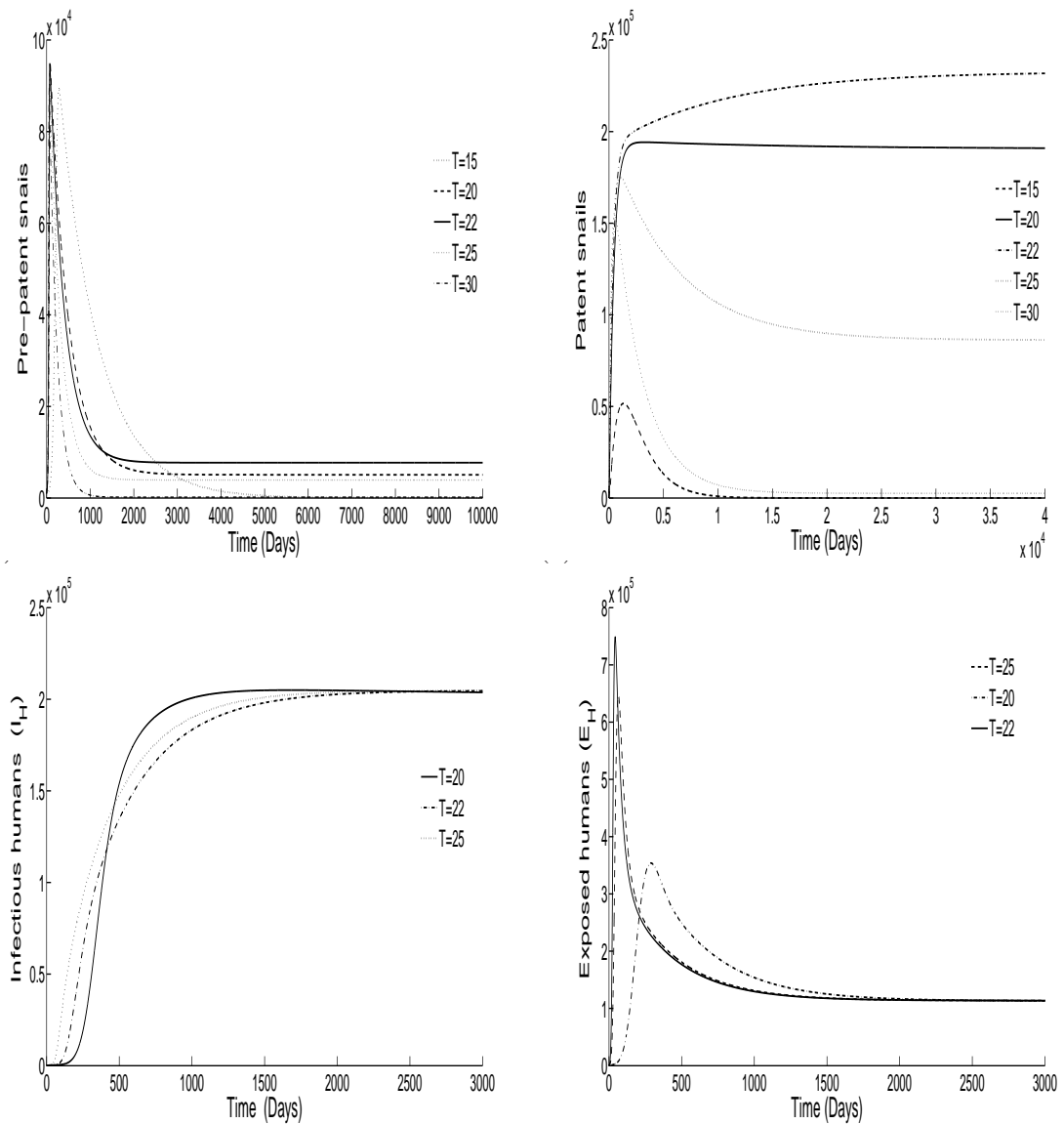Figure 4.4 shows different reproduction numbers across Zimbabwe. Cooler and warmer colours represent low and high reproduction numbers respectively. Thus based on temperature alone highest reproduction numbers are in the lower veld and the Zambezi valley catchment area. Higher reproduction numbers signify higher incidences of schistosomiasis. Based on these results which are temperature dependant, it is shown that most major towns have very low incidence of schistosomiasis if we are to base the results on temperature only.
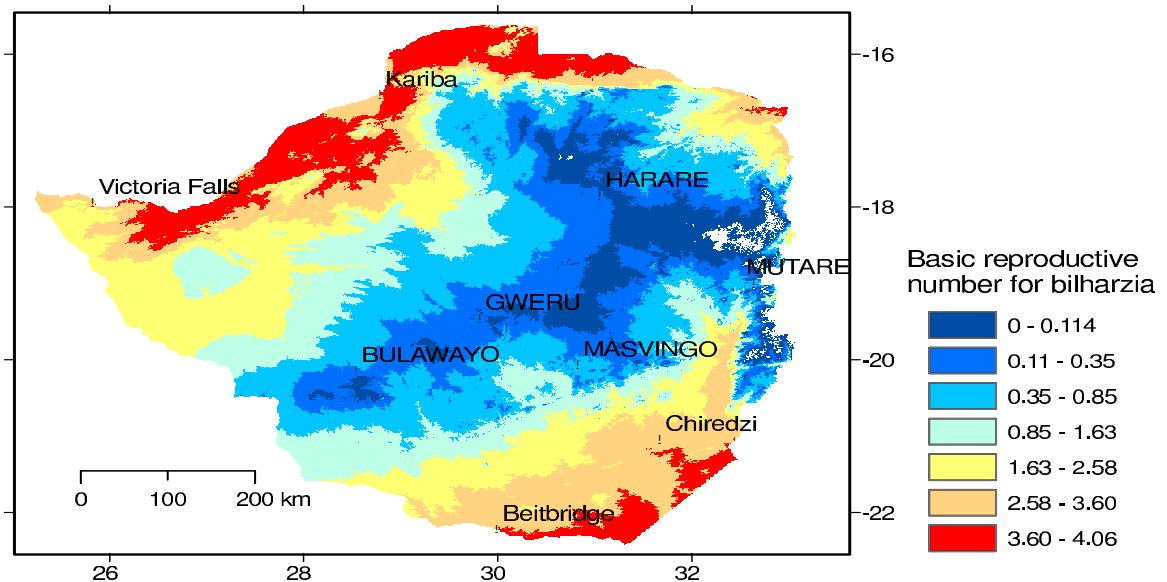
Figure 4.4: Variation of reproduction number R_s as a function of temperature in Zimbabwe.

In Figure 4.5, the combined effects of temperature and rainfall patterns in Zimbabwe from 1950-2000 were used to map the reproduction number risk map for schistosomiasis transmission. As the intensity of the colour increases, the reproduction number also increases. Therefore, high reproductive numbers are found in the lower veld of Zimbabwe and along the Zambezi valley catchment area. This correlates with high incidence of schistosomiasis. This result is in total agreement

with Midzi *et al* (2014) who obtained similar results for the cross-sectional survey of 280 primary schools country wide. The combined effect of rainfall and temperature seem to lower the reproduction number as the reproduction number is a decreasing function of rainfall.
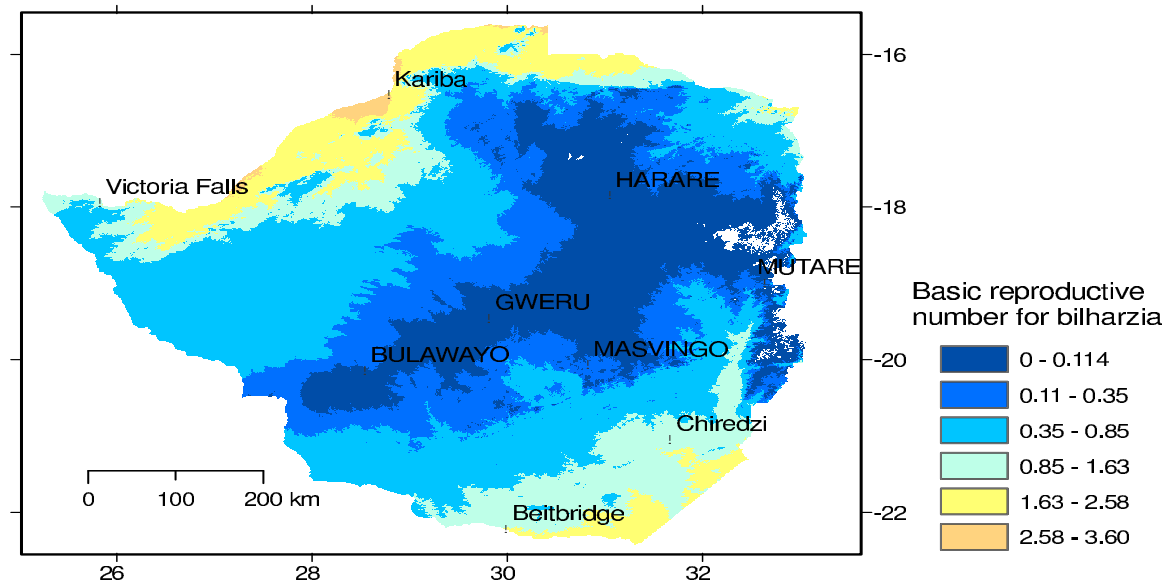
Figure 4.5: Variation of reproduction number R_s as a function of temperature and rainfall in Zimbabwe.

4.5. Discussion

In this chapter, a mathematical model to explore the impact of temperature and water bodies taken in the context of rainfall on schistosomiasis transmission is presented as a system of differential equations and analysed. In agreement with Dagal *et al.* (1986), the model analysis suggests that the temperature range of 18^oC to 28^oC is found to be ideal for schistosomiasis transmission. The reproduction number increases as temperature increases to attain a maximum around 23^oC,

beyond which the reproduction number starts declining. This result suggests the optimal temperature for schistosomiasis transmission is around 23^oC. The analytic results are also supported by numerical simulations which show an increased infection among snails at 22^oC as compared to at 20^oC and 25^oC. At 30^oC the infection dies out. Amongst humans however, the infection is endemic from $20-25^oC$ and the differences in transmission in relation to temperatures are minimal. Geographical information systems (GIS) was used to map the reproduction number on the Zimbabwe map using temperature and rainfall data from 1950-2000. It was noted that high reproduction numbers are found in the Zambezi valley catchment area and the lower veld of the country. High reproduction numbers suggest high incidences of schistosomiasis. The results of this manuscript can be used to identify areas which need special attention with regard to schistosomiasis control. Chiredzi, a known irrigated sugarcane producing area and Mushandike areas in the lowveld of Zimbabwe are among those requiring special attention in the fight against schistosomiasis. This can be extended to incorporate other aspects like the terrain of the country under study to capture the real dynamics of what happens on the ground.

Chapter 5

Mapping malaria and schistosomiasis coinfection in Africa and South America

5.1. Introduction

Malaria and schistosomiasis are the worlds two most important parasitic infections in terms of distribution, morbidity, and mortality. Both infections are highly endemic in tropical and sub tropical areas (Adegnika and Kremsner, 2012; Akue *et al.*, 2011; Brooker *et al.*, 2007). In the tropics, Sub Saharan Africa bears the heaviest burden of Plasmodium infections and 90% of all schistosomiasis cases worldwide are confined into this part of the world (Hotez and Kamath 2009; Simoonga *et al.* 2009). In areas where Plasmodium and Schistosoma species are both endemic,

coinfections are common. Research on parasitic infections has over the years been focused on a singular disease, in recent years however there has been a growing recognition that patients in tropical regions worldwide often experience dual infections (Keusch and Migasena, 1982). In parasitic coinfection, the interactions between diseases can cause altered immunologic and pathological outcomes compared to what usually occurs with single infections (Supali *et al.*, 2010).

Epidemiological studies have shown that heavy schistosomiasis mansoni infections are associated with a significant increase in the incidence of malaria among school-age children (Ndefo Mbah *et al.* 2014). In this chapter, we extend the work done in Chapters 2, 3 and 4 to come up with coinfection of the two tropical infections. The current work is focused on predicting the coinfection pattern of schistosomiasis and malaria, laying the basis for public health management system to map intervention strategies and allocate resources accordingly for eliminating the diseases.

5.2. Model formulation

A mathematical model for the interplay between malaria and S. mansoni is developed. Malaria and schistosomiasis transmission is modeled as follows: At each point in time people can be in one of seven states: susceptible (S), malaria exposed (E_{HM}), malaria infectious (I_{HM}), recovered with temporary immunity (R), schistosomiasis exposed (E_{HS}), schistosomiasis infectious (I_{HS}) and schistosomiasis and malaria coinfected (X).

Upon infection with the malaria parasite, individuals will then move to the ex-

posed class E_{HM}, where parasites in their bodies are still in the asexual stages. Both human and mosquito infections take time to develop into an infectious state. We assume that exposed individuals are not capable of transmitting the disease to susceptible mosquitoes as they do not have gametocytes. Humans exposed to the malaria parasite progress at a rate κ_H to the infectious class, in which they now have gametocytes in their bloodstream making them capable of infecting the susceptible anopheles mosquitoes. Treated individuals recover at a rate α_M with temporary immunity and enter the class R. Temporarily immune individuals lose immunity at a rate γ and join the susceptible class. Infected individuals who do not seek treatment die from malaria infection at a rate η. The birth rate for humans is θ and individuals die naturally at a rate μ_H. Within host parasite dynamics are weather independent, but within vector parasite dynamics, as well as the mosquito life cycle are weather dependent. The mosquito population is divided into the juvenile ($J_M(t)$) and adult population which is subdivided into three classes: susceptible ($S_M(t)$), exposed $E_M(t)$ and infectious ($I_M(t)$). Adult mosquitoes are recruited from the juvenile mosquito population at a rate Λ_M. The rate of infecting a susceptible mosquito depends on the mosquitoes' biting rate a and the proportion of bites by susceptible mosquitoes on infected humans that produce infection b_M. Susceptible mosquitoes that feed on infectious humans will take gametocytes in blood meals, but as they do not have sporozoites in their salivary glands, they enter into the exposed class. After fertilisation, sporozoites are produced and migrate to the salivary glands ready to infect any susceptible host, the vector is then considered as infectious. Mosquitoes die at a rate μ_M which is independent of infection status.

Infected mosquitoes are not harmed by the infection, never clear their infection and the infective period of the mosquito ends with its death.

For schistosomiasis transmission, the model is based on monitoring the dynamics of the populations at any time t of susceptible humans S_H, exposed humans E_{HS}, infected humans I_{HS}, miracidia M, susceptible snails U, prepatent snails L patent snails I_S and the cercariae C. The susceptible population is the same population susceptible to malaria. Susceptible individuals acquire infection at a rate $\lambda_H = \dfrac{\beta_H C(t)}{C_0 + \epsilon C(t)}$, where β_H is the cercarial infection rate, C_0 is a saturation constant for the cercariae and ϵ is the limitation of the growth velocity of cercariae with the increase of cases. Upon infection, an individual does not automatically become infectious but enters an exposed class as the incubation period of schistosomiasis ranges from 4-8 weeks for schistosomiasis mansoni and schistosomiasis japonicum, respectively (Cohen, 1977; Spira, 2003). Individuals then progress to the infectious compartment at a rate κ_{HS}. Susceptible and infected individuals suffer from natural death rate μ_H, but infectious individuals have an additional host mortality δ_H. Treated individuals recover at a rate α_s to join the class R with temporary immunity. Adult schistosomes within infected human hosts produce eggs which hatch and develop to free-swimming miracidia at a net rate θ_M. Miracidia either die at a rate δ_M or infect uninfected snails at rate $\lambda_S = \dfrac{\beta_S M}{M_0 + \epsilon M}$. Adult snails are recruited into the susceptible snail population at a rate Λ_S. Upon infection, snails enter the latently infected class from which they progress to the patent infected class at a rate κ_S. Adult snails die naturally at rate μ_S and infected adult snails also die due

to parasite-induced mortality at an additional rate α. The patent infected snails will then release a second form of free swimming larvae called cercariae at a rate θ_C which is capable of infecting humans. Cercariae die naturally at the rate δ_C.

Individuals can be dually infected by malaria and schistosomiasis. We assume that individuals who aquire malaria infection while they are already infected with schistosomiasis will progress to being malaria infectious faster. Individuals who are already malaria infectious cannot aquire schistosomiasis because of reduced contact with water as they are already considered less mobile due to malaria disease. Individuals who show symptoms of schistosomiasis when further infected with malaria parasites, quickly progress to the infectious state of malaria hence the modification parameter p. Thus the coinfection compartment X consists of individuals who are dually infected. Individuals in the compartment X recover from treatment of both malaria and schistosomiasis at a rate α_{SM} to join the class R. Individuals who are not treated from compartment X as a result of dual infection die at a rate η_{SM}.

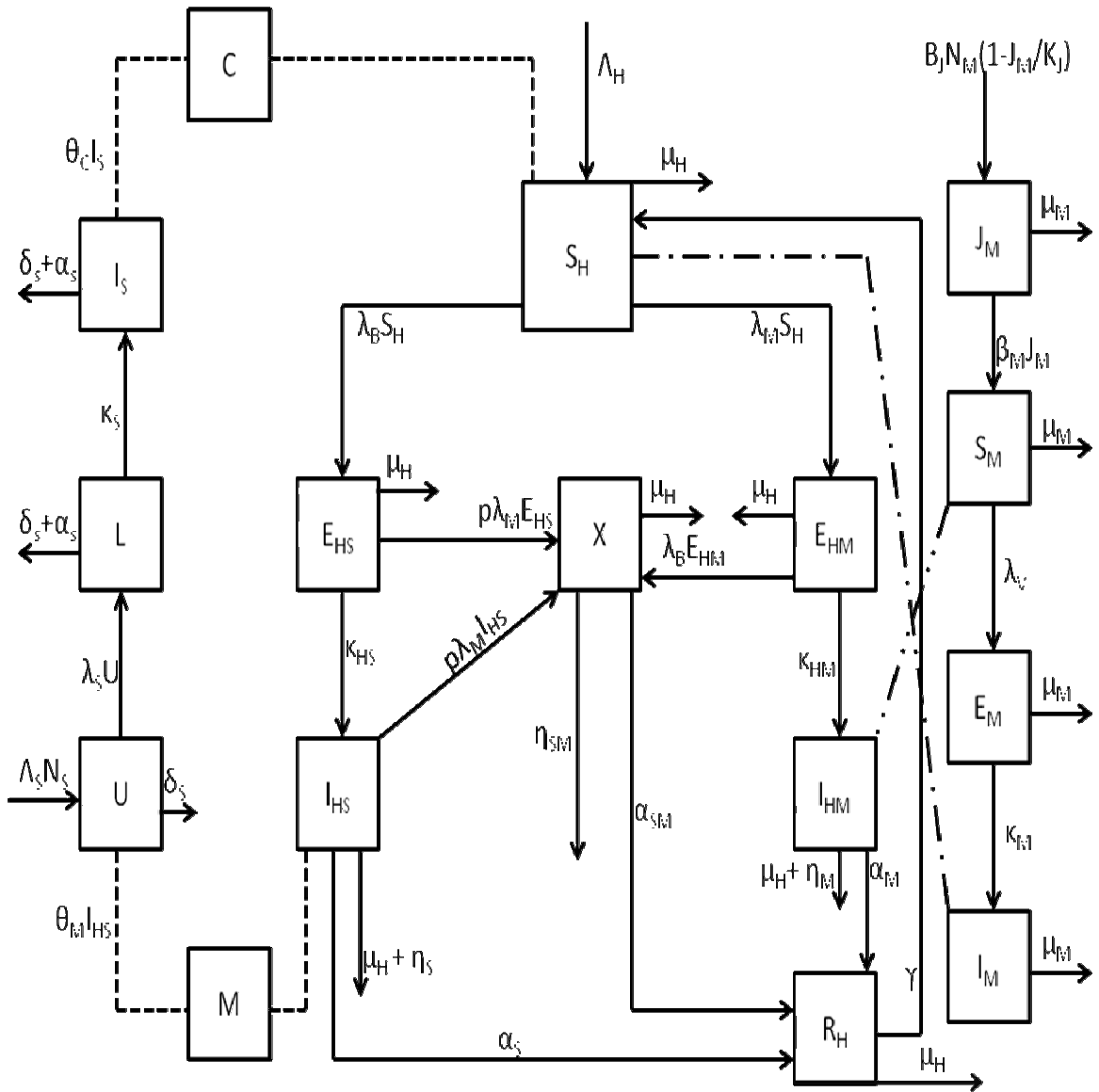The model flow diagram is presented in Figure 5.1.

Figure 5.1: Malaria schistosomiasis coinfection model.

The model equations describing the dynamics of infection are as follows

$$S'_H(t) = \Lambda_H - \lambda_M(T,R)S_H - \lambda_B(T,R)S_H - \mu_H S_H + \alpha_S I_{HS} + \gamma R,$$

$$E'_{HM}(t) = \lambda_M(T,R)S_H - (\kappa_{HM} + \mu_H)E_{HM},$$

$$I'_{HM}(t) = \kappa_{HM}E_{HM} - (\mu_H + \alpha_M + \eta)I_H,$$

$$R'_H(t) = \alpha I_{HM} - (\gamma + \mu_H)R_H,$$

$$J'_M(t) = \beta_J(T)N_M(1 - \frac{J_M}{K}) - \mu_J(T)\ J_M - \beta_M(T)J_M,$$

$$S'_M(t) = \beta_M(T)J_M - \lambda_V(T,R)S_M - \mu_M(T)S_M,$$

$$E'_M(t) = \lambda_V(T,R)S_M - (\kappa_M(T) + \mu_M(T))E_M,$$

$$I'_M(t) = \kappa_M(T)E_M - \mu_M(T)I_M,$$

$$E'_{HS}(t) = \frac{\beta_H C S_H}{C_0 + \epsilon C} - (\kappa_{HS} + \mu_H)E_{HS}, \tag{5.1}$$

$$I'_{HS}(t) = \kappa_{HS}E_{HS} - (\mu_H + \delta_H + \gamma_H)I_{HS},$$

$$M'(t) = \theta_M I_H - \frac{\beta_S M U}{M_0 + \epsilon M} - \delta_M M,$$

$$U'(t) = \Lambda_S - \frac{\beta_S M U}{M_0 + \epsilon M} - \mu_S U,$$

$$L'(t) = \frac{\beta_S M U}{M_0 + \epsilon M} - (\mu_S + \alpha + \kappa)L,$$

$$I'_S(t) = \kappa L - (\mu_S + \alpha)I_S,$$

$$C'(t) = \theta_C I_S - \frac{\beta_H C S_H}{C_0 + \epsilon C} - \delta_C C,$$

$$X'(t) = \lambda_M(E_{HS} + I_{HS}) + \lambda_B E_{HM} - \alpha_{SM} X - \mu_H X,$$

where, $\lambda_M = \dfrac{a(T,R)b_H I_M}{N_M}$, $\lambda_V = \dfrac{a(T,R)b_M I_{HM}}{N_H}$, $\lambda_B = \dfrac{\beta_H C}{C_0 + \epsilon C}$ and $\lambda_S = \dfrac{\beta_S M}{M_0 + \epsilon M}$.

Note that

$$N_H = S_H + E_{HM} + I_{HM} + R + E_{HS} + I_{HS} + X,$$

$$N_V = S_M + E_M + I_M,$$

$$N_S = U + L + I_S.$$

(5.2)

5.2.1. Positivity and boundedness of solutions

Model (5.1) describes the human, juvenile mosquito, adult mosquito, snail, miracidia and cercarea populations and therefore it can be shown that the associated state variables are non-negative for all time $t \geq 0$ and that the solutions of the model (5.1) with positive initial data remains positive for all time $t \geq 0$. We assume the associated parameters are nonnegative for all time $t \geq 0$. We show that all feasible solutions are uniformly bounded in a proper subset $\Psi = \Psi_H \times \Psi_J \times \Psi_V \times \Psi_S \times \Psi_C \times \Psi_M$.

Theorem 5.1. *Solutions of the model (5.1) are contained in the region* $\Psi = \Psi_H \times \Psi_J \times \Psi_V \times \Psi_S \times \Psi_C \times \Psi_M$.

Proof. To show that all feasible solutions are uniformly-bounded in a proper subset Ψ, we split the model (5.1) into the human component (N_H), juvenile mosquito component J_M, the adult mosquito component (N_V), the snail component (N_S), the miracidia component (M) and the cercarea component (C) given by equations (5.2).

Let

$$(S_H, E_{HM}, I_{HM}, R, E_{HS}, I_{HS}, X) \in \mathbb{R}^7_+$$

be any solution with non-negative initial conditions. From the theorem by Birkhoff and Rota (1989) on differential inequality it follows that

$$\limsup_{t \to \infty} S_H(t) \leq \frac{\Lambda_H}{\mu_H}.$$

Taking the time derivative of N_H along a solution path of the model (5.1) gives

$$\frac{dN_H}{dt} = \Lambda_H - \mu_H N_H - \eta_M I_{HM} - \eta_S I_{HS} - \eta_{SM} X.$$

Then,

$$\frac{dN_H}{dt} \leq \Lambda_H - \mu_H N_H.$$

From the theorem by Birkhoff and Rota (1989) on differential inequality it follows that

$$0 \leq N_H \leq \frac{\Lambda_H}{\mu_H} + N_H(0) e^{-\mu_H t}$$

where $N_H(0)$ represents the value of (5.2) evaluated at the initial values of the respective variables. Thus as $t \to \infty$, we have

$$0 \leq N_H \leq \frac{\Lambda_H}{\mu_H}.$$

This shows that N_H is bounded and all the feasible solutions of the human only component of model (5.1) starting in the region Ψ_H approach, enter or stay in the

region, where

$$\Psi_H = \left\{ (S_H, E_{HM}, I_{HM}, R, E_{HS}, I_{HS}, X) : N_H \leq \frac{\Lambda_H}{\mu_H} \right\}. \tag{5.3}$$

Similarly, let

$$(S_V, E_V, I_V) \in \mathbb{R}_+^3$$

be any solution with non-negative initial conditions. Then

$$\limsup_{t \to \infty} S_V(t) \leq \frac{\Lambda_V}{\mu_V}.$$

Taking the time derivative of N_V along a solution path of the model (5.1) gives

$$\frac{dN_v}{dt} = \Lambda_V - \mu_V N_V.$$

The mosquito-only component (5.2) has a constant population size. Therefore,

$$\frac{dN_V}{dt} \leq \Lambda_V - \mu_V N_V.$$

From the theorem by Birkhoff and Rota (1989) on differential inequality it follows that

$$0 \leq N_V \leq \frac{\Lambda_V}{\mu_V} + N_V(0)e^{-\mu_V t},$$

where $N_V(0)$ represents the value of (5.2) evaluated at the initial values of the respective variables. Thus as $t \to \infty$, we have

$$0 \leq N_V \leq \frac{\Lambda_V}{\mu_V}.$$

This shows that N_V is bounded and all the feasible solutions of the mosquito only component of model (5.1) starting in the region Ψ_V approach, enter or stay in the region, where

$$\Psi_V = \{(S_V, E_V, I_V) : N_V \le \Lambda_V \mu_V\}. \tag{5.4}$$

Similarly, let

$$(U, L, I_S) \in \mathbb{R}^3_+$$

be any solution with non-negative initial conditions. Then

$$\limsup_{t\to\infty} U(t) \le \frac{\Lambda_S}{\mu_S}.$$

Taking the time derivative of N_S along a solution path of the model (5.1) gives

$$\frac{dN_S}{dt} = \Lambda_S - \alpha(L + I_S) - \mu_S N_S.$$

The snails-only component (5.2) has a varying population size. Therefore,

$$\frac{dN_S}{dt} < \Lambda_S - \mu_S N_S.$$

From the theorem by Birkhoff and Rota (1989) on differential inequality it follows that

$$0 \le N_S \le \frac{\Lambda_S}{\mu_S} + N_S(0)e^{-\mu_S t},$$

where $N_S(0)$ represents the value of (5.2) evaluated at the initial values of the

respective variables. Thus as $t \to \infty$, we have

$$0 \leq N_S \leq \frac{\Lambda_S}{\mu_S}.$$

This shows that N_S is bounded and all the feasible solutions of the snails only component of model (5.1) starting in the region Ψ_S approach, enter or stay in the region, where

$$\Psi_S = \{(U, L, I_S) : N_S \leq \frac{\Lambda_S}{\mu_S}\}. \tag{5.5}$$

All feasible solutions of model system (5.1) enter the region

$$\Psi = \begin{cases} \Psi_H = (S_H, E_{HM}, I_{HM}, R, E_{HS}, I_{HS}, X) \in \mathbb{R}_+^7 : N_H \leq \frac{\Lambda_H}{\mu_H}, \\[2em] \Psi_J = J_M \in \mathbb{R}_+ : J_M \leq K, \\[2em] \Psi_V = (S_V, E_V, I_V) \in \mathbb{R}_+^3 : N_V \leq \frac{\Lambda_V}{\mu_V}, \\[2em] \Psi_S = (U, L, I_S) \in \mathbb{R}_+^3 : N_S \leq \frac{\Lambda_S}{\mu_S}, \\[2em] \Psi_M = M \in \mathbb{R}_+ : M \leq \frac{\theta_M \Lambda_H}{\delta_M \mu_H}, \\[2em] \Psi_C = C \in \mathbb{R}_+ : C \leq \frac{\theta_C \Lambda_S}{\delta_C \mu_S}, \end{cases} \tag{5.6}$$

which is positively invariant and attracting and it is sufficient to consider solutions in Ψ. Existence, uniqueness and continuation results for system (5.1) hold in this region and all solutions starting in Ψ remain in there for all $t \geq 0$. Hence, (5.1) is mathematically and epidemiologically well-posed and it is sufficient to consider the

dynamics of the flow generated by the model system (5.1) in Ψ. Also, all parameters and state variables for model system (5.1) are assumed to be non-negative since it monitors human, mosquito, snail, miracidia and cercariae populations.   □

5.2.2.   Disease free equilibrium (DFE)

The disease free equilibria,

$$E^0 = (\frac{\Lambda_H}{\mu_H}, 0, 0, 0, \frac{\beta_J N_M K}{\beta_J + K(\mu_J + \beta_M)}, \frac{\beta_M \beta_J N_M K}{\mu_M[\beta_J + K(\mu_J + \beta_M)]}, 0, 0, 0, 0, 0, \frac{\Lambda_S}{\mu_S}, 0, 0, 0, 0).$$

The coinfection reproduction number

$$R_{sm} = \max \left\{ \sqrt{\frac{a^2 b_H b_M \kappa_H \kappa_M S_H S_M}{Z_1}}, \sqrt{\frac{\beta_H \beta_S \theta_C \theta_M \kappa_{HS} \kappa_S S_H U}{Z_2}} \right\},$$

$$= max\left\{ R_m, R_s \right\},$$

(5.7)

where

$$Z_1 = \mu_M N_H N_M (\eta + \alpha_M + \mu_H)(\kappa_{HM} + \mu_H)(\kappa_M + \mu_M),$$

and

$$Z_2 = C_0 M_0 \delta_C \delta_M (\gamma_H + \delta_H + \mu_H)(\kappa_{HS} + \mu_H)(\alpha + \mu_S)(\alpha + \kappa_S + \mu_S).$$

The parameters used for numerical simulations are taken from Tables 3.1 and 4.1

5.3.   Results

Figure 5.2 shows the simulated basic reproduction numbers for malaria and schistosomiasis on the African continent and the Americas based on the baseline cli-

mate. This ideally shows the regions where the environmental ambient conditions allow malaria endemicity alone, schistosomiasis endemicity alone or coinfection insighted from the model.
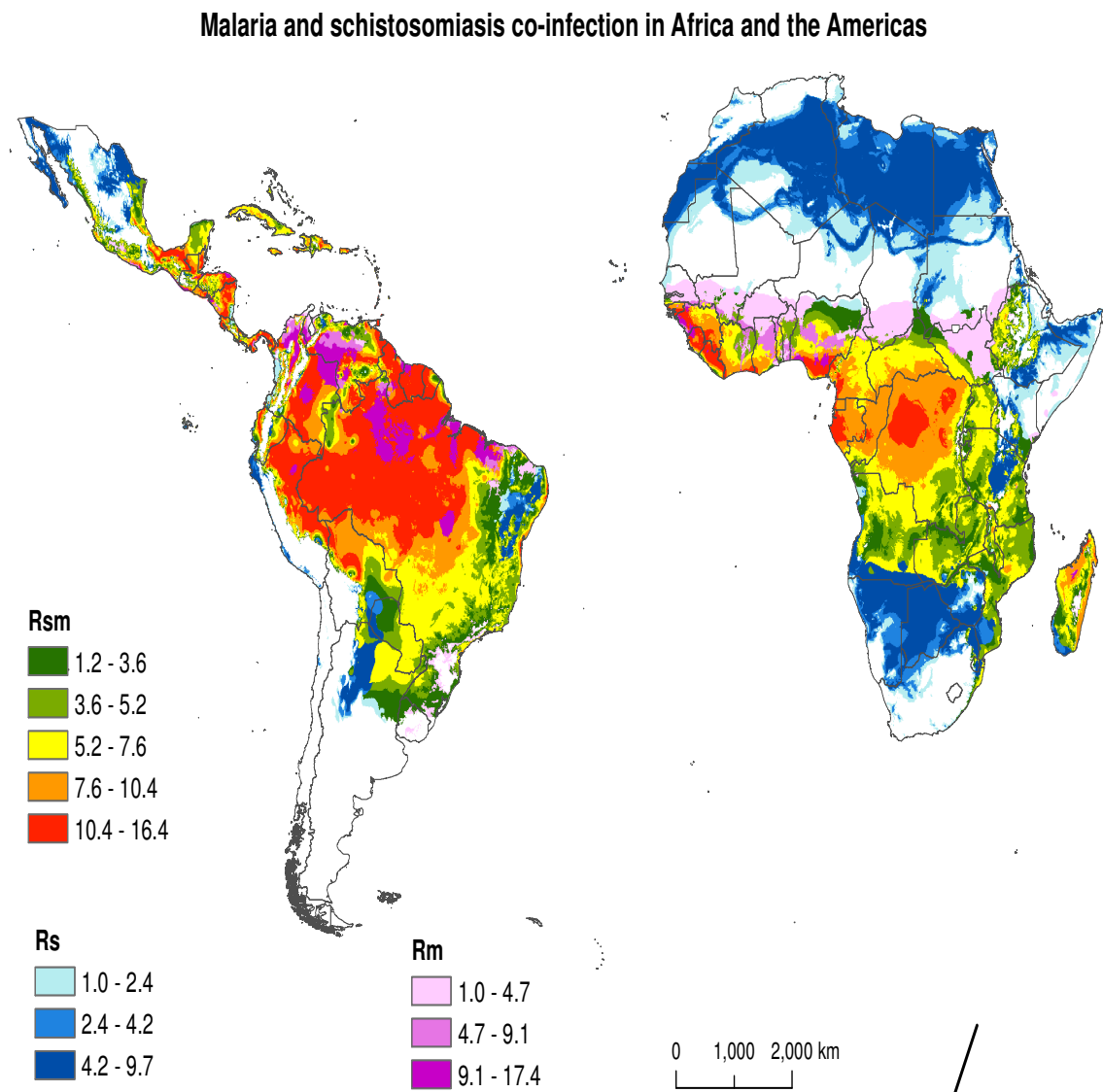
Malaria and schistosomiasis co-infection in Africa and the Americas

Figure 5.2: Malaria schistosomiasis coinfection pattern.

5.4. Discussion

A mathematical model for schistosomiasis and malaria coinfection incorporating rainfall and temperature is analysed. The coinfection reproduction number is computed and mapped on the continents of Africa and South America. Results from the mapping suggest that environmental ambient conditions in the equatorial regions of Africa and Latin America promote malaria and schistosomiasis coinfection with a heavier burden of coinfection in South America especially Brazil. Within Africa, there are some countries where it is beneficial to target both diseases for example DRC, Angola, Madagascar except the southern tip. The same pattern of coinfection is observed in South America. However there are some areas where targeting Malaria only is warranted. In the sub-tropical regions, including Namibia, South Africa and the greater part of Zimbabwe schistosomiasis is more dominant than malaria. The same goes for the areas on the northern fringe of the Sahara. Results show that coinfection is a greater problem in general in South America than in Africa. These results also suggest that one of the reasons why malaria mortality is higher in Africa may not necessarily be because of endemicity but of poor and failing health systems. Results of this current work also correspond with the targerted areas of control of schistosomiasis in South America (CDC, 2012). However health systems should target both diseases in Africa and the Americas as schistosoma infection enhances malaria incidence (Ndeffo *et al.*, 2014).

Chapter 6

Conclusion

6.1. Introduction

In this study, climate driven deterministic models of malaria, schistosomiasis and a coinfection model for malaria and schistosomiasis were developed. Temperature and rainfall were incorporated in the models to explore the effects of climate variability and change on the disease transmission dynamics. Calculated reproductive rates of the models were mapped to determine whether results from mathematical models agree with the situation on the ground. Projections were made for future transmission dynamics in order to inform policy makers on how to deal with diseases in the future.

6.2. Summary and concluding remarks

In Chapter 2, a human-mosquito population model for malaria dynamics incorporating temperature dependant parameters was developed. Results from the model suggests that temperature range 23^0C to 38^0C is ideal for malaria transmission. Beyond 38^0C mosquito mortality is extremely high and the reproduction number drops below unit. The model suggests that optimal temperature for malaria transmission is around 31^0C. The analysed results are also supported by numerical simulations which show an increase in malaria cases as temperature increases to about 38^0C and a decrease thereafter. Results of the partial rank correlation coefficients (PRCCs) illustrated that the death rate of mosquitoes has a negative impact on the reproduction number. This then suggests that any factor which contributes to increased mosquito mortality has potential to reduce malaria transmission.

In Chapter 3 the aspect of water bodies as a result of rainfall is incorporated into the model formulated in Chapter 2. Apart from the optimal temperature for malaria transmission being around 31^0C, results from the model analysis suggested a daily rainfall in the range of $15 - 17mm$ is ideal for the spread of malaria. The reproduction number dependent on both temperature and rainfall is applied to gridded temperature and rainfall datasets to determine the transmission pattern of malaria across Africa. The results of the transmission pattern fall within the observed falciparum limit of 2010 Gething *et al.* (2011). The reproduction number is also applied to projected datasets of temperature and rainfall to predict the future impact of climate change on malaria transmission. Results from the study

suggest that in future, malaria will die out on the southern fringe of the disease in Africa, giving hope for malaria eradication in Southern Africa. However malaria will remain endemic in the tropics and coastal areas of East Africa. Furthermore, results of the study suggest an upward shift of the northern limit of falciparum malaria and endemic malaria will become a problem in the African highlands.

In Chapter 4 a schistosomiasis transmission model with parameters related to snails and parasite dynamics dependent on temperature is developed. The snail recruitment rate was dependant on both temperature and rainfall. The mathematical analysis of the model was done and the reproduction number for schistosomiasis transmission was mapped to temperature and rainfall datasets from Zimbabwe. Environmental ambient conditions suitable for endemic schistosomiasis were suggested to be in the lower veld of Zimbabwe and along the Zambezi valley catchment area. Results of the study suggest an optimal temperature for schistosomiasis transmission around 23^0C.

In Chapter 5 a rainfall and temperature dependent malaria and schistosomiasis coinfection model is developed. The coinfection reproduction number is also computed and mapped to show the effect of climate variability on the pattern of coinfection in Africa and the Americas. Results from the study suggest a high burden of schistosomiasis coinfection in Africa and Latin America along the tropics and subtropics. These results suggest both schistosomiasis and malaria control programmes in these areas. In countries on the northern fringe of the Sahara, and the sub tropical regions of Africa including Namibia, South Africa and the greater part

of Zimbabwe, channelling resources towards eliminating schistosomiasis should be a priority.

6.3. Future research directions

The results of this thesis leave room for possible future research. We propose the following extensions.

- In this study we have gained insight into the effects of climate variability on the dynamics of schistosomiasis and the effect of climate change on the dynamics of malaria. The knowledge gained from this theoretical study can be used in the implementation of a practical project, thus a possible extension of this thesis would be to consider the implementation of practical projects in the light of this work for African countries.

- Given that lymphatic filariasis is also a mosquito transmitted infection, its coinfection with malaria may also be investigated in light of climate change.

- Possible extensions of this thesis are to incorporate other aspects like human migration, relative humidity, the role of socio-economic factors and the spatial variation of the countries under study to capture the the real transmission dynamics of schistosomiasis and malaria.

Bibliography

Adegnika AA, Kremsner PG. Epidemiology of malaria and helminth interaction: a review from 2001 to 2011, (2012). *Curr. Opin. HIV AIDS*.7:221-224.221224. doi: 10.1097/COH.0b013e3283524d90.

Akue JP, Nkoghe D, Padilla C, Moussavou G, Moukana H, Mbou RA, Ollomo B, Leroy EM, (2011). Epidemiology of concomitant infection due to Loa loa and Mansonella perstans in Gabon. *PLoS Negl Trop Dis*. doi: 10.1371/journal.pntd.0001329.

Alemu A, Abebe G, Tsegaye W, Golassa L, (2011). Climatic variables and malaria transmission dynamics in Jimma town, southwest Ethiopia. *Parasites & Vectors*. 4:30-41. 10.1186/1756-3305-4-30.

Alonso D, Bouma MJ and Pascual M, (2010). Epidemic malaria and warmer temperatures in recent decades in an East African highland. *Proc. R. Soc. Lond.B Biol. Sci.*, 278:1661-1669.

Anderson RM, May RM, (1991). Infectious diseases of humans: dynamics and control London: Oxford University Press.

Anderson RM, May RM, (1985). Helminth infections of humans: mathematical models, population dynamics, and control. *Adv Parasitol*. 24:1-101.

Andrade ZA, Bina JC, 1983. The pathology of the hepatosplenic form of Schistosoma mansoni infection. Memorial Institute. Oswaldo Cruz., 78:285-305.

Bailey NJT, (1975) The mathematical theory of infectious diseases, 2nd ed., Hafner, New York.

Barbour AD, (1996). Modeling the transmission of schistosomiasis: an introductory view. *Am. J. Trop. Med. Hyg*. 55:S135-S143.

Barbour AD, (1978). Macdonalds model and the transmission of bilharzia. *Trans Roy Soc Trop Med Hyg* 72:6-15.

Birkhoff G and Rota GC, (1989). Ordinary differential equations, 4th Edition, John Wiley and Sons, Inc., New York.

Blayneh K, Cao Y, and Kwon H, (2009). Optimal Control of Vector-borne Diseases: Treatment and Prevention.*DCDS Ser. B.* 11(3):587-611.

Bradley DJ and May RM, (1978). Consequences of helminth aggregation for dynamics if schistosomiasis. *Trans. Roy. Soc. Trop. Med. Hyg*. 72:262-273.

Brooker S, (2007). Spatial epidemiology of human schistosomiasis in Africa: risk models, transmission dynamics and control. *Trans. Roy. Soc. Trop. Med. Hyg*, 101:1-8

Brooker S, Akhwale W, Pullan R, Estambale B, Clarke SE, Snow RW, Hotez PJ, (2007). Epidemiology of plasmodium-helminth co-infection in Africa: populations at risk, potential impact on anemia, and prospects for combining control. *Am J Trop Med Hyg*. 77: 88-98.

De jesus AR, Gonzalez Miranda D, Gonzalez Miranda R, Arau Jo I, Andrea Magalha? ES, Bacellar M, Carvalho EM, (2000). Morbidity associated with schistosoma mansoni infection determined by ultrasound in an endemic area of Brazil. Caatinga do Moura. *Am. J. Trop. Med. Hyg*. 63:1-4.

CDC, Malaria facts. http://www.cdc.gov/malaria/about/facts.html

Center for Disease Control and Prevention,http://wwwnc.cdc.gov/travel/yellowbook/2012/chapter-3-infectious-diseases-related-to-travel/ schistosomiasis2696.

Chan MS, Isham VS, (1998). A stochastic model of schistosomiasis immunoepidemiology. *Math Biosci* 151:179-198.

Chan MS, Mutapi F, Woolhouse MEJ, Isham VS, (2000.) Stochastic simulation and the detection of immunity to schistosome infections. *Parasitology*. 120:161-169.

Castillo-Chavez C, Song B,(2004). Dynamical models of tuberculosis and their applications, *Math. Biosci. Eng*. 1:361-404.

Chitsulo L, Engels D, Montresor A, Savioli L,(2000). The global status of schistosomiasis and its control. *Acta Trop*. 77:41-51.

Chiyaka C, Tchuenche JM, Garira W, Dube S, (2007). A mathematical analysis of the effects of control strategies on the transmission dynamics of malaria, *Applied Mathematics and Computation*. 195(2):641-662.

Chiyaka E, Garira W, (2009). Mathematical Analysis of the Transmission Dynamics of Schistosomiasis in the Human-Snail Hosts, *J. Biol. Syst*. 17:397-423.

Cohen JE, (1977). Mathematical Models of Schistomiasis. Ann. Rev. *Ecol. Syst*. 8:209-33.

Colley DG, Bustinduy AL, Secor WE, King CH, (2014) Human schistosomiasis. *Lancet*. 383:2253-64.

Craig MH, Snow RW and le Sueur D, (1999). A Climate-based Distribution Model of Malaria Transmission in Sub-Saharan Africa. *Parasitology Today*. 15:105-111.

Dagal MA, Upatham ES, Kruatrache M, Viyanant V, (1986). Effects of some physico-chemical factors on the hatching of egg masses and on the survival of juvenille and adult snails of bilunus (physopsis) abyssinicus. *ScienceAsia* 12:023-030

Daley D.J and Gani J, (1999). Epidemic modelling : An introduction. Cambridge University Press.

Diekmann O, Heestterbeek JAP, Metz JAP, (1990). On the computation of the basic reproduction ratio R_0 in models for infectious diseases in heterogenous populations. *J. Math. Biol.*, **28**:365-382.

Dietz K, (1967). Epidemics and rumours: A survey, *J Roy Statist Soc Ser A*. 130:505-528.

Dietz K, (1988) The first epidemic model: A historical note on P. D. Enko, Austral. *J. Statist*. 30:56-65.

Feng Z, Li CC, Milner FA, (2002). Schistosomiasis models with density dependence and age of infection in snail dynamics. *Math Bioscience*. 177:271-286.

Gething P.W et al. (2011) A new world malaria map: Plasmodium falciparum endemicity in 2010, *Malar. J*. 10: 378.

Gubler DJ (1998) Resurgent vector-borne diseases as a global health problem. *Emerg Infect Dis* 4(3):442-450.

Hamer WH, (1906) Epidemic disease in England, *Lancet* 1:733-739.

Hay SI et al (2002) Climate change and the resurgence of malaria in the Eastern African highlands. *Nature* 415:905-909.

Heffernan JM, Smith RJ and Wahl LM, (2005). Perspectives on the basic reproductive ratio, *J R Soc Interface* 2(4):281293, 2005.

Hethcote HW, (2000). The mathematics of infectious diseases, *SIAM review*. 42(4):599-653.

Hoshen MB, Morse AP, (2005). A model structure for estimating malaria risk. In:Environmental change and malaria risk global and local implications, *Springer Dordrecht*, 41-50. ISBN 1-4020-3927-1.

Hotez PJ, Kamath A, (2009). Neglected tropical diseases in sub-saharan Africa: review of their prevalence, distribution, and disease burden. *PLoS Negl Trop Dis*. 3:e412. doi: 10.1371/journal.pntd.0000412.

Hotez PJ, Molyneux DH, Fenwick A, Ottesen E, Ehrlich Sachs S, et al. (2006) Incorporating a rapid-impact package for neglected tropical diseases with programs for HIV/AIDS, tuberculosis, and malaria. *PLoS Med* 3:e102. Available: http://dx.plos.org/10.1371/journal.pmed.0030102. Accessed 3 June 2013.

Hurlimann E, Schur N, Boutsika K, Stensgaard A-S, Laserna de Himpsl M, et al. (2011) Toward an open-access global database for mapping, control, and surveillance of neglected tropical diseases. *PLoS Negl Trop Dis* 5:e1404. Available:http://dx.plos.org/10.1371/journal.pntd.0001404. Accessed 30 June 2013.

Intergovernmental Panel on Climate Change, (2007). Working Group III Fourth Assessment Report, IPCC. See http://www.ipcc.ch/publications and data/publications and data reports.shtml.

Jia Li (2011) Malaria model with stage-structured mosquitoes, *Mathematical Biosciences and Engieering*. 8(3):753-768.

Killeen G, Fillinger U, Kiche I , Gouagna L and Knols B, (2002). Eradication of Anopheles gambiae from Brazil: lessons for malaria control in Africa?, *Lancet Infect Dis.*, 10:618-627.

Keusch GT, Migasena P. 1982. Biological implications of polyparasitism. *Rev. Infect. Dis.* 4:880-882.

Kochar DK, Kochar SK, Saxena V, Sirohi P, Garg S, Kochar A, Khatri MP, Gupta V, (2009) Severe Plasmodium vivax malaria: A report on serial cases from Bikaner in Northwestern India. *Am J Trop Med Hyg* 80(2):194-198.

Lawi GO, Mugisha JYT and Omolo-Ongati N, (2011). Mathematical Model for Malaria and Meningitis Co-infection among Children. *Applied Mathematical Sciences*. 47:2337-2359.

Lee KL. and Lewis ER, (1976). Delay time models of population dynamics with application to schistosomiasis control. I.L.E.E. *Trans Biomed Eng* 23:225-233.

Liang S, Maszle D and Spear RC, (2002. A quantitative framework for a multigroup model of Schistosomiasis japonicum transmission dynamics and control in Sichuan, *China. Acta Trop* 82:263-277.

Liang S, Spear ,; Seto E, Hubbard A, Qui D, (2005). A multi-group model of Schistosoma japonicum transmission dynamics and control: model calibration and control prediction. *Tropical medicine and International health*. 3:263-278.

Lindsay SW and Martens WJM (1998) Malaria in the African highlands: past, present and future. *Bulletin of the World Health Organisation* 76(1):33-45.

Macdonald G, (1965). The dynamics of helminth infections, with special reference to schistosomes. *Transactions of the Royal Society of Tropical Medicine and Hygiene* 59:489-506.

Mangal TD, Paterson S, Fenton A, (2008) Predicting the impact of long-term temperature changes on the epidemiology and control of schistosomiasis: a mechanistic model. *PLoS One*. 3:e1438.

McDonald G, (1957). The epidemiology and control of malaria . London : *Oxford University Press*.

Martens WJM, Jetten TH, Rotmans J, Niessen LW, (1995). Climate change and vector-borne diseases: a global modelling perspective. *Glob. Environ. Chang*. 5:195-209.

Martens WJM, Jetten TH, Focks DA, (1997). Sensitivity of malaria, schistosomiasis and dengue to global warming. *Clim Change*, 35:145-156.

Martens P, Niessen LW, Rotmans J et al, (1995). Potential impact of global climate change on malaria risk. *Environ Health Perspective* 103(5):458-464.

Martens WJM, Jetten TH, and Focks DA, (1997.) Sensitivity of malaria, schistosomiasis and dengue to global warming, *Clim.Change* 35:145-156.

Martens P, Thomas C, (2005). Climate change and malaria risk: Complexity and scaling. In W. Takken, P. Martens, R. Bogers (Eds.), Environmental change and malaria risk: global and local implications. Dordrecht: Springer

Mas-Coma S, Valero MA, Bargues MD, (2009). Climate change effects on trematodiases, with emphasis on zoonotic fascioliasis and schistosomiasis. *Vet Parasitol* 163:264-280.

McCreesh N, Booth M, (2014). The effect of increasing water temperatures on Schistosoma mansoni transmission and Biomphalaria pfeifferi population dynamics: An agent-based modelling study. *PLoS One* 9:e101462.

McMichael AJ, Haines, Sloof, Kovats, (1996). Climate Change and Human Health, *World Health Organization*, 78-86.

Mendis K, Sina BJ, Marchensini P, Carter R, (2001) The neglected burden of Plasmodium vivax malaria. *A J Trop Med Hyg*. 64(Suppl 1/2):97-106

Midzi *et al.*, (2014). Distribution of Schistosomiasis and Soil Transmitted Helminthiasis in Zimbabwe: Towards a National Plan of Action for Control and Elimination. *PLoS Negl Trop Dis* 8(8): e3014. doi:10.1371/journal.pntd.0003014

Mordecai E A et al, (2013.) Optimal temperature for malaria transmission is dramatically lower than previously predicted, *Ecology Letters* 16:22-30.

Nasell I, (1976). A hybrid model of schistosomiasis with snail latency. *Theor Pop Biol*. 10:47-69.

Ndeffo Mbah Martial L et al. (2014). Impact of Schistosoma mansoni on Malaria Transmission in Sub-Saharan Africa. *PLoS Negl Trop Dis*. 8(10):32-34.

Ngarakana-Gwasira ET, Bhunu CP & Mashonjowa E, (2014). Assessing the impact of temperature on malaria transmission dynamics. *Afrika Matematika*, Vol 25:1095-1112.

Ngarakana-Gwasira ET, Bhunu CP, Masocha M, Mashonjowa E, (2016). Transmission dynamics of schistosomiasis in Zimbabwe: A mathematical and GIS Approach. *Communication in Nonlinear Science and Numerical Simulation*, 35:137-147.

Ngarakana-Gwasira ET, Bhunu CP, Masocha M, Mashonjowa E, (2016). Assessing the Role of Climate Change in Malaria Transmission in Africa. *Malar Res Treat*, Article ID 7104291.

Paaijmans KP, Cator LJ, Thomas MB, (2013). Temperature-Dependent Pre-Bloodmeal Period and Temperature-Driven Asynchrony between Parasite Development and Mosquito Biting Rate Reduce Malaria Transmission Intensity. *PLOS ONE*. 8(1):e55777.

Parham, PE, and Michael E, (2010). Modelling climate change and malaria transmission, *Adv Exp Med Biol* 673:184-99.

Parham, P.E. & Michael, E. (2010) Modeling the Effects of Weather and Climate Change on Malaria Transmission. *Environmental Health Perspectives* 118(5):620-626.

Remai, J, (2010). Modeling Environmentally Mediated Infectious Diseases of Humans: Transmission Dynamics of Schistosomiasis in China. *Adv Exp Med Biol.*, 673:79-98.

Remais J, Hubbard A, Zisong W and Spear RC, (2007). Weather-driven dynamics of an intermediate host: mechanistic and statistical population modelling of Oncomelania hupensis.*Journal of Applied Ecology*. 44:781-791.

Remais J, Akullian A, Ding L, Seto E, (2010). Analytical methods for quantifying environmental connectivity for the control and surveillance of infectious disease spread. *J R Soc Interface*. 7(49):1181-93.

Roberts MG and Heesterbeek JAP , (2003). Mathematical Models in Epidemiology in Mathematical Models, [Eds. Filar JA and Krawczyk JB], in Encyclopedia of Life Support Systems (EOLSS), Developed under the auspices of the UNESCO, Eolss Publishers, Oxford, UK, [http://www.eolss.net].

Ross R, (1911) The prevention of malaria London: John Murray.

Ross R, (1915). Some a priori pathometric equations. *Br Med J* 1:546-447.

Ross R, (1916). An application of the theory of probabilities to the study of a priori pathometry - I. *Proc R Soc*, A92:204-230.

Ross R, (1916.) An application of the theory of probabilities to the study of a priori pathometry - II. *Proc R Soc*, A93:212-225.

Ross R, (1916). Hudson HP: An application of the theory of probabilities to the study of a priori pathometry - III. *Proc R Soc*, A93:225-240.

Rubel F, Brugger K, Hantel M, Chvala-Mannsberger S, Bakonyi T, Weissenbo H, Nowotny N, (2008). Explaining Usutu virus dynamics in Austria: Model development and calibration. *Preventive Veterinary Medicine*, 85:166-186.

Sambo LG, Ki-Zerbo G, Kirigia JM (2011) Malaria control in the African Region: perceptions and viewspoints on proceedings of the Africa Leaders Malaria Alliance (ALMA). *BMC Proc* 5 Suppl 5:S3.

Shetty P. Climate Change and Insect-borne Disease: Facts and Figures - SciDev.Net. http://www.scidev.net/en/south-east-asia/features/climate-change-and-insect-borne-disease-facts-and–1.html

Simoonga C, Utzinger J, Brooker S, Vounatsou P, Appleton C, Stensgaard As O, Kristensen T, (2009). Remote sensing, geographical information system and spatial analysis for schistosomiasis epidemiology and ecology in Africa. *Parasitology*. 136:1683-1693. doi: 10.1017/S0031182009006222.

Siraj AS et al, (2014.) Altitudinal Changes in Malaria Incidence in Highlands of Ethiopia and Colombia. *SCIENCE* 343:1154-1158.

Smith DL, McKenzie FE (2004.) Statics and dynamics of malaria infection in Anopheles mosquitoes. *Malar J* 3:13.

Spira AM, (2003). Assessment of travelers who return home ill. *THE LANCET*, 361:1459-69

Steinmann P, Keiser J, Bos R, Tanner M, Utzinger J, (2006). Schistosomiasis and water resources development: systematic review, meta-analysis, and estimates of people at risk. *Lancet Infect Dis*. 6:411-25.

Stensgaard A-S, Utzinger J, Vounatsou P, Hurlimann E, Schur N, et al. (2011.) Large-scale determinants of intestinal schistosomiasis and intermediate host snail distribution across Africa: Does climate matter? Acta Trop null. Available: http://dx.doi.org/10.1016/j.actatropica.2011.11.010. Accessed 28 June 2013.

Stocker TF, Qin D, Plattner G-K, Tignor M, Allen SK, Boschung J, Nauels A, Xia Y, Bex V, Midgley PM, (2013). Climate change : The physical science basis. In Intergovernmental Panel on Climate Change, Working Group I Contribution to the IPCC Fifth Assessment Report (AR5). New York: *Cambridge Univ Press*.

Sturrock RF, (1993). The intermediate hosts and host-parasite relationships. In P Jordan, G Webbe, RF Sturrock (eds), Human Schistosomiasis, CAB International, Wallingford, 33-85:

Supali T, et al. (2010). Polyparasitism and its impact on the immune system. *Int. J. Parasitol*. 40:1171-1176.

Thieme HR, (2003). Mathematics in Population Biology, *Princeton University Press*, Princeton.

Thomas CJ, Davies G and Dunn C, (2004). Mixed picture for changes in stable malaria distribution with future climate in Africa. *Trends in Parasitology* 20:216-220.

Ukoroije BR, Abowei JFN, (2012). Some Occupational Diseases in Culture Fisheries Management and Practices Part Two: Schistosomiasis and Filariasis, International Journal of Fishes and Aquatic Sciences 1(1):64-71.

Van der Werf MJ, de Vlas SJ, Brooker S, Looman CWN, Nagelkerke NJD, et al. (2003) Quantification of clinical morbidity associated with schistosome infection in sub-Saharan Africa. *Acta Trop* 86:125-139.

Volker Et, Fink A, Morse A and Paeth H, (2012). The impact of Regional Climate Change on Malaria Risk due to Greenhouse Forcing and Land -Use Changes in Tropical Africa. *Environmental Health Perspectives* 120:77-84.

Vos T, Flaxman AD, Naghavi M, Lozano R, Michaud C, Ezzati M, et al. (2012.) Years lived with disability (YLDs) for 1160 sequelae of 289 diseases and injuries 19902010: a systematic analysis for the Global Burden of Disease Study 2010. *Lancet*. 380:2163-96.

van den Driessche P and Watmough J, (2002) Reproduction numbers and the sub-threshold endemic equilibria for compartmental models of disease transmission. *Math. Biosci*., 180:29-48.

WHO 1993. The control of schistosomiasis. Geneva: World Health Organisation, Technical Report Series, No. 830.

WHO Expert Committee, (2002). Prevention and control of schistosomiasis and soil-transmitted helminthiasis. *World Health Organ Tech Rep Ser*. 912:1-57.

WHO, (2014). Schistosomiasis: number of people receiving preventive chemotherapy in 2012. *Wkly Epidemiol Rec*. 89:21-28.

WHO, (2013). Schistosomiasis: progress report 20012011 and strategic plan 20122020. Geneva: World Health Organization.

http://www.who.int/malaria/media/worldmalariareport2014/en/

http://www.who.int/malaria/media/worldmalariareport2015/en/

World Health Organization, (2012). Accelerating work to overcome the global impact of neglected tropical diseases: a roadmap for implementation. Geneva, Switzerland: World Health Organization.

Woolhouse MEJ, (1991). On the application of mathematical models of schistosome transmission dynamics. I. Natural transmission. *Acta Trop* 49:241-270.

Woolhouse MEJ (1992) On the application of mathematical models of schistosome transmission dynamics. II. Control. *Acta Trop* 50: 189-204.

Woolhouse MEJ, Chandiwana SK, (1990). Population dynamics model for Bulinus globosus, intermediate host for Schistosoma haematobium, in river habitats. *Acta Trop* 47:151-160.

World Malaria Report, (2011). World Health Organisation, Geneva, 278.

WHO (2013.) www.who.int/features/factfiles/malaria/en/.

World Malaria Report, (2014). www.who.int/malaria/publications/world-malaria-report-2014/en/.

World Health Organisation, (2015). http://www.who.int/mediacentre/factsheets/fs115/en/.

World clim database, www.worldclim.org

Zhou XN, Yang GJ, Yang K, Wang XH, Hong QB, Sun LP, Malone JB, Kristensen TK, Bergquist NR, Utzinger J, (2008) Potential impact of climate change on schistosomiasis transmission in China. *Am J Trop Med Hyg*, 78:188-194.

.

Appendix

The matlab code for numerical simulations in Figure 4.3 is presented below.

function dx = bilharzia(t,x) global PiH BH C0 epsilon muH deltaH gammaH a K piS deltaE thetaE lambdaM BS M0 deltaM deltaJ thetaS deltaS kappah kappas alpha lambdaC deltaC deltaP LambdaS $dx = zeros(8, 1);$

$T = 40;$

$a = 0.23;$

$b = -1.05;$

$c = 0.1;$

$P = 30;$

$Bm = 0.849;$

$BH = (-2.2957184151497) + (0.44586818702128) * log(T) + (2.95983357327484)/(log(T));$

$C0 = 90000000;$

$epsilon = 0.2;$

$muH = 0.00000384;$

$kappah = 0.017857;$

$deltaH = 0.0039;$

$gammaH = 0.006;$

$LambdaS = 2000 * exp(351.04480681884 + (-1925.49534415329)/T + (-85.1815135926783) * log(T));$

$kappas = 1/10 * (T/(6271.093098237131 + 165.427360339652 * T + (-1946.87993772373 * sqrt(T))));$

$thetaE = 0.0318402041755522/(1 + (-0.0416780520469753) * T + 0.000577602879269135 * T. * T);$

$lambdaM = 500;$

$BS = -8.59111 + 855/T - 31487.35/T^2 + 574921.12/T^3 - 5188906/T^4 + 18196700/T^5;$

$M0 = 100000000;$

$deltaM = 1/1000 * ((3.98974358865154E - 07) * T^5 + (-3.7263403251269E - 05) * T^4 + (4.96981351536597E - 04) * T^3 + (3.99238927794239E - 02) * T^2 + (-1.14921235431391) * T + 9.58999999983625);$

$deltaJ = (-2.19004925774938E - 04) + (2.66513140443254E - 07). * T. * T. * T +$

$(5.98522430001724E - 18). * exp(T);$

$thetaS = T/(79196.0253972279 + 3446.39220863669 * T + (-32898.311685307) * sqrt(T));$

$alpha = 1/100 * ((-1.333627E - 02) + 8.738295237E - 06 * T^2.5 + 1334.208298 * exp(-T));$

$deltaP = (8.45272006716759E - 02) + (4.86602370933418E - 18). * exp(T) + (-4.00521351511864E -$
$03). * (T^(0.5)). * log(T);$

$lambdaC = 6.44999999999998 * T. * T + 40.1900000000012 * T + (-907.850000000018);$

$deltaC = 0.004;$

$PiH = 800;$

$deltaS = 1/100 * (11.4266138930207 + (-126.890461063771)/log(T) + (525.291589814963)/(log(T))$
$(-960.378832397901)/(log(T))^3 + (654.302614387871)/(log(T))^4);$

$dx(1) = PiH - (BH * x(8) * x(1))/(C0 + epsilon * x(8)) - muH * x(1) + gammaH * x(3);$

$dx(2) = (BH * x(8) * x(1))/(C0 + epsilon * x(8)) - (muH + kappah) * x(2);$

$dx(3) = kappah * x(2) - (muH + deltaH + gammaH) * x(3);$

$dx(4) = LambdaS - (BS * x(7) * x(4))/(M0 + epsilon * x(7)) - deltaS * x(4);$

$dx(5) = (BS * x(7) * x(4))/(M0 + epsilon * x(7)) - (alpha + deltaS + kappas) * x(5);$

$dx(6) = kappas * x(5) - (alpha + deltaS) * x(6);$

$dx(7) = lambdaM * x(3) - deltaM * x(7);$

$dx(8) = lambdaC * x(6) - deltaC * x(8);$

global PiH BH C0 epsilon muH deltaH gammaH a K deltaE thetaE lambdaM BS

M0 deltaM deltaJ thetaS deltaS kappah kappas alpha lambdaC deltaC deltaP

hold on

$[t, x] = ode45('bilharzia', [0.0 : 0.1 : 4000.0], [1000000.0, 5000.0, 200.0, 100000.0, 1000.0, 100.0, 1000$

$plot(t, x(:, 1), 'r', 'Linewidth', 1.5)$

$plot(t, x(:, 2), 'b', 'Linewidth', 1.5)$

$plot(t, x(:, 3), 'r', 'Linewidth', 1.5)$

$plot(t, x(:, 4), 'r', 'Linewidth', 1.5)$

$plot(t, x(:, 5), 'b', 'Linewidth', 1.5)$

$plot(t, x(:, 6), 'b', 'Linewidth', 1.5)$

$plot(t, x(:, 7), 'r', 'Linewidth', 1.5)$

$plot(t, x(:, 8), 'g', 'Linewidth', 1.5)$

hold off